

---

Masters Theses

Student Theses and Dissertations

---

Spring 2015

## Impact of configuration variations on small modular reactor core performance

William Kirby Compton

Follow this and additional works at: [https://scholarsmine.mst.edu/masters\\_theses](https://scholarsmine.mst.edu/masters_theses)



Part of the [Nuclear Engineering Commons](#)

Department:

---

### Recommended Citation

Compton, William Kirby, "Impact of configuration variations on small modular reactor core performance" (2015). *Masters Theses*. 7391.

[https://scholarsmine.mst.edu/masters\\_theses/7391](https://scholarsmine.mst.edu/masters_theses/7391)

This thesis is brought to you by Scholars' Mine, a service of the Missouri S&T Library and Learning Resources. This work is protected by U. S. Copyright Law. Unauthorized use including reproduction for redistribution requires the permission of the copyright holder. For more information, please contact [scholarsmine@mst.edu](mailto:scholarsmine@mst.edu).

**IMPACT OF CONFIGURATION VARIATIONS ON SMALL MODULAR  
REACTOR CORE PERFORMANCE**

**by**

**WILLIAM KIRBY COMPTON**

**A THESIS**

**Presented to the Faculty of the Graduate School of the**

**MISSOURI UNIVERSITY OF SCIENCE AND TECHNOLOGY**

**In Partial Fulfillment of the Requirements for the Degree**

**MASTER OF SCIENCE IN NUCLEAR ENGINEERING**

**2015**

**Approved by**

**Dr. Ayodeji B. Alajo, Advisor**

**Dr. Carlos H. Castano**

**Dr. Shoaib Usman**



## ABSTRACT

One of the most promising new reactor designs is the Small Modular Reactor (SMR). These reactors, which operate under 300 MWe, will help bring cheap and safe nuclear energy to remote and centralized locations alike. Their ease of construction, advanced passive safety features, and cost effectiveness make these reactors an intriguing option for the near future.

In the work presented here, a neutronics analysis of the Westinghouse SMR was performed. Westinghouse's SMR design is a scaled down version of their AP1000 plant and will produce about 225 MWe of power. Though the parameters of the reactor core will be modeled after the AP1000, the exact layout of the core has not been released. For this research project, six initial core configurations have been proposed. The Monte Carlo method was used to calculate several reactor parameters by means of the MCNP6 code. Beginning of life calculations such as effective multiplication factor, delayed neutron fraction, temperature coefficients of reactivity, and neutron flux profile have been performed. Three refueling cycles have then been completed to observe how the six cores perform within the cycle up to the point when an equilibrium fuel cycle has been reached, while extracting data pertaining to multiplication factor, burnup, composition of spent fuel, and flux profile. These calculations will help to determine the feasibility and the effectiveness of the six potential core configurations.

## ACKNOWLEDGEMENTS

I would like to express a great thanks to my research advisor Dr. Ayodeji Alajo for his guidance throughout the duration of this project and sharing with me his expertise in the areas of reactor physics and MCNP simulations. I would also like to thank my committee members Dr. Carlos Castano and Dr. Shoaib Usman for their support in this process. I also give thanks to my fellow graduate students, particularly Brendan D'Souza for sharing this two-year struggle with me and having some fun along the way. I thank my mom Nancee, my dad Ron, and my two sisters Kelsey and Emma for their ongoing support and willingness to do what they could to help me every step of the way. Finally I'd like to acknowledge the financial assistance provided to me through the NRC Fellowship Grant awarded to me by the Nuclear Engineering Department at Missouri University of Science and Technology.

## TABLE OF CONTENTS

ABSTRACT .....	iii
ACKNOWLEDGMENTS .....	iv
LIST OF ILLUSTRATIONS.....	vii
LIST OF TABLES.....	x
NOMENCLATURE .....	xi
 SECTION	
1. INTRODUCTION.....	1
1.1. SMALL MODULAR REACTORS.....	1
1.2. WESTINGHOUSE SMR.....	2
1.2.1. Safety Features.....	3
1.2.2. Core Design.....	3
1.3. RESEARCH OBJECTIVES AND OVERVIEW.....	4
2. METHODS.....	5
2.1. DESIGNING THE SMR CORE.....	5
2.2. GEOMETRY MODELING AND MATERIALS.....	10
2.3. COMPUTATIONAL METHODS.....	18
2.3.1. Beginning of Cycle Calculations.....	18
2.3.2. In-Cycle Calculations.....	23
3. RESULTS AND DISCUSSIONS.....	27
3.1. BEGINNING OF LIFE RESULTS.....	27
3.2. MID-CYCLE RESULTS.....	40

3.2.1. Burn Cycle 1.....	41
3.2.2. Burn Cycle 2.....	47
3.2.3. Burn Cycle 3.....	53
4. CONCLUSIONS.....	60
APPENDICES	
A. BEGINNING OF LIFE NEUTRONICS DATA.....	62
B. SAMPLE MCNP INPUT FILE.....	64
BIBLIOGRAPHY.....	89
VITA.....	91

## LIST OF ILLUSTRATIONS

Figure	Page
1.1. Diagram of Westinghouse SMR Containment Vessel Interior.....	3
2.1. AP1000 Core Configuration.....	6
2.2. Proposed Core 1 Configuration.....	7
2.3. Proposed Core 2 Configuration.....	8
2.4. Proposed Core 3 Configuration.....	8
2.5. Proposed Core 4 Configuration.....	9
2.6. Proposed Core 5 Configuration.....	9
2.7. Proposed Core 6 Configuration.....	10
2.8. Horizontal Cross Section of Standard Fuel Rod.....	11
2.9. Horizontal Cross Section of IFBA Rod.....	12
2.10. Horizontal Cross Section of Pyrex Rod.....	14
2.11. Positions of Pyrex Rods in Fuel Assemblies.....	15
2.12. Positions of IFBA Rods in Fuel Assemblies.....	15
2.13. Sample Fuel Assembly from MCNP Geometry Model.....	16
2.14. Full MCNP Core Geometry Model.....	17
2.15. Diagram of Eightfold-Symmetry of Core Layout.....	24
2.16. SMR Core Reloading Pattern.....	25
3.1. Beginning of Life k-effective and $\beta$ -effective Results.....	27
3.2. Beginning of Life Excess Reactivity and Shutdown Margin Results.....	28
3.3. k-effective vs. Dissolved Boric Acid Concentration.....	31



3.4. Beginning of Life Core 1 Normalized Radial Flux Profile and Flux Slice.....	33
3.5 Beginning of Life Core 1 Normalized Axial Flux.....	33
3.6. Beginning of Life Core 2 Normalized Radial Flux Profile and Flux Slice.....	34
3.7. Beginning of Life Core 2 Normalized Axial Flux.....	34
3.8. Beginning of Life Core 3 Normalized Radial Flux Profile and Flux Slice.....	35
3.9. Beginning of Life Core 3 Normalized Axial Flux.....	35
3.10. Beginning of Life Core 4 Normalized Radial Flux Profile and Flux Slice.....	36
3.11. Beginning of Life Core 4 Normalized Axial Flux.....	36
3.12. Beginning of Life Core 5 Normalized Radial Flux Profile and Flux Slice.....	37
3.13. Beginning of Life Core 5 Normalized Axial Flux.....	37
3.14. Beginning of Life Core 6 Normalized Radial Flux Profile and Flux Slice.....	38
3.15. Beginning of Life Core 6 Normalized Axial Flux.....	38
3.16. $k_{\text{eff}}$ vs. Time for Three MCNP Burn Cycles.....	40
3.17. Normalized Weight Percentages of Transuranics Present in Fuel After Cycle 1.....	43
3.18. Burn Cycle 1 Core 1 Normalized Radial Flux Profile and Flux Slice.....	44
3.19. Burn Cycle 1 Core 2 Normalized Radial Flux Profile and Flux Slice.....	44
3.20. Burn Cycle 1 Core 3 Normalized Radial Flux Profile and Flux Slice.....	45
3.21. Burn Cycle 1 Core 4 Normalized Radial Flux Profile and Flux Slice.....	45
3.22. Burn Cycle 1 Core 5 Normalized Radial Flux Profile and Flux Slice.....	46
3.23. Burn Cycle 1 Core 6 Normalized Radial Flux Profile and Flux Slice.....	46
3.24. Normalized Weight Percentages of Transuranics Present in Fuel After Cycle 2.....	49
3.25. Burn Cycle 2 Core 1 Normalized Radial Flux Profile and Flux Slice.....	49
3.26. Burn Cycle 2 Core 2 Normalized Radial Flux Profile and Flux Slice.....	50

3.27. Burn Cycle 2 Core 3 Normalized Radial Flux Profile and Flux Slice.....	50
3.28. Burn Cycle 2 Core 4 Normalized Radial Flux Profile and Flux Slice.....	51
3.29. Burn Cycle 2 Core 5 Normalized Radial Flux Profile and Flux Slice.....	51
3.30. Burn Cycle 2 Core 6 Normalized Radial Flux Profile and Flux Slice.....	52
3.31. Normalized Weight Percentages of Transuranics Present in Fuel After Cycle 3.....	55
3.32. Burn Cycle 3 Core 1 Normalized Radial Flux Profile and Flux Slice.....	55
3.33. Burn Cycle 3 Core 2 Normalized Radial Flux Profile and Flux Slice.....	56
3.34. Burn Cycle 3 Core 3 Normalized Radial Flux Profile and Flux Slice.....	56
3.35. Burn Cycle 3 Core 4 Normalized Radial Flux Profile and Flux Slice.....	57
3.36. Burn Cycle 3 Core 5 Normalized Radial Flux Profile and Flux Slice.....	57
3.37. Burn Cycle 3 Core 6 Normalized Radial Flux Profile and Flux Slice.....	58

## LIST OF TABLES

Table	Page
2.1. Composition of Zirconium Alloy Used in Cladding.....	11
2.2. Composition of IFBA Material.....	12
2.3. Composition of Pyrex.....	13
2.4. Fuel Assembly Rod Makeup.....	14
2.5. SMR Core Design Specifications.....	18
3.1. Reactivity Coefficient KCODE Results.....	29
3.2. Temperature Coefficients of Reactivity Calculations.....	30
3.3. Critical Boric Acid Concentration Calculations.....	32
3.4. Beginning of Life Peak to Average Flux Ratios.....	39
3.5. Burn Cycle 1 Numerical Results (600 days).....	41
3.6. Normalized Weight % of Key Actinides Found in Fuel after Burn Cycle 1.....	42
3.7. Burn Cycle 1 Peak to Average Flux Ratios.....	47
3.8. Burn Cycle 2 Numerical Results (400 days).....	47
3.9. Normalized Weight % of Key Actinides Found in Fuel After Burn Cycle 2.....	48
3.10. Burn Cycle 2 Peak to Average Flux Ratios.....	52
3.11. Burn Cycle 3 Numerical Results (400 days).....	53
3.12. Normalized Weight % of Key Actinides Found in Fuel After Burn Cycle 3.....	54
3.13. Burn Cycle 3 Peak to Average Flux Ratios.....	58

## NOMENCLATURE

<b>Symbol</b>	<b>Meaning</b>
SMR	Small Modular Reactor
LWR	Light-Water Reactor
LEU	Low-Enriched Uranium
PWR	Pressurized Water Reactor
RFA	Westinghouse Robust Fuel Assembly
MCNP	Monte-Carlo N-Particle Transport Code
$k_{\text{eff}}$	Effective Neutron Multiplication Factor
$\beta_{\text{eff}}$	Effective Delayed Neutron Fraction
$\rho_{\text{ex}}$	Core Excess Reactivity
SDM	Shutdown Margin
$\alpha_{\text{M}}$	Moderator Temperature Coefficient of Reactivity
$\alpha_{\text{F}}$	Fuel Temperature Coefficient of Reactivity
IFBA	Integral Fuel Burnable Absorber
$k_{\text{prompt}}$	Prompt Multiplication Factor Due to Prompt Neutrons Only
$\nu_{\text{avg}}$	Average Number of Neutrons Released per Fission
$Q_{\text{avg}}$	Average Energy Released per Fission
$\sigma_x$	Uncertainty in Measurement 'x'

# 1. INTRODUCTION

## 1.1. SMALL MODULAR REACTORS

Currently, every commercial power reactor in the United States is a light-water reactor (LWR) that is fueled by low-enriched Uranium (LEU). LWRs have long been relied upon due to their relative ease of construction and maintenance, their safety record, and their ability to effectively produce power. With the bulk of the country's reactor fleet advancing towards their eventual decommission, new reactors will need to be constructed in the coming years. Some new designs such as Westinghouse's Advanced Passive 1000 (AP1000) PWR-type reactor have already undergone the first stages of construction. The first two AP1000 reactors are currently being constructed at the Plant Vogtle site in Burke County, Georgia. However with increasing demand for cheaper and more accessible power, one concept that is quickly gaining traction throughout the nuclear world is the Small Modular Reactor (SMR).

The US Department of Energy defines a Small Modular Reactor as any reactor that produces 300 MWe or less of power. SMRs have numerous advantages. Firstly, they are considered to be "modular" in that they can be completely assembled and constructed in the factory and subsequently shipped to the plant site by either train or truck. Conversely, larger scale reactors require a substantial amount of on-site construction. Having this self-contained fabrication plan helps to reduce the initial capital cost as well, since the units can be produced more quickly and easily than a large reactor [1]. Furthermore, one plant can contain multiple SMR units, so this modularity makes it convenient to scale the power output of a plant to the desired level by simply installing more reactors. Another key benefit to the SMR is that they are a viable way of delivering power to more remote areas.

It is not always feasible or cost-effective to run electricity over long distances. A power plant consisting of SMR units can establish a smaller more localized electrical grid for a remote population area without having to build a superfluous and expensive large-scale plant such as the AP1000 [1]. Many of the SMR designs feature extensive passive safety features that rely on natural convection to help remove heat from the core during an accident scenario. The first SMR is on track to be deployed within the next ten years.

## **1.2. WESTINGHOUSE SMR**

One of the companies developing a Small Modular Reactor in the United States is Westinghouse Electric Company. Their SMR will operate at 800 MWt which corresponds to about 225 MWe. The containment vessel, which has a height of 27.1 m and an outer diameter of 9.7 m will enclose several essential parts of the reactor including the core, the pressurizer, the coolant pumps, and the steam generators [2]. This reactor will also have load following capabilities and can operate anywhere from 20% to 100% of full power when in a daily load following cycle [3]. The following shows a diagram highlighting key structures within the SMR containment vessel.

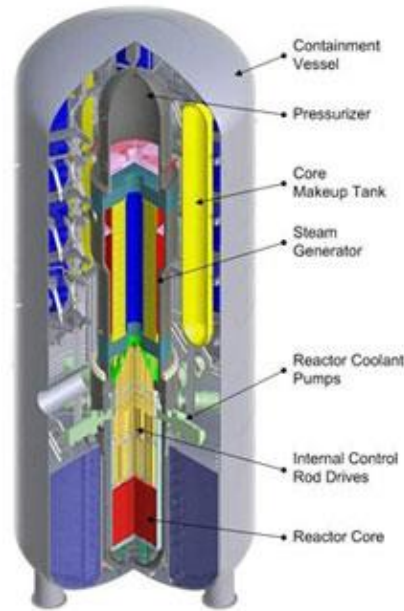


Figure 1.1. Diagram of Westinghouse SMR Containment Vessel Interior

**1.2.1. Safety Features.** In nuclear reactor design, safety is always of utmost importance. Westinghouse has incorporated several innovative passive safety features into their SMR. The heat removal and coolant flow from the core can be accomplished completely by natural circulation and do not require any additional operator intervention. In the event of an accident scenario, the control rods drop and highly borated water falls into the core due to gravity. Furthermore, the reactor will continue to remove heat for seven days without the need for any human intervention [2]. These safety features make the SMR an even more appealing design.

**1.2.2. Core Design.** The Westinghouse SMR core will be similar to their AP1000 core, but scaled down to account for the reduction in power output. The core will consist of 89 17x17 Robust Fuel Assemblies (RFA) which have been proven to be effective as part of the AP1000 core. The fuel used will be low enriched Uranium. There will be three

different enrichments used among the 89 assemblies, the highest of which will be 4.95% enriched in  $^{235}\text{U}$ . It also will use the same control rod drive mechanisms as the AP1000 reactor [2].

### **1.3. RESEARCH OBJECTIVES AND OVERVIEW**

While it is known that the Westinghouse SMR core will be a very similar but scaled-down version of their AP1000 core, the exact layout has yet to be released. For this project, six core configurations have been proposed and modeled. The performance of each core layout will be tested in several calculations at both the beginning of life and during multiple refueling cycles. This process was carried out using the Monte Carlo method facilitated by transport code MCNP6, which has been developed by Los Alamos National Laboratory. The goal of this research was to determine the feasibility of the six cores and decide which of them had the best performance and which should be discarded if any of them displayed poor performance. First, the six configurations were planned. Key features of the AP1000 core were preserved, such as the three zones of varying enrichment. The six proposed cores are not drastically different from each other, but each one shows some variation in the location and content of the different fuel assemblies used. Once the six configurations were decided, a geometry model was written in MCNP. The individual fuel rods were created and then arranged into their slots in the 17x17 assemblies. The assemblies were then placed into the core configuration as dictated by the layout design. Once the geometry model was complete, the data collection began. Several beginning of life calculations were performed, including effective multiplication factor ( $k\text{-eff}$ ), delayed neutron fraction ( $\beta$ ), the excess reactivity at startup ( $\rho$ ), the reactor shutdown margin, the



critical concentration of Boric Acid dissolved in the coolant, the moderator temperature coefficient of reactivity ( $\alpha_M$ ), and the fuel temperature coefficient of reactivity ( $\alpha_T$ ). In addition, the two-dimensional radial and axial flux profiles were plotted using an MCNP mesh tally. Next, the first three fuel cycles were completed using the burnup capabilities of MCNP6. Throughout the burn cycles, k-effective was tracked as well as fuel composition, total burnup, and radial flux profile. These results were compared in order to determine the suitability of all six configurations and which core layout gave the best performance.

## 2. METHODS

### 2.1. DESIGNING THE SMR CORE

When creating the SMR core, several different types of fuel assemblies are considered. Each assembly has its own enrichment in  $^{235}\text{U}$ , a number of fuel rods coated with  $\text{ZrB}_2$  which are known as Integral Fuel Burnable Absorber (IFBA) rods and a number of borosilicate glass or Pyrex rods. The IFBA and Pyrex rods are used to suppress initial excess reactivity in the core. The variation in the locations and amount of the IFBA fuel rods and the Pyrex rods will account for most of the differences among the six cores that have been modeled. Because the SMR core layout will be heavily based on the AP1000 core layout, it was important to first examine the AP1000 core. The following figure shows the AP1000 core map. The enrichment is color-coded and the number of Pyrex rods and IFBA-coated rods are indicated in the overlaid text.

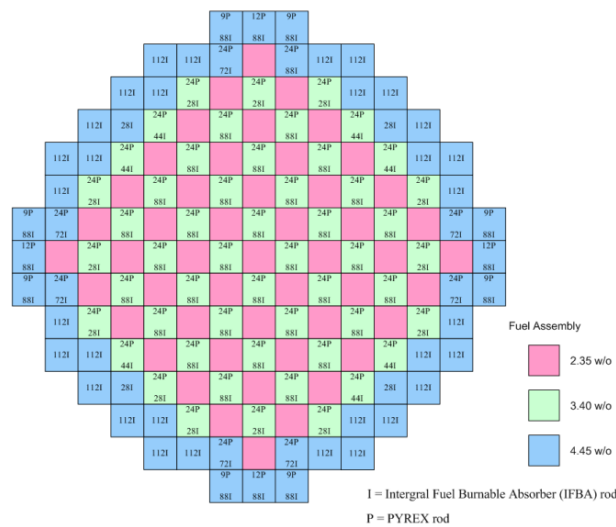


Figure 2.1. AP1000 Core Configuration [4]

The AP1000 Core has 157 fuel assemblies each of which falls into one of three enrichment zones. The highest enrichment used is 4.45% by weight in  $^{235}\text{U}$ , the middle enrichment value is 3.40%, and the lowest enrichment value is 2.35%. The three enrichment zones are used in order to flatten the power profile [4]. Since the center of the core will be the hottest, creating a perimeter of fuel with a higher enrichment while putting the fuel with a lower enrichment towards the center will help achieve this goal of lowering the maximum-to-average flux ratio.

Because Westinghouse has specified that the highest enrichment used in the SMR is 4.95% by weight, all three zones have been scaled from the AP1000 values. Therefore, the enrichment values used for this project are 4.95% for the highest, 3.78% for the middle, and 2.61% for the lowest. Each SMR core will have 89 fuel assemblies. 48 of these will be enriched to 4.95%, 16 will be enriched to 3.78%, and 25 will be enriched to 2.61%. The six proposed configurations can be seen below.

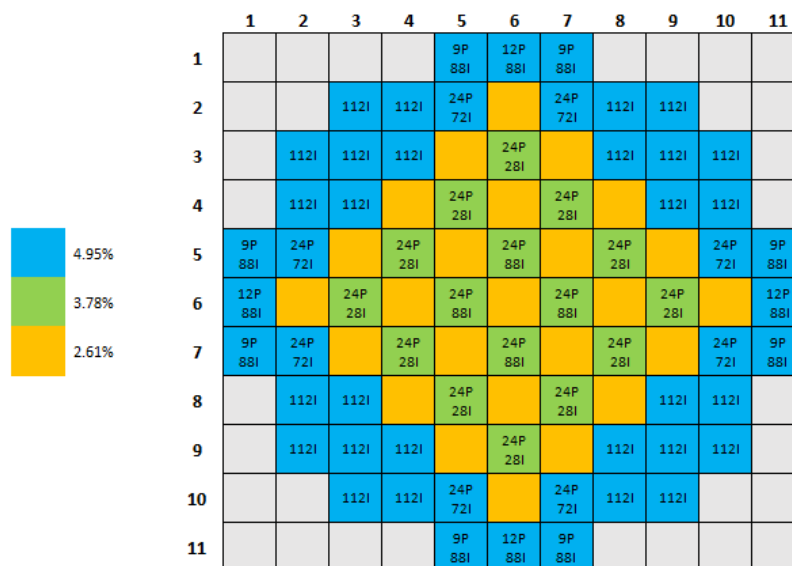


Figure 2.2. Proposed Core 1 Configuration

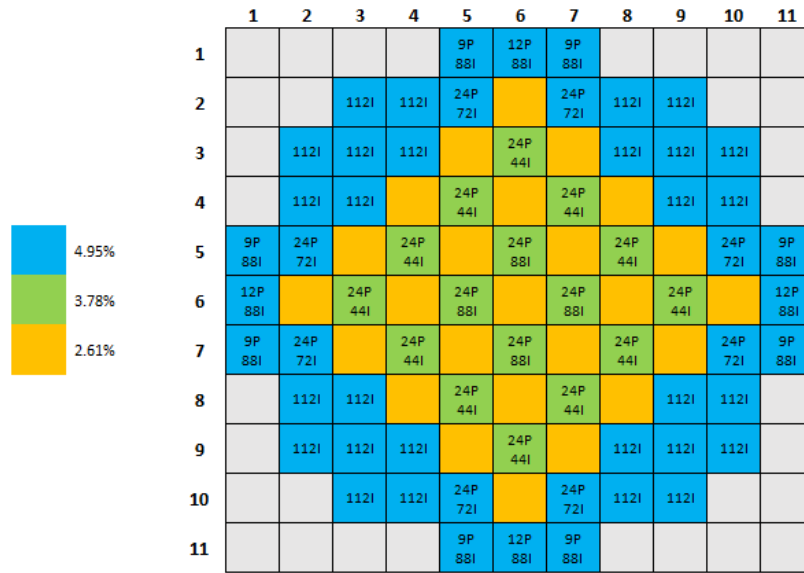


Figure 2.3. Proposed Core 2 Configuration

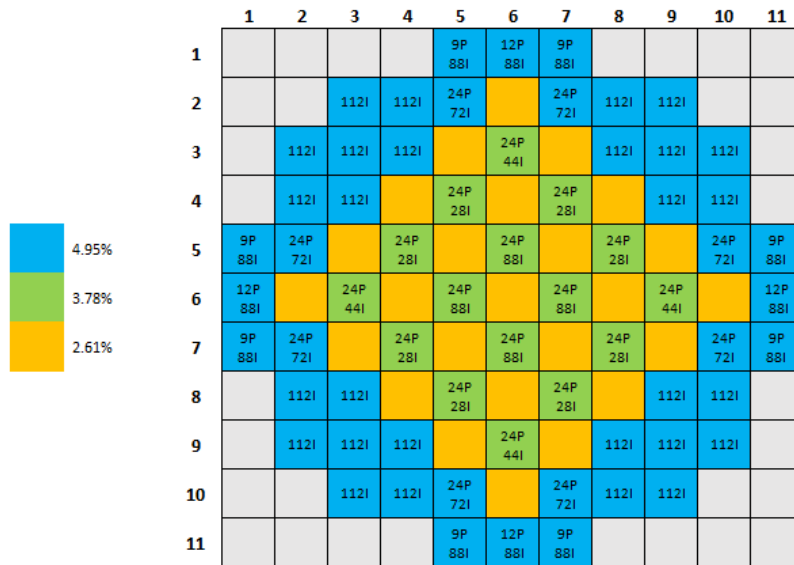


Figure 2.4. Proposed Core 3 Configuration

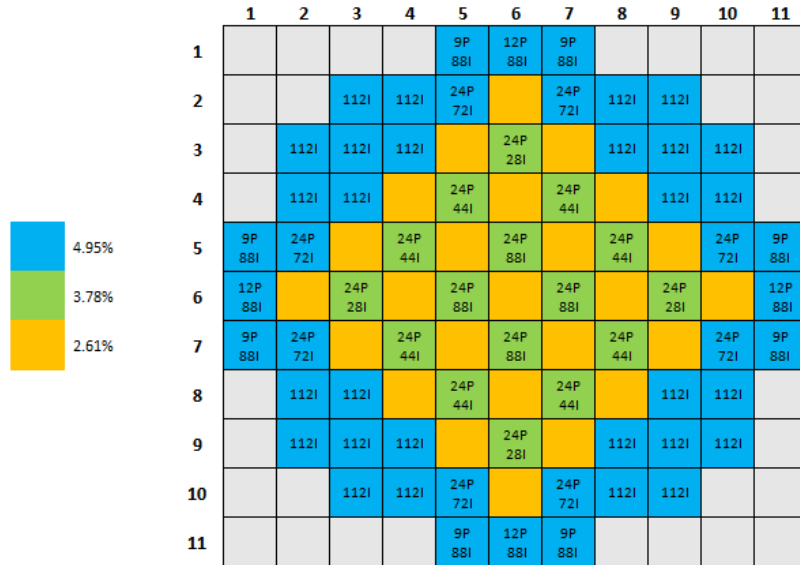


Figure 2.5. Proposed Core 4 Configuration

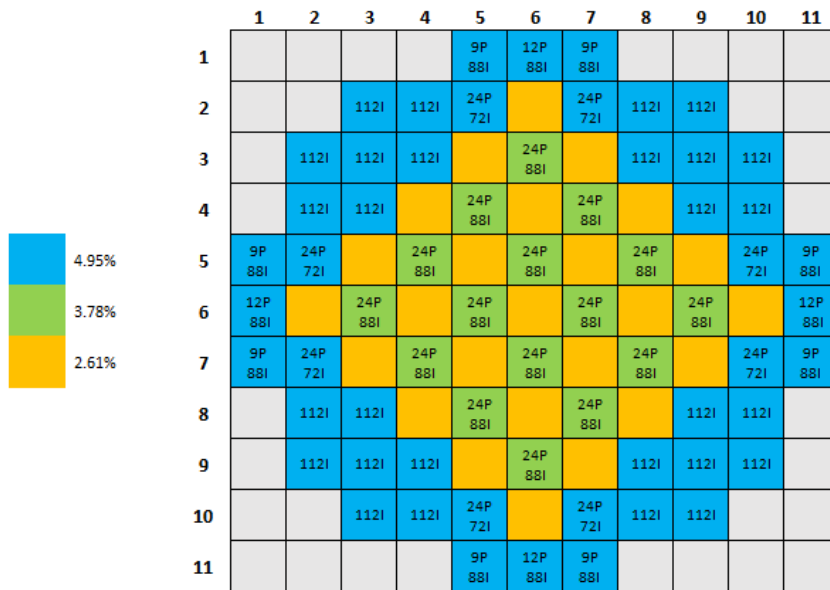


Figure 2.6. Proposed Core 5 Configuration

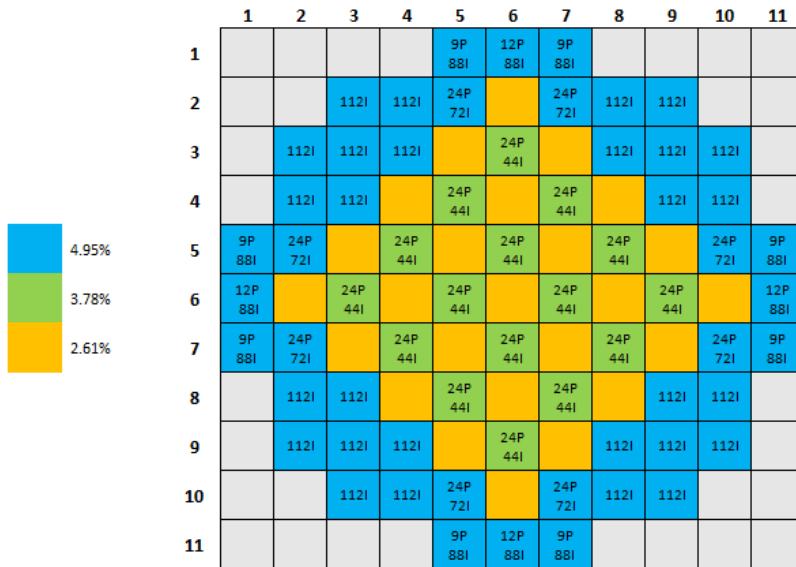


Figure 2.7. Proposed Core 6 Configuration

These six layout patterns have varying numbers of Pyrex and IFBA-coated rods.

They were each modeled and tested in MCNP in order to evaluate their performance.

## 2.2. GEOMETRY MODELING AND MATERIALS

The first structures modeled were the fuel pins. The fuel was composed of  $UO_2$ , with the majority of the Uranium being  $^{238}U$  with each of the three level of enrichments having a small contribution from  $^{235}U$ . It is assumed that the fresh fuel is “pure” in that it consists only of the three isotopes  $^{238}U$ ,  $^{235}U$ , and  $^{16}O$ . The cladding material for the Westinghouse SMR is their patented zirconium alloy Zirlo, but for this simulation a similar Zirconium alloy will be used. The elemental composition for the Zirconium alloy, which has a density of  $6.50 \text{ g/cm}^3$ , can be seen in the following table:

Table 2.1. Composition of Zirconium Alloy Used in Cladding

Element	Composition (Weight Percentage)
Zirconium	98.23%
Tin	1.45%
Iron	0.21%
Chromium	0.1%
Hafnium	0.01%

The standard fuel pins had a radius of the fuel of 4.096 mm. There is a Helium gap of thickness 0.083 mm between the fuel pellet and the cladding to allow for thermal expansion of the fuel. The cladding has a thickness of 0.571 mm and consists of the aforementioned Zirconium alloy. A view of the standard fuel pin from the MCNP plotter window can be seen below.

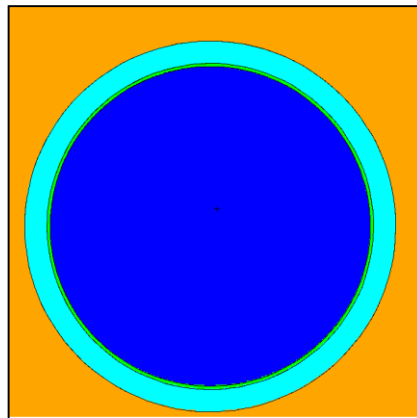


Figure 2.8. Horizontal Cross Section of Standard Fuel Rod

As previously discussed, many of the fuel pins will have their pellets coated with the IFBA material  $ZrB_2$ . This is a measure taken to suppress the initial excess reactivity and control the power distribution. The composition of the IFBA material by isotope can be seen in the following table.

Table 2.2. Composition of IFBA Material

Isotope	Composition (Weight Percentage)
$^{10}\text{B}$	3.531503%
$^{11}\text{B}$	3.293305%
$^{90}\text{Zr}$	40.990457%
$^{91}\text{Zr}$	9.038548%
$^{92}\text{Zr}$	13.967492%
$^{94}\text{Zr}$	14.463039%
$^{96}\text{Zr}$	2.37937%

The thickness of the IFBA coating was 0.0256 mm. A diagram of the IFBA-coated fuel pins can be seen below. Because the thickness of the coating is so small compared to the rest of the rod, a close-up view of the edge of the fuel rod is also shown.

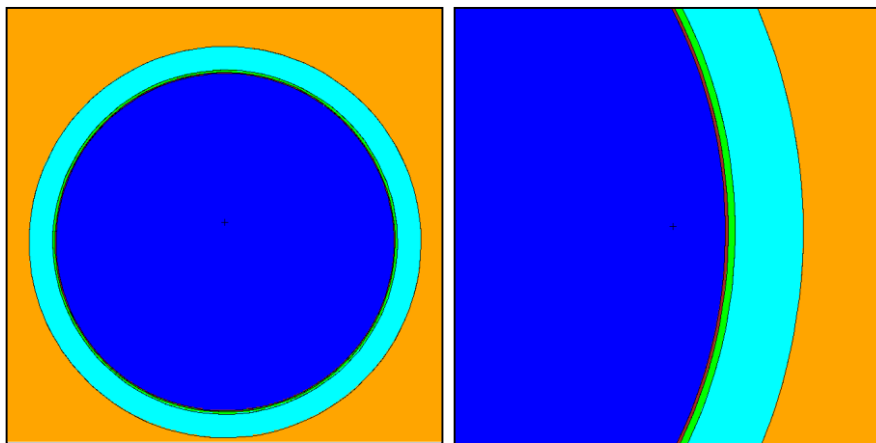


Figure 2.9. Horizontal Cross Section of IFBA Rod

The above images come from the MCNP plotter where each material in the program is assigned a color. In this case, the fuel is the dark blue, the cladding is the light blue, the



IFBA coating is the dark red, and the Helium gap is the light green, while the orange is the coolant and moderator (water).

The 17x17 Robust Fuel Assemblies contain 289 total rod positions, but only 264 are occupied by fuel. One spot in the center of the assembly is used for instrumentation. This leaves 24 open positions. In the various assemblies used in these cores, either 9, 12, or all 24 of these positions are occupied by Pyrex rods enclosed in stainless steel. In this case, the steel used is SS 316. The borosilicate glass is another strong neutron absorber that is used to quell initial excess reactivity. The composition of the Pyrex used can be seen in the following table.

Table 2.3. Composition of Pyrex

<b>Isotope</b>	<b>Composition (Weight Percentage)</b>
<sup>10</sup> B	0.744139%
<sup>11</sup> B	3.293305%
<sup>16</sup> O	54.012447%
<sup>23</sup> Na	2.967434%
<sup>27</sup> Al	1.587757%
<sup>28</sup> Si	34.355993%
<sup>29</sup> Si	1.801744%
<sup>30</sup> Si	1.237181%

The cross section of the Pyrex rods can be seen in the diagram below. The center of the rod is a Helium gap (green), there are layers of SS 316 (pink) and Pyrex (purple), and the entire rod is enclosed in a SS 316 guide tube.

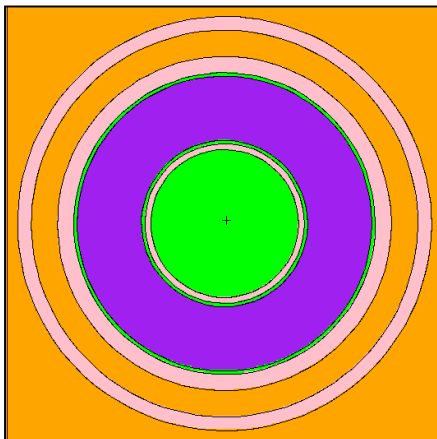


Figure 2.10. Horizontal Cross Section of Pyrex Rod

Once all rod-related cells had been constructed, each type of assembly was constructed using the various rods and ultimately the assemblies were combined to form an entire core. There were nine different assembly configurations used in total. The table below lists each of the types of 17x17 RFA used along with its important parameters.

Table 2.4. Fuel Assembly Rod Makeup

<b>ID Number</b>	<b>Enrichment</b>	<b>Number of Pyrex Rods</b>	<b>Number of IFBA Rods</b>
1	2.61%	0	0
2	3.78%	24	28
3	3.78%	24	44
4	3.78%	24	88
5	4.95%	0	28
6	4.95%	0	112
7	4.95%	9	88
8	4.95%	12	72
9	4.95%	12	88

The locations of the Pyrex and IFBA rods in the assemblies were determined based on the known pattern from the AP1000 reactor core. The specific layouts can be seen in the following figures.

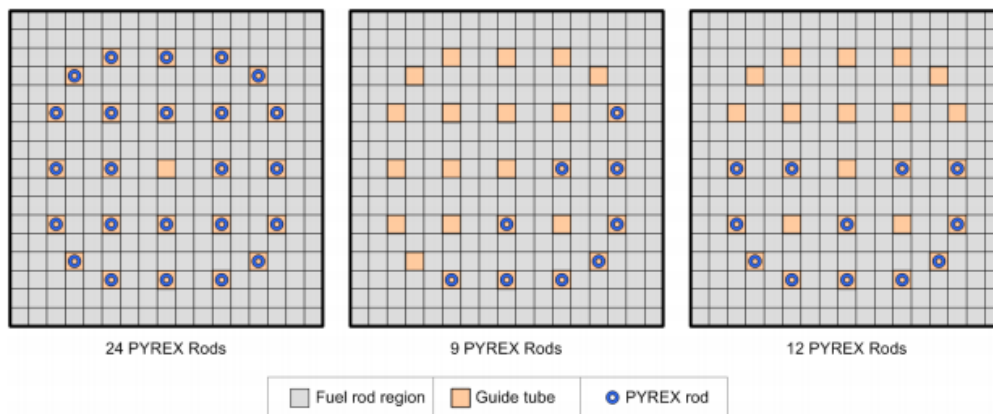


Figure 2.11. Positions of Pyrex Rods in Fuel Assemblies [4]

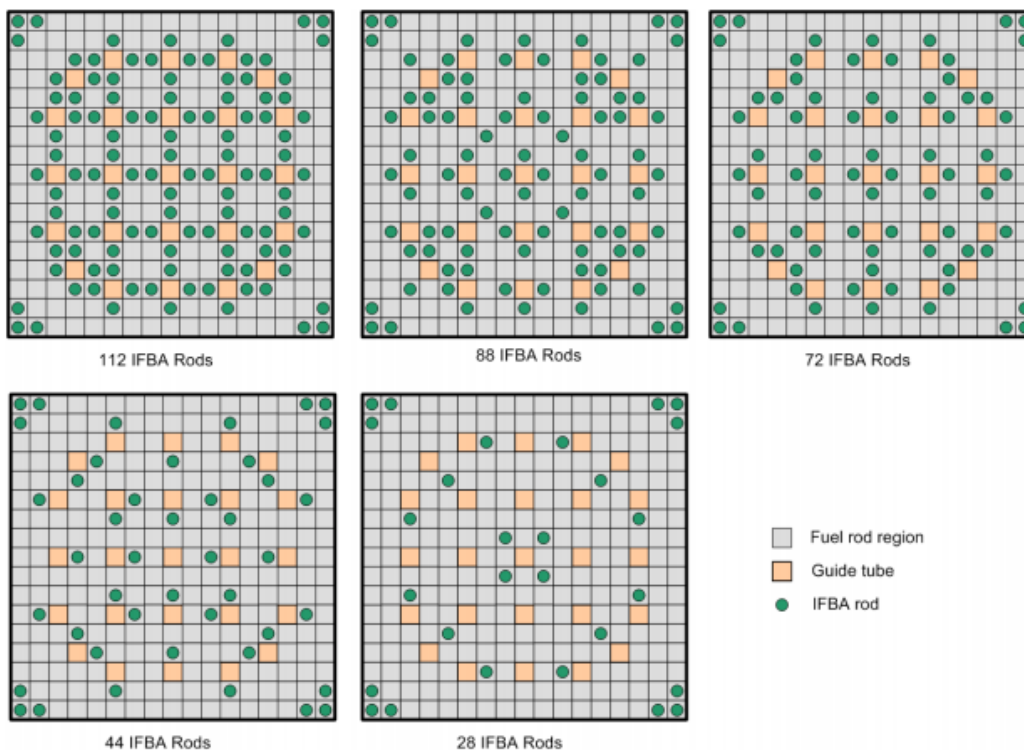


Figure 2.12. Positions of IFBA Rods in Fuel Assemblies [4]

Due to symmetry considerations, the assemblies with 9 and 12 Pyrex rods needed to be created in MCNP four separate times, to account for the four possible alignments within the core. For example in the case of 9 Pyrex rods, the rod layout as seen in the middle frame of Figure 2.11 could feature the Pyrex rods in the bottom right corner, the bottom left corner, the upper right, or the upper left. Using these guidelines, the fuel assemblies were created in the MCNP input file. The following figure shows one example of a fuel assembly as viewed from the MCNP plotter window. This sample assembly is type 2, meaning it has 3.78% enrichment, 24 Pyrex rods and 28 IFBA rods.

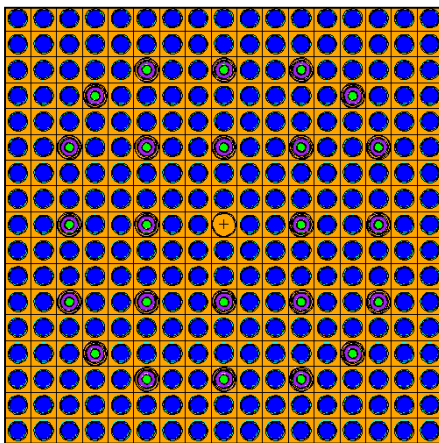


Figure 2.13. Sample Fuel Assembly from MCNP Geometry Model

Once each fuel assembly was compiled, each of the six cores was concocted in six different input files. The fuel assemblies were placed in the correct pattern in a lattice which was divided up into 21.42 cm x 21.42 cm boxes. The core was surrounded by a stainless-steel barrel and the entire structure was filled with pure light water. The full geometry model for

the core layout in MCNP can be seen below. In this figure, the Core 1 model is laid out in the MCNP Visual Editor (VisEd).

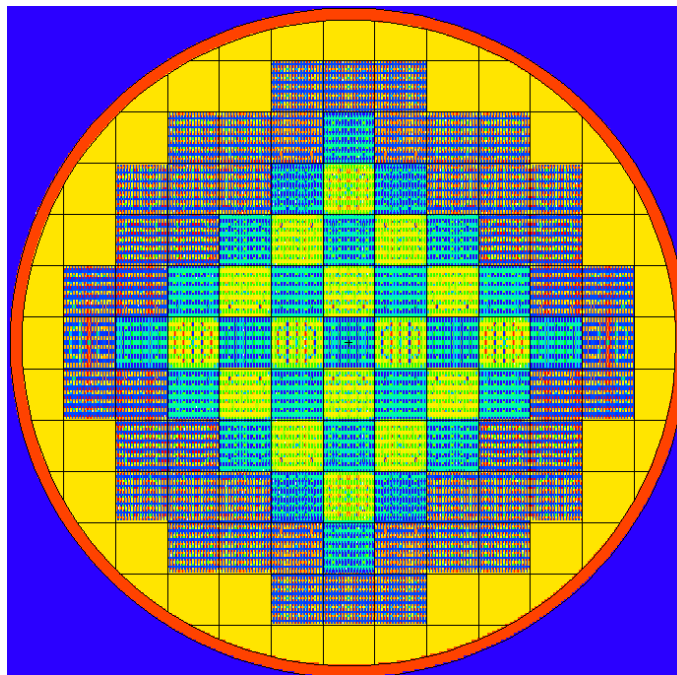


Figure 2.14. Full MCNP Core Geometry Model

The specifications used for creating this geometry model have been compiled into the following table.

Table 2.5. SMR Core Design Specifications

<b>Fuel Material</b>	Low Enriched UO <sub>2</sub>
<b>Rod Diameter</b>	8.192 mm
<b>Helium Gap Thickness</b>	0.083 mm
<b>Cladding Material</b>	Zircaloy-4
<b>Cladding Thickness</b>	0.571 mm
<b>IFBA Coating Material</b>	ZrB <sub>2</sub>
<b>IFBA Thickness</b>	0.0256 mm
<b>Rod Pitch</b>	12.6 mm
<b>Assembly Type</b>	17x17 Robust Fuel Assembly
<b>Number of Assemblies</b>	89
<b>Assembly Dimensions</b>	21.42 cm x 21.42 cm
<b>Active Fuel Height</b>	244 cm
<b>Guide Tube Material</b>	SS316
<b>Core Barrel Material</b>	SS316
<b>Coolant/Moderator Material</b>	H <sub>2</sub> O
<b>Control Rod Material</b>	Ag-In-Cd alloy

## 2.3. COMPUTATIONAL METHODS

The bulk of the calculations were performed by MCNP6, the most current version of the often-used Monte-Carlo transport code developed during the middle of the 20<sup>th</sup> century and maintained and updated at Los Alamos National Lab. The calculations performed fall into two categories: beginning of life and in-cycle

**2.3.1. Beginning of Life Calculations.** For the beginning of life portion of the project, nearly every result was found using a KCODE simulation. For this procedure, a fission source was placed in nearly the exact center of the core. The exact center was not the location of the source because the middle pin in each assembly is used for instrumentation; therefore a pin adjacent to the center of the array was used. The source was planted using the KSRC card in MCNP. The first calculation performed sought to determine the effective multiplication factor  $k_{\text{eff}}$  at operating conditions. 400 cycles of

100,000 particles each were run in these initial KCODE simulations. It is necessary for criticality to be achieved in the reactor and have some excess reactivity in order to continue to remain at least slightly supercritical while the fuel is depleted over time.

The next calculation was the delayed neutron fraction  $\beta_{eff}$ . It is crucial for nuclear reactors to have delayed neutrons present since they act to control how quickly the reactor can increase in power. Without delayed neutrons, a reactor would increase in power to such a magnitude and in such a short time period that significant damage would result [5]. The effective delayed neutron fraction can be determined by the following equation:

$$\beta_{eff} = \frac{k_{eff} - k_{prompt}}{k_{eff}} \quad (1)$$

In this equation,  $k_{prompt}$  is the effective multiplication factor when only prompt neutrons are considered. The method for obtaining this result in MCNP is rather simple. By using the data card TOTNU and setting its value to ‘NO’ while keeping the same KCODE parameters as before, MCNP was able to calculate  $k_{prompt}$  [5]. The results were then plugged into Eq. 1 along with the results from the initial  $k_{eff}$  calculation to determine the value of  $\beta_{eff}$  for each core.

The next calculation made was the excess reactivity,  $\rho_{ex}$ . For a low-enriched Uranium PWR-type reactor such as the Westinghouse SMR, some excess reactivity is needed upon startup in order to maintain criticality for the duration of the operation period, however a higher reactivity means the amount of reactivity control must also increase. The excess reactivity is calculated as the amount by which the reactor is supercritical when all possible sources of negative reactivity (such as control rods or borated water) are absent from the core [6]. The value is taken as a fraction of the initial  $k_{eff}$  and is given by the following formula:

$$\rho_{ex} = \frac{k_{eff} - 1}{k_{eff}} \quad (2)$$

With excess reactivity present in the core, it is imperative that the reactor has enough control elements that it can inject enough negative reactivity to shut itself down, which is accomplished by bringing the reactor subcritical. For the sake of a conservative calculation, the shutdown margin (SDM) is calculated with all control rods inserted except for the rod bundle with the highest negative worth [6]. For this simulation, all control rods were identical so the rod cluster for the central assembly was the one chosen to be left out of the shutdown margin calculation. The formula used to determine the shutdown margin was as follows:

$$SDM = \frac{k_{rod\,dis\,n\,s\,e\,r\,t\,e\,d} - 1}{k_{rod\,dis\,n\,s\,e\,r\,t\,e}} \quad (3)$$

35 of the 36 control rod bundles composed of a Silver-Cadmium-Indium alloy were fully inserted in order to find the shutdown margin for each core.

Another important safety feature of any nuclear reactor is how its reactivity responds as a function of temperature. This is quantified by the temperature coefficient of reactivity  $\alpha_T$ . This temperature coefficient is defined mathematically by the following equation:

$$\alpha_T = \frac{\partial \rho}{\partial T} \quad (4)$$

Here,  $\rho$  is the reactivity and  $T$  is the temperature. Plugging in Eq. 2 for  $\rho$  and performing the differentiation gives the following form for  $\alpha_T$ :

$$\alpha_T = \frac{1}{k^2} \frac{dk}{dT} \approx \frac{1}{k} \frac{dk}{dT} \quad (5)$$



Since  $k_{\text{eff}}$  is reasonably close to 1, the approximation that  $k^2 \approx k$  can be made [7]. It is necessary for the value of the temperature coefficient to be negative, which indicates that as temperature increases, the total reactivity and therefore power will decrease. It is helpful to further divide this into a moderator temperature coefficient of reactivity (how the reactivity changes with respect to a change in the moderator temperature) and fuel temperature coefficient of reactivity (how the reactivity changes with respect to a change in the fuel temperature). To first find the moderator temperature coefficient of reactivity  $\alpha_{T,M}$ , the moderator temperature was lowered from operating temperature (600K) to room temperature (293.6K) and  $k_{\text{eff}}$  was calculated in MCNP. The temperature of the simulation was lowered by changing two parameters. First, the cross section libraries for the materials used in the moderator (Hydrogen and Oxygen) were changed from the .71c library to the .70c library, which correspond to 600K and 293.6K respectively. Secondly, the density of the water was changed. Under operating conditions of 600K and 2200 psia, the density of water is found to be approximately 0.67 g/cm<sup>3</sup>. At room temperature, water has a density of 1 g/cm<sup>3</sup>, so this was adjusted accordingly. The moderator coefficient was determined by the following relation:

$$\alpha_{T,M} = \frac{k_1 - k_2}{k_1} \frac{1}{\Delta T} \quad (6)$$

Here,  $k_1$  is measured with both moderator and fuel at operating temperature and  $k_2$  is measured with the moderator lowered to room temperature while the fuel stays at operating temperature. Next, the fuel temperature was lowered from operating to room temperature in order to find the fuel temperature coefficient of reactivity,  $\alpha_{T,M}$ . Because changing the temperature of UO<sub>2</sub> has a negligible effect on its density, the only parameter changed for

this part was the cross section library. The fuel coefficient was found by the following relation:

$$\alpha_{T,M} = \frac{k_2 - k_3}{k_2} \frac{1}{\Delta T} \quad (7)$$

Here,  $k_3$  is measured with both fuel and moderator at 293.6K. KCODE simulations were performed in MCNP to find  $k_1$ ,  $k_2$ , and  $k_3$  and from there the temperature coefficients were calculated.

It is known that Boron, specifically the isotope  $^{10}\text{B}$ , has a large neutron absorption cross section. With this in mind, the element is used in reactors to act as a chemical control element. This is accomplished in the Westinghouse SMR by dissolving Boric acid ( $\text{H}_3\text{BO}_3$ ) in the coolant. Boric acid is used to help suppress initial excess reactivity in the core. It would therefore be useful to know how much Boric acid needs to be added to the water in order to reduce the  $k_{\text{eff}}$  from its initial supercritical value down to a critical value of 1. This was done by gradually adding the Boric acid into the material card for water in the MCNP code. Increases were made in increments of 500 parts per million from 0 ppm to 4000 ppm until the reactor dropped to a subcritical state. In this case one part per million will refer to one molecule of acid, so due to the isotopic abundance of  $^{10}\text{B}$ , for roughly every five parts per million there will be one atom of  $^{10}\text{B}$ . The results were plotted in order to observe the behavior of the reactor with this chemical control and to determine the value in parts per million where the  $k_{\text{eff}}$  value dropped to 1.

The final calculations performed for the beginning of cycle time period were the two-dimensional radial and axial flux profiles. The FMESH4 tally was used in MCNP with a rectangular mesh overlaid. For the radial profile, a slice was taken in the X-Y plane and the flux in each cell was averaged over the entire height of the core (260 cm). Each of the

78,400 cells in the 280x280 mesh array had dimensions 5 mm by 5 mm. The data was also used to calculate the maximum-to-average flux ratio to ensure that there was a reasonably flat power distribution. For the axial flux profile, a 10x10 cm<sup>2</sup> vertical slice was taken and 260 meshes in the Z-direction of 1 cm each were created. This gave the value of the flux at these points along the vertical axis. For both flux profiles, the tally data was read into MATLAB and the plots were generated in the form of a surface plot for the radial profile and a line plot for the axial profile.

**2.3.2. In-Cycle Calculations.** After the core parameters with fresh fuel had been calculated, the MCNPX capabilities of MCNP6 were utilized in order to track the cores' performance over time while operating at a power of 800 MW. The BURN data card was used with a time set for 600 days in 100-day intervals. Westinghouse projects 24-month refueling cycles but this research project is only considering 18-month refueling cycles. Three types of materials were burned: the fuel, the IFBA, and the Pyrex. In order to most effectively simulate the refueling process in the MCNP input file, the eightfold-symmetry of the core was taken advantage of and the assemblies were divided eight ways. Within that octant, the sixteen assemblies contained had their materials burned and each of those was reflected and copied eight times to complete the full core. The core octant with numbering system is shown below.

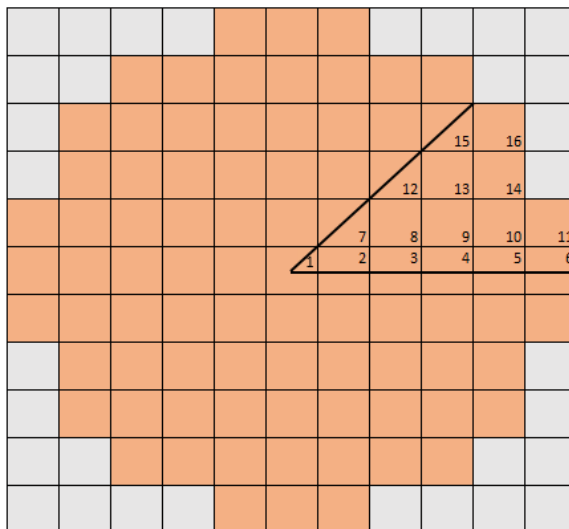


Figure 2.15. Diagram of Eightfold-Symmetry of Core Layout

After each burn cycle was completed, the MCNP output file gave both the relevant neutronics and burnup information in addition to the inventory of materials present in the core. Using this material inventory, the new material cards for the next burn cycles were meticulously formulated. The actinide inventory was of particular note, and the content of isotopes of Uranium, Neptunium, Plutonium, Americium, and Curium were tracked. The suggested pattern for refueling this SMR has been released in a document by Westinghouse. This map, seen below, indicates which assemblies should be replaced in which cycle.

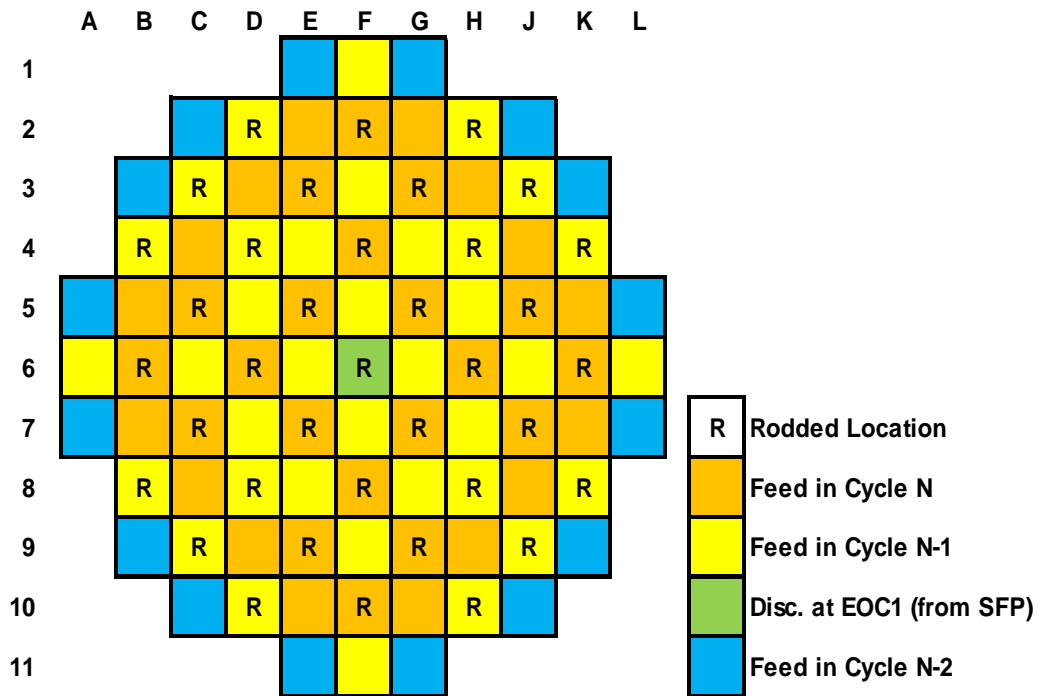


Figure 2.16. SMR Core Reloading Pattern [13]

This diagram, which also dictates the locations of the control rod clusters, shows the assemblies that will be replaced in each of three refueling cycles before an equilibrium cycle is achieved. Two of the cycles replace 36 assemblies while the final refueling replaces 16 assemblies. In this research, the center assembly will also be included in the third cycle as a simplification to make for a total of 17 assemblies removed in the third cycle.

The parameters given for each time-step in the burn cycle output file include  $k_{\text{eff}}$ , average flux, average number of neutrons produced per fission ( $\nu$ ), average Q-value, and burnup in units of GWd/MTU. After each cycle, plots of  $k_{\text{eff}}$  vs. time were produced in order to determine how long the fuel lasted before the core became subcritical. Once again, the radial flux profile was calculated by means of an FMESH4 tally using the same

parameters as during the beginning of life calculations. This data was then used to generate the two-dimensional flux maps in MATLAB.

### 3. RESULTS AND DISCUSSION

#### 3.1. BEGINNING OF LIFE RESULTS

The first simulations were carried out in order to find the  $k_{\text{eff}}$  and  $\beta_{\text{eff}}$  values. The delayed neutron fraction was calculated by running a KCODE first with both prompt and delayed neutrons then again using only prompt neutrons. After this, Eq. 2 was applied to obtain the value. The results from the beginning of life KCODE simulations are found in the following figure.

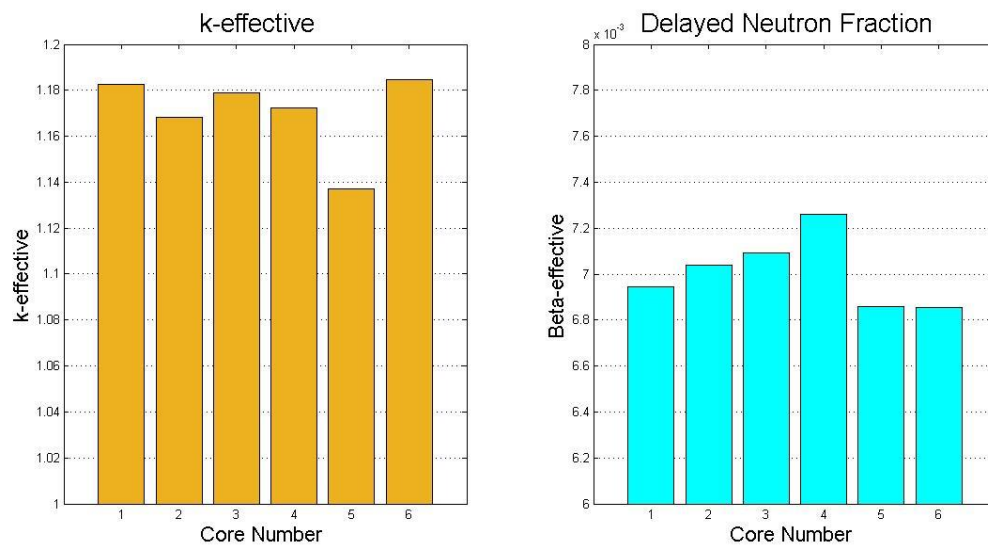


Figure 3.1. Beginning of Life k-effective and  $\beta$ -effective Results

The values for  $k_{\text{eff}}$  were in an acceptable range for a freshly fueled reactor with no control rods or chemical control elements of any kind in the core. The Westinghouse AP1000 is designed to have an initial  $k_{\text{eff}}=1.205$  under the same conditions of a fresh core with no external control elements present [8]. One thing that was immediately evident was that

Core 5 had a substantially lower starting criticality value at  $k_{\text{eff}}=1.13702$ , whereas the other five cores had values ranging from 1.168-1.85. This was not surprising, since Core 5 has the highest number of IFBA-coated rods out of all cores. The values for  $\beta_{\text{eff}}$  all fell in the range between 0.0068 and 0.0073. The expected delayed neutron fraction from the fission of  $^{235}\text{U}$  is 0.0065, so it was realistic to see all six cores have a delayed neutron fraction greater than this expected value [7]. According to its design document, the AP1000 has a delayed neutron fraction of  $\beta_{\text{eff}}=0.0075$  [8]. The large number of particles tracked in the KCODE run has rendered the uncertainties in these calculations to be rather small.

Next, the reactivity parameters were calculated. The following figure shows the results for excess reactivity (found using Eq. 2) and shutdown margin (found by Eq. 3).

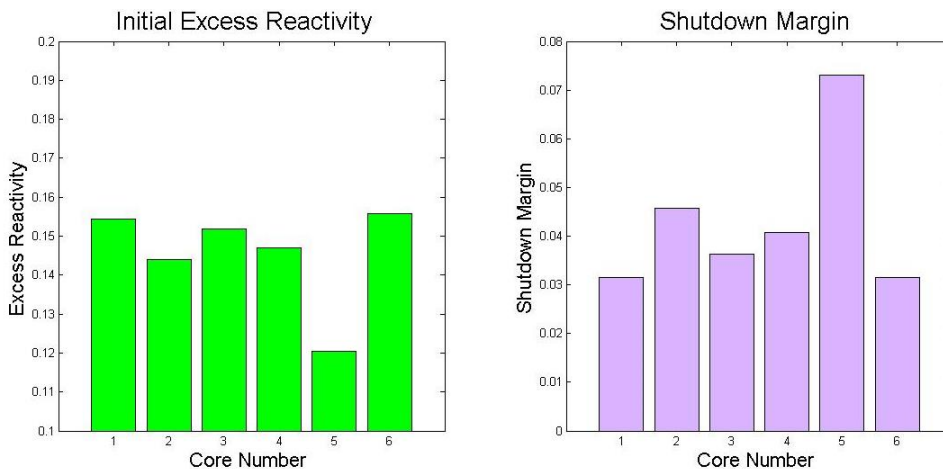


Figure 3.2. Beginning of Life Excess Reactivity and Shutdown Margin Results

The excess reactivity was calculated only using the  $k_{\text{eff}}$  result, so there were again no surprises and these values were reasonable for a PWR. The typical absolute minimum



allowed shutdown margin for a PWR is 1%, so it is good that all six of these cores exhibited a shutdown margin of 3% or larger [9]. Intuitively, the higher the starting k-effective, the lower the initial shutdown margin will be. For example, Core 5 had the lowest initial excess reactivity and therefore had the highest shutdown margin.

The next quantities calculated were the temperature coefficients of reactivity. In accordance with Eq. 6 and Eq. 7, three different values of  $k_{\text{eff}}$  were determined. The value  $k_1$  came when both moderator and fuel were at operating temperature of 600K,  $k_2$  came with the moderator at 293.6 K and the fuel at 600K, while  $k_3$  came when both moderator and fuel were at 293.6K. The results from these three KCODE simulations can be seen in the table below.

Table 3.1. Reactivity Coefficient KCODE Results

	<b>k<sub>1</sub></b>	<b>k<sub>2</sub></b>	<b>k<sub>3</sub></b>
<b>Core 1</b>	1.18278	1.24995	1.25904
<b>Core 2</b>	1.16867	1.23442	1.24298
<b>Core 3</b>	1.17997	1.24389	1.25633
<b>Core 4</b>	1.17323	1.23699	1.24896
<b>Core 5</b>	1.13588	1.19912	1.20920
<b>Core 6</b>	1.18593	1.25075	1.25867

After these criticality values were calculated for the three temperature situations, the equations were applied and the temperature coefficients of reactivity were calculated. The results can be found in the following table.

Table 3.2. Temperature Coefficients of Reactivity Calculations

	$\alpha_{T,M}$ (pcm/K)	$\sigma_{\alpha,M}$	$\alpha_{T,F}$ (pcm/K)	$\sigma_{\alpha,F}$	$\alpha_{Total}$ (pcm/K)	$\sigma_{\alpha,tot}$
<b>Core 1</b>	-18.53	0.15	-2.37	0.15	-20.90	0.30
<b>Core 2</b>	-18.36	0.14	-2.26	0.13	-20.62	0.27
<b>Core 3</b>	-17.68	0.13	-3.26	0.13	-20.94	0.26
<b>Core 4</b>	-17.74	0.13	-3.16	0.12	-20.90	0.25
<b>Core 5</b>	-18.17	0.16	-2.74	0.13	-20.91	0.29
<b>Core 6</b>	-17.84	0.13	-2.07	0.13	-19.91	0.26

Standard error propagation techniques were used to calculate the uncertainty for these values. The moderator coefficients all fell in the range between -17.6 and -18.6, while the fuel coefficients all fell in the range between -2.0 and -3.3. The anticipated range for these values in a PWR have been calculated or estimated in previous studies. For such a PWR-type reactor, the moderator temperature coefficient should be of the order of -10 to -60 pcm/K [10]. The results found from these simulations agreed with this estimate. The fuel temperature coefficient has been calculated using MCNP for several values of enrichment in UO<sub>2</sub>. Using the enrichment and number of assemblies in each zone, a simple weighted average can be calculated, and it is found that the effective average enrichment is 4.08%. According to the benchmarking that has been previously done, the value for the fuel temperature coefficient should be roughly -2 pcm/K [11]. All of the values calculated in this research are slightly higher than that, but were still in the general area for a reasonable result. The most important consideration is that all coefficients were indeed negative, indicating that an increase in temperature will lead to a decrease in reactor power.

Next, the concentration of Boric acid needed to be dissolved in the coolant in order to bring the k-effective value down to 1.00 was determined. Molecules of Boric acid (H<sub>3</sub>BO<sub>3</sub>) were added in increments of 500 ppm until the reactor was subcritical. The critical

value was found by applying a best-fit line to the data and finding point on the x-axis that corresponded to  $k_{\text{eff}}=1$ . The results for all six cores are shown in the following figure.

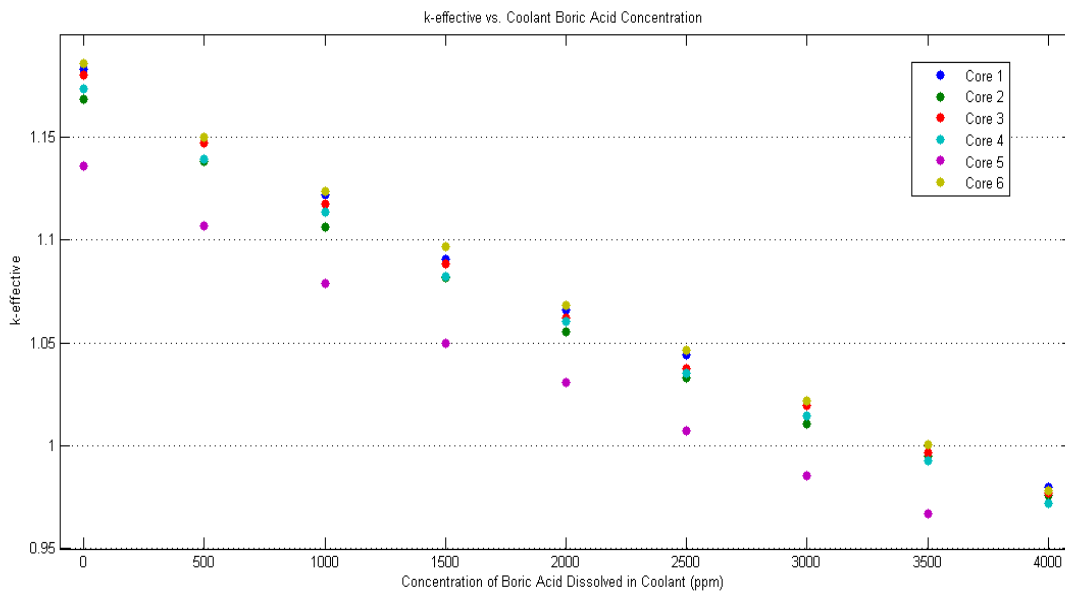


Figure 3.3. k-effective vs. Dissolved Boric Acid Concentration

The critical concentration was found by applying a linear trend to the above data. An equation for each of the six lines was used to calculate the correct value for Boron concentration. The results can be seen in the table below.

Table 3.3. Critical Boric Acid Concentration Calculations

	<b>Trend Line Equation</b>	<b>R<sup>2</sup> Value</b>	<b>Critical Boric Acid Concentration (ppm)</b>
<b>Core 1</b>	$y=-5E-5x+1.1740$	0.9934	3480
<b>Core 2</b>	$y=-5E-5x+1.1589$	0.9900	3178
<b>Core 3</b>	$y=-5E-5x+1.1703$	0.9916	3406
<b>Core 4</b>	$y=-5E-5x+1.1640$	0.9938	3280
<b>Core 5</b>	$y=-5E-5x+1.1278$	0.9930	2556
<b>Core 6</b>	$y=-5E-5x+1.1769$	0.9952	3538

Five of the six cores displayed Boric acid concentrations above 3170 ppm. The only core that deviates from this pattern is Core 5, which started with the lowest initial excess reactivity. Therefore, it makes sense that the critical concentration of Boric acid would be substantially lower than the others, as seen in these results.

Finally, the neutron flux was plotted in each cell of a 280x280 mesh with cell size 5 mm by 5 mm. The two-dimensional flux profiles for the beginning of life were created using MATLAB and can be seen in the following figures. For the radial flux, both the full core layout and a slice through the center of the core are shown in order to visualize the full flux profile and a line flux profile. The line profile will make it easier to see how the neutron flux decreases with distance from the center assembly.

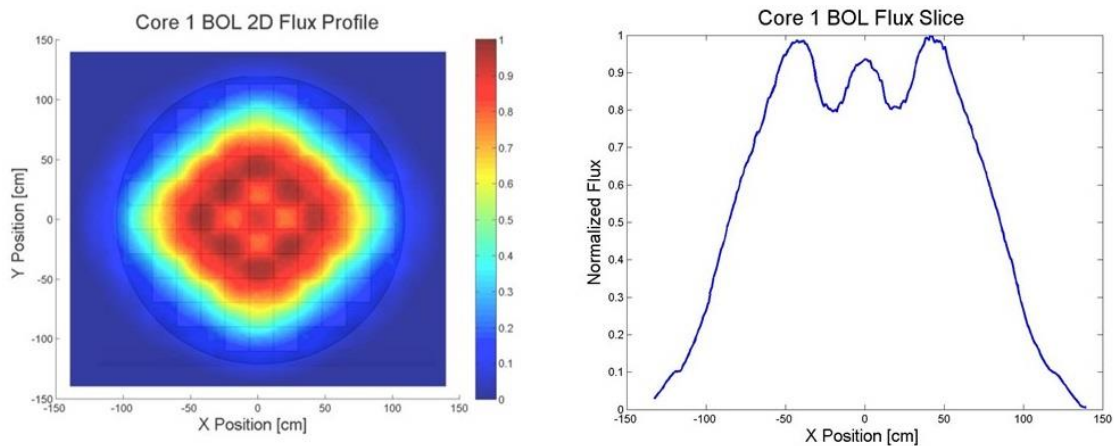


Figure 3.4. Beginning of Life Core 1 Normalized Radial Flux Profile and Flux Slice

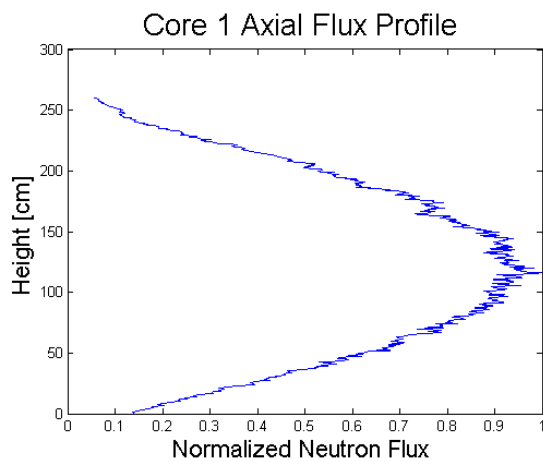


Figure 3.5 Beginning of Life Core 1 Normalized Axial Flux

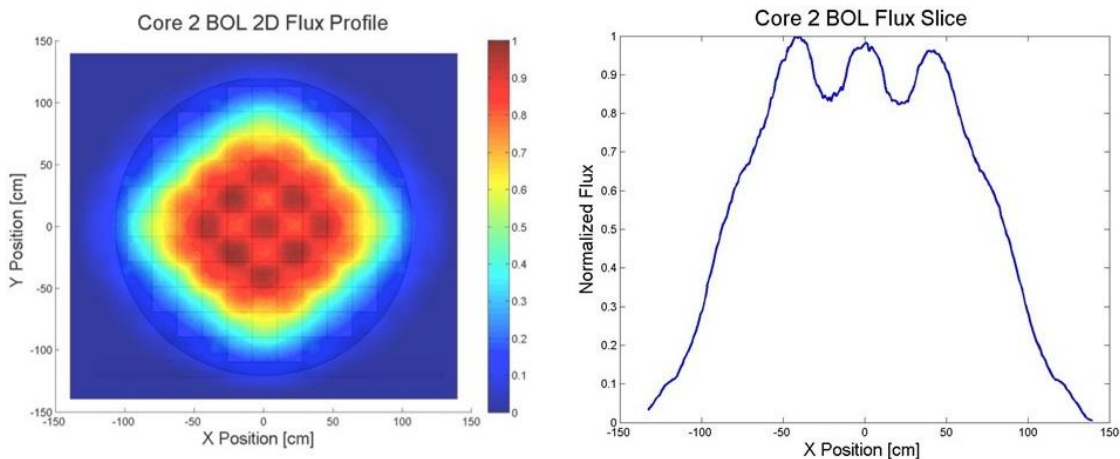


Figure 3.6. Beginning of Life Core 2 Normalized Radial Flux Profile and Flux Slice

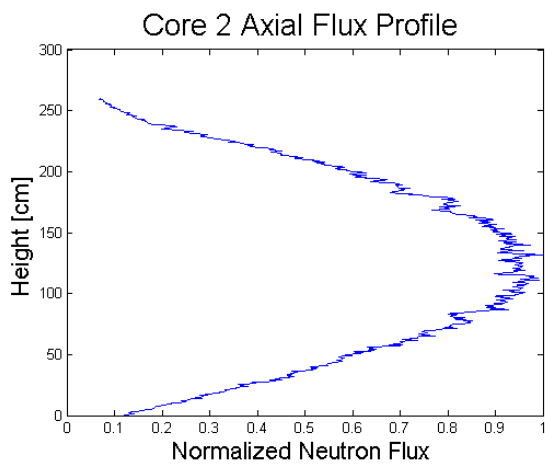


Figure 3.7. Beginning of Life Core 2 Normalized Axial Flux

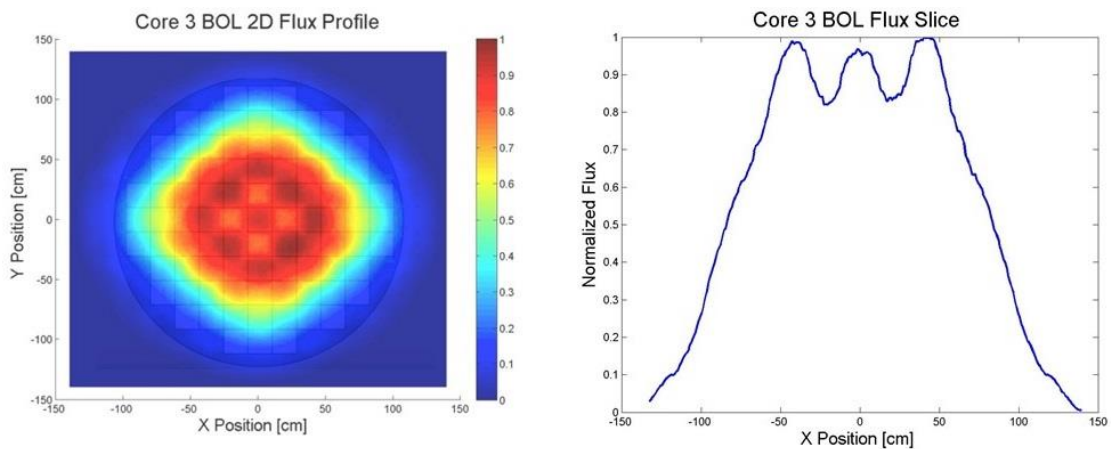


Figure 3.8. Beginning of Life Core 3 Normalized Radial Flux Profile and Flux Slice

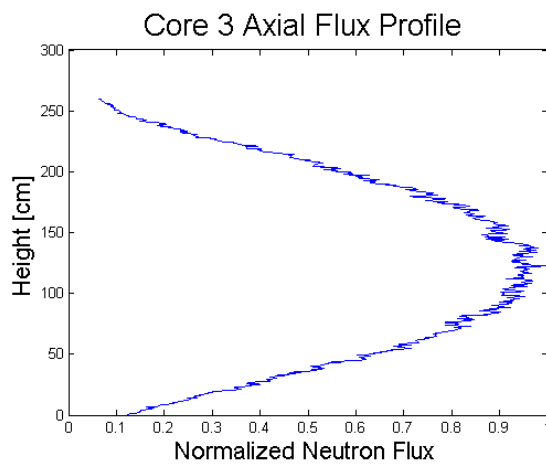


Figure 3.9. Beginning of Life Core 3 Normalized Axial Flux

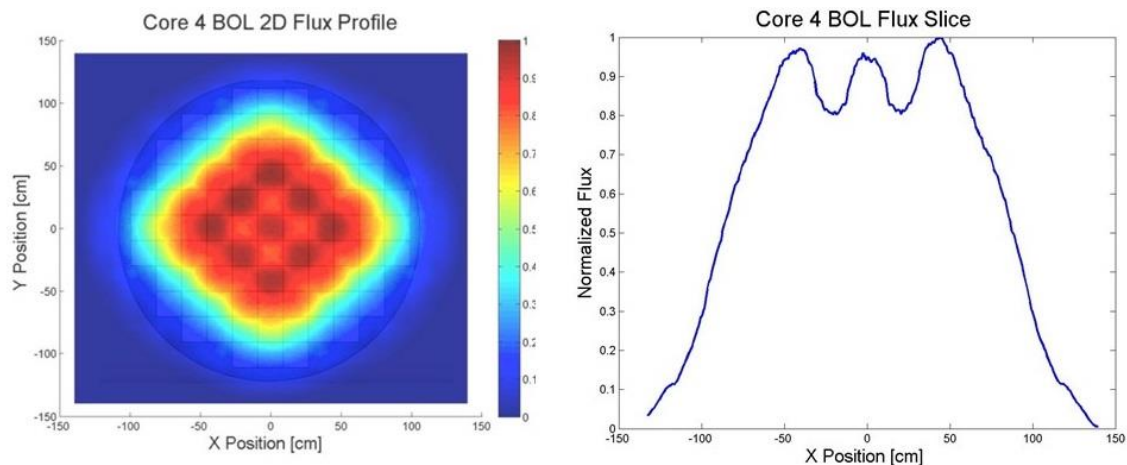


Figure 3.10. Beginning of Life Core 4 Normalized Radial Flux Profile and Flux Slice

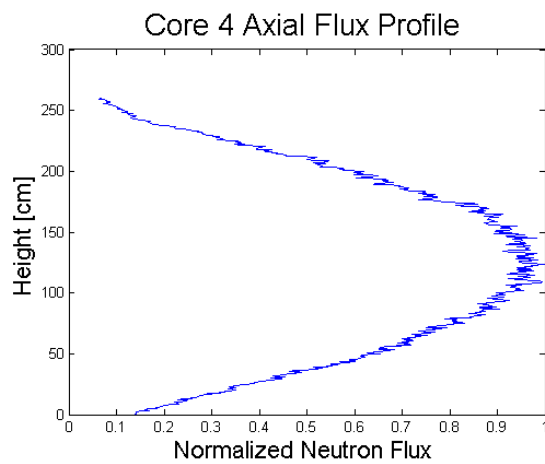


Figure 3.11. Beginning of Life Core 4 Normalized Axial Flux



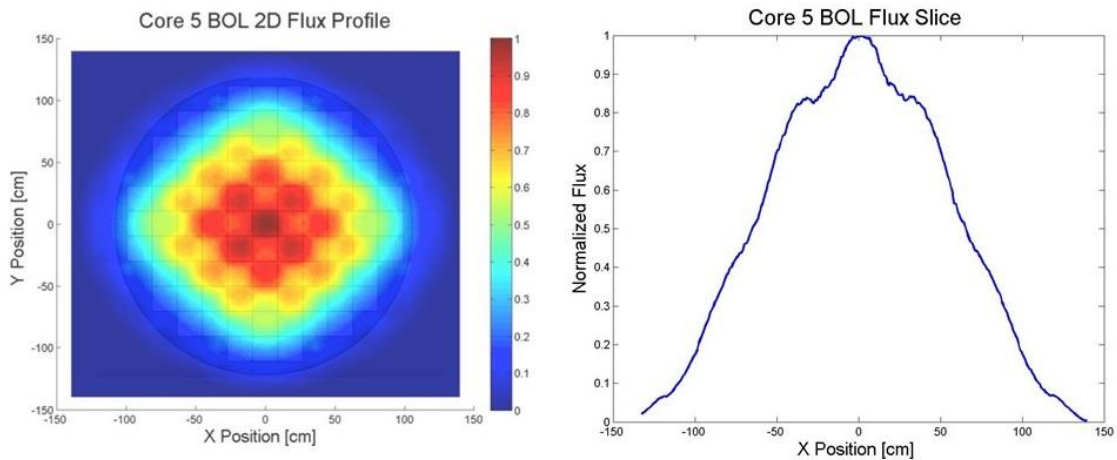


Figure 3.12. Beginning of Life Core 5 Normalized Radial Flux Profile and Flux Slice

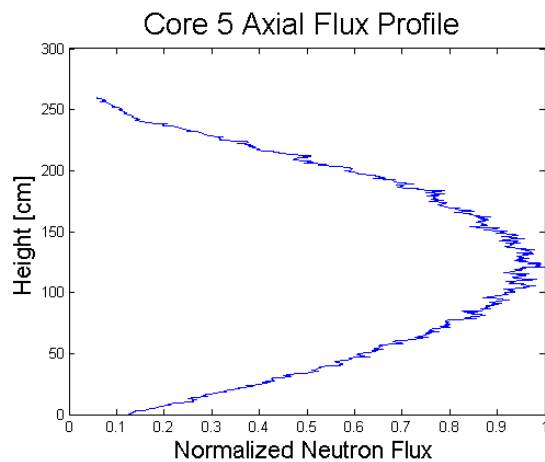


Figure 3.13. Beginning of Life Core 5 Normalized Axial Flux

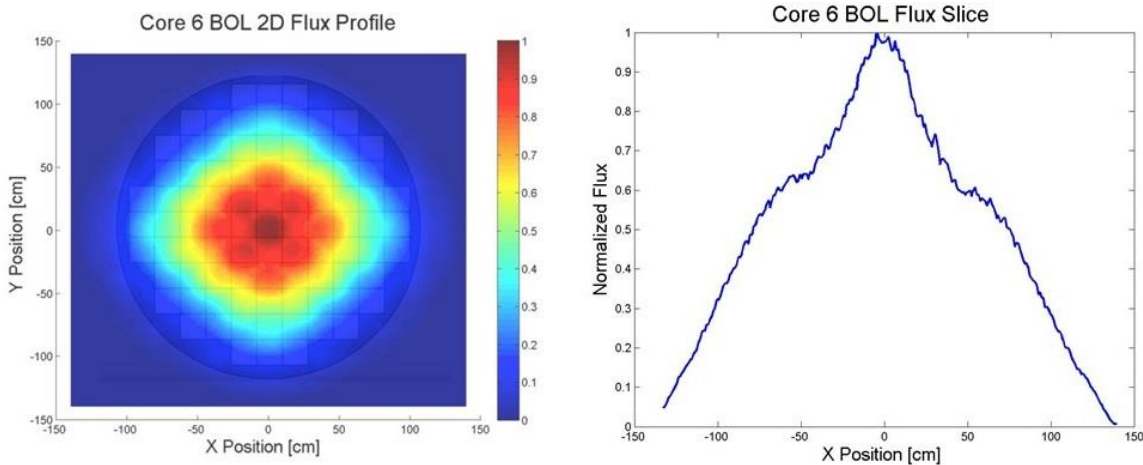


Figure 3.14. Beginning of Life Core 6 Normalized Radial Flux Profile and Flux Slice

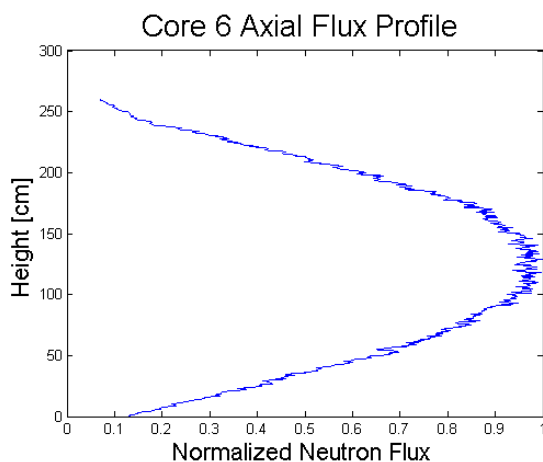


Figure 3.15. Beginning of Life Core 6 Normalized Axial Flux

These flux values were all normalized by dividing all values in the mesh tally result by the largest constituent of that array. The visualizations of the radial flux are in line with expectations. The hottest region is at the very center, and throughout the ‘checkerboard’ region of 2.61% and 3.78% enrichments towards the center of the core, localized hot spots corresponding to those assemblies containing 2.61% enriched  $\text{UO}_2$  are clearly visible. The design goal in such a reactor core layout is to minimize the maximum to average flux ratio.

This ratio for the six cores was calculated by finding the area of the core cross section, dividing that by the total mesh area, then using that fraction to take the correct number of values from an ordered list of the flux. The results for the peak to average flux ratios can be seen in the following table.

Table 3.4. Beginning of Life Peak to Average Flux Ratios

	<b>Maximum to Average Ratio</b>
<b>Core 1</b>	2.7475
<b>Core 2</b>	2.7399
<b>Core 3</b>	2.8462
<b>Core 4</b>	2.6620
<b>Core 5</b>	2.9039
<b>Core 6</b>	3.5966

All cores showed a maximum to average flux ratio of less than 3 except for Core 6, which showed a noticeably higher ratio at nearly 3.6. Since the neutron flux and reactor power are linearly proportional, these numbers give an idea of the reactor's power peaking factor. The power peaking factor for the AP1000 core with both IFBA rods and Pyrex rods included has been previously calculated to be 2.3 [12]. These values were all slightly higher, but once again were reasonably close and were in an acceptable range.

In summary, all values obtained from the beginning of life calculations fell within a reasonable range compared to previous experiments and simulations or the design specifications of the AP1000, whose core the Westinghouse SMR is based upon.

### 3.2. MID-CYCLE RESULTS

Upon completion of the beginning of life portion of this project, the BURN card was used in MCNP to simulate and track the performance of the cores over time and refuel the reactor when it became subcritical. Along the way, the burnup, Q-value, and average number of neutrons per fission of each core were also obtained from the output file. The behavior of  $k_{\text{eff}}$  vs. time for three burn cycles can be seen in the following figure.

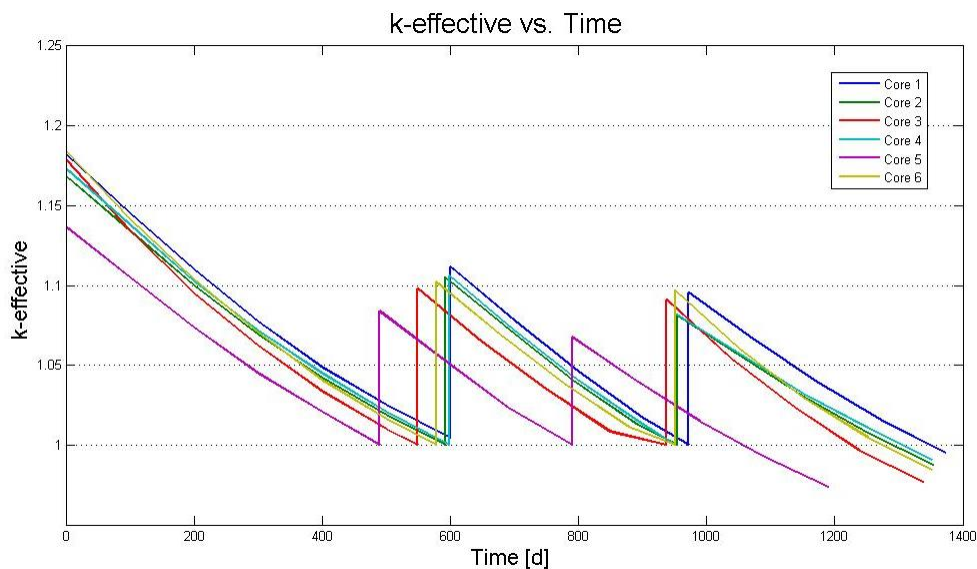


Figure 3.16.  $k_{\text{eff}}$  vs. Time for Three MCNP Burn Cycles

During the first burn cycle, all cores besides Core 5 lasted at least 550 days before going subcritical. Core 5 (which had the smallest starting  $k_{\text{eff}}$ ) dropped below  $k=1$  first after 490 days. The initial estimate for this project was for 18 month (540 day) refueling cycles. Once a value of  $k=1$  was reached, the refueling was performed and the new cycle started.

It is important to note that the refuels happen at different times for different cores, since each core reached  $k=1$  at a different time. Beyond the first cycle, the core is no longer completely fresh and some of the Uranium has been depleted. Because of this, each core becomes subcritical between 300 and 400 days. Ideally, the time before these cores fell subcritical would be about 100 days longer, and the reasons for the shortcoming in this regard will be investigated further.

**3.2.1. Burn Cycle 1.** The numerical results for the pertinent parameters from the first burn cycle can be seen in the following table.

Table 3.5. Burn Cycle 1 Numerical Results (600 days)

	<b><math>k_{eff}</math></b>	<b><math>\nu_{avg}</math></b>	<b><math>Q_{avg}</math> (MeV)</b>	<b>Burnup (GWd/MTU)</b>
<b>Core 1</b>	1.00457	2.667	205.193	20.79
<b>Core 2</b>	0.99832	2.664	205.129	20.79
<b>Core 3</b>	0.98959	2.669	205.213	20.79
<b>Core 4</b>	0.99954	2.666	205.174	20.79
<b>Core 5</b>	0.97857	2.662	205.081	20.79
<b>Core 6</b>	0.99529	2.668	205.200	20.79

The values for average number of neutrons, average Q-value, and burnup were pretty consistent throughout all six cores. For every core, 20.79 GWd of energy were produced per metric ton of Uranium burned. The values for  $\nu_{avg}$  and  $Q_{avg}$  are expected to be around 2.4 and 200 MeV respectively when dealing with fission of  $^{235}\text{U}$ , so these results matched up well with these quantities.

The next thing considered was the composition of the fuel at the end of each cycle. During each refuel, one third of the core was replaced with pristine, pure  $\text{UO}_2$ , however

roughly two thirds remained in the core as a mixture of several isotopes. These included several isotopes of Plutonium and other minor actinides such as Neptunium, Americium, and Curium that contribute to fission and decay heat, among other things. A table containing the amount of certain key transuranics present after the first burn cycle can be seen below. The values are normalized and represent percentages of the total transuranic content in the used fuel.

Table 3.6. Normalized Weight % of Key Actinides Found in Fuel after Burn Cycle 1

	<b>Core 1</b>	<b>Core 2</b>	<b>Core 3</b>	<b>Core 4</b>	<b>Core 5</b>	<b>Core 6</b>
<b>Np-237</b>	0.0309	0.0303	0.0275	0.0305	0.0301	0.0308
<b>Pu-238</b>	0.0084	0.0080	0.0071	0.0082	0.0080	0.0090
<b>Pu-239</b>	0.6674	0.6715	0.6859	0.6697	0.6764	0.6693
<b>Pu-240</b>	0.1471	0.1456	0.1348	0.1466	0.1430	0.1474
<b>Pu-241</b>	0.0785	0.0772	0.0686	0.0778	0.0760	0.0768
<b>Other</b>	0.0678	0.0674	0.0762	0.0673	0.0665	0.0667

One of the biggest contributors to decay heat in commercial nuclear reactors is  $^{238}\text{Pu}$ , which as seen in the table above is accounting for only about 0.8% of the total weight of the transuranic content in most of the cores and even a little less than that in Core 3. Clearly the most dominating presence among all transuranics was  $^{239}\text{Pu}$ . The normalized values for actinide inventory can be seen graphically in the following figure.

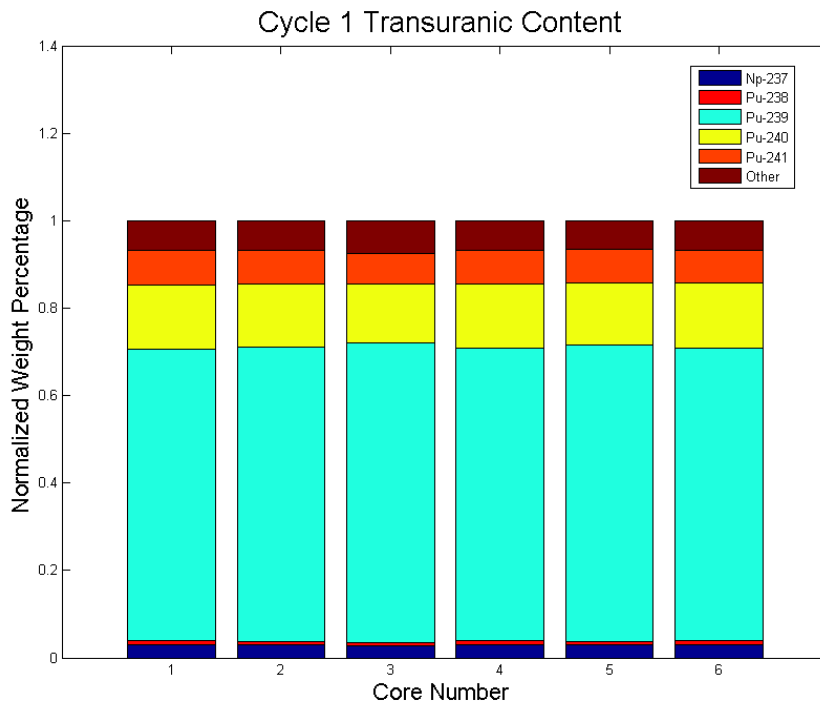


Figure 3.17. Normalized Weight Percentages of Transuranics Present in Fuel After Cycle 1

As previously in the case of the beginning of cycle, a fine mesh was overlaid on the core after each burn cycle. The flux profile was once again obtained using an FMESH4 tally and plotted in MATLAB. The results for the two dimensional flux maps and line profiles can be seen in the following figures.

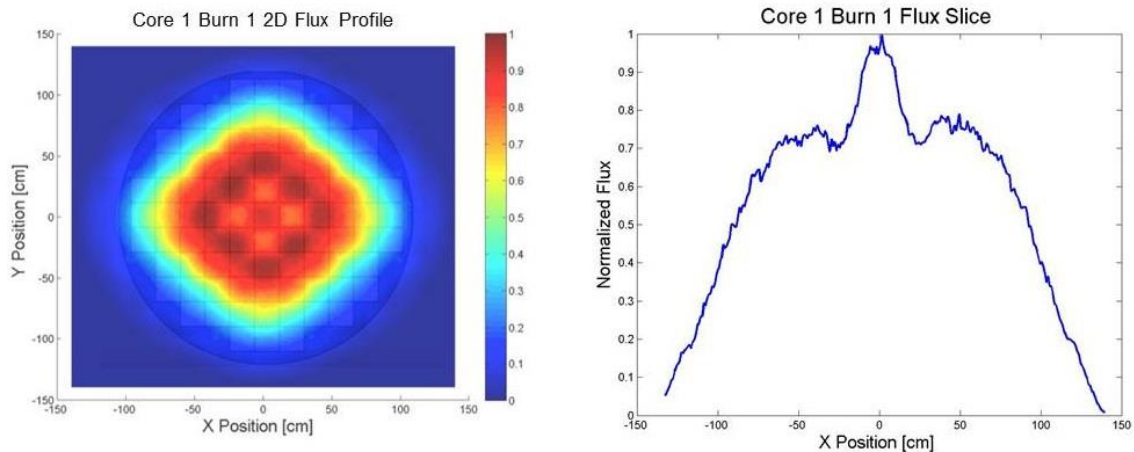


Figure 3.18. Burn Cycle 1 Core 1 Normalized Radial Flux Profile and Flux Slice

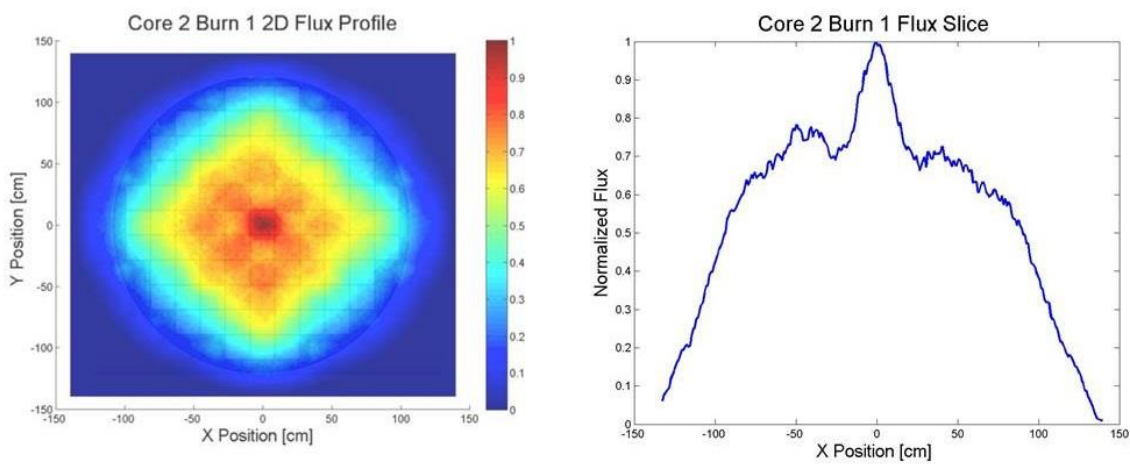


Figure 3.19. Burn Cycle 1 Core 2 Normalized Radial Flux Profile and Flux Slice



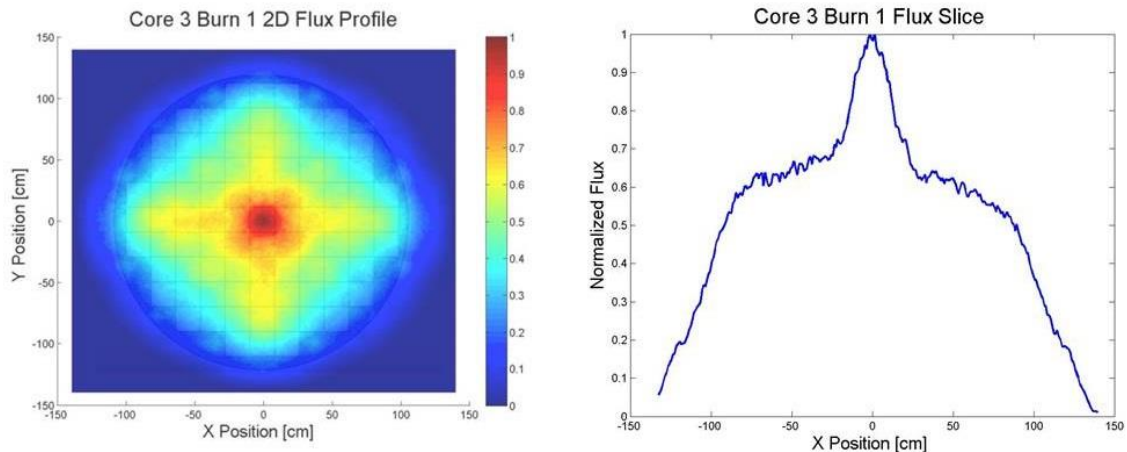


Figure 3.20. Burn Cycle 1 Core 3 Normalized Radial Flux Profile and Flux Slice

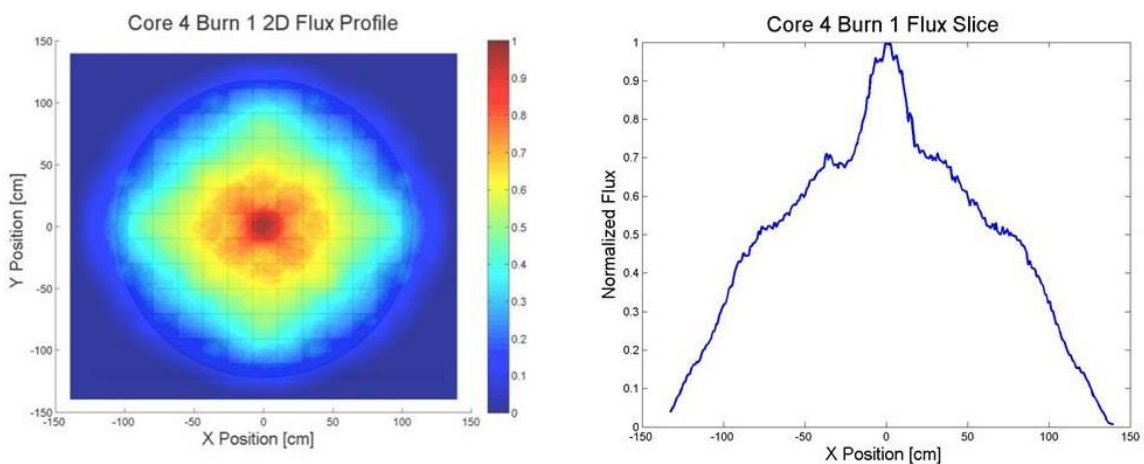


Figure 3.21. Burn Cycle 1 Core 4 Normalized Radial Flux Profile and Flux Slice

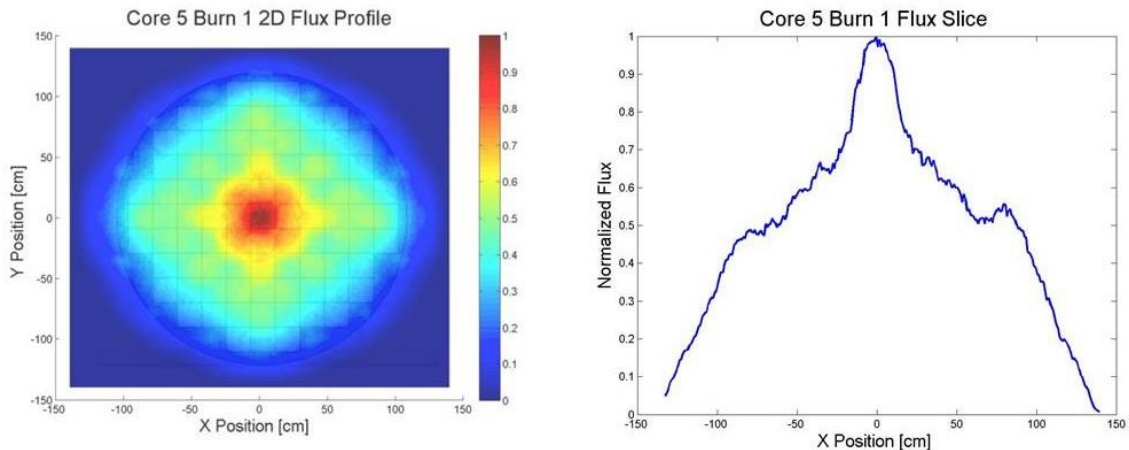


Figure 3.22. Burn Cycle 1 Core 5 Normalized Radial Flux Profile and Flux Slice

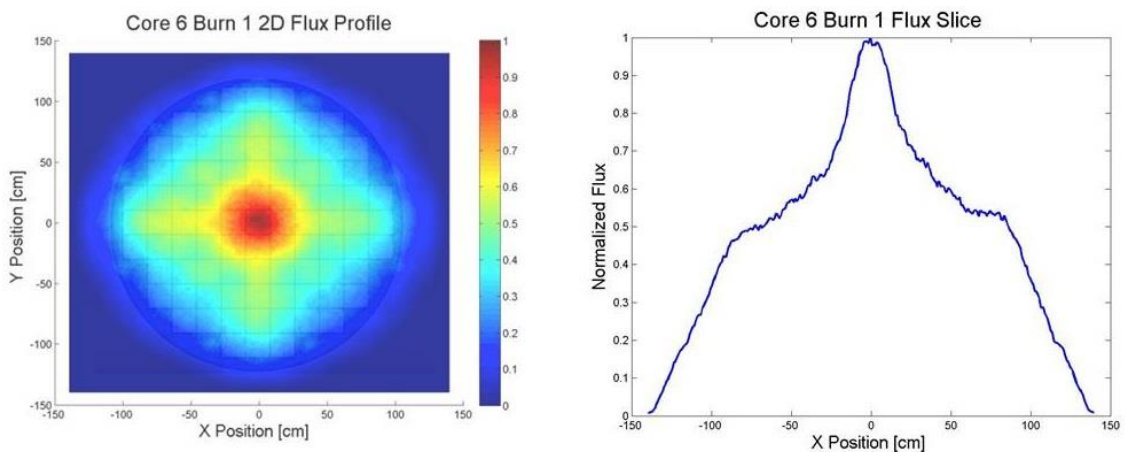


Figure 3.23. Burn Cycle 1 Core 6 Normalized Radial Flux Profile and Flux Slice

These visualizations show very similar characteristics to the previous 2D flux maps. A clearly visible peak occurs in the center of the core, and the neutron flux eventually decreases as distance from the center increases. Based on this data, the maximum to average flux ratios were calculated. The results from these calculations are found in the following table.

Table 3.7. Burn Cycle 1 Peak to Average Flux Ratios

	<b>Maximum to Average Ratio</b>
<b>Core 1</b>	2.7262
<b>Core 2</b>	2.7804
<b>Core 3</b>	3.0419
<b>Core 4</b>	3.1321
<b>Core 5</b>	3.1426
<b>Core 6</b>	3.3475

These values for maximum to average flux ratio which give an estimate for the reactor's power peaking factor are on average slightly higher after the first burn cycle than during the beginning of cycle, but not by enough to present any worrisome trouble.

**3.2.2. Burn Cycle 2.** For a second time, roughly one third of each of the six cores was refueled in accordance with Fig. 2.16. The pertinent neutronics information can be found in the table below.

Table 3.8. Burn Cycle 2 Numerical Results (400 days)

	<b>k<sub>eff</sub></b>	<b>v<sub>avg</sub></b>	<b>Q<sub>avg</sub> (MeV)</b>	<b>Burnup (GWd/MTU)</b>
<b>Core 1</b>	0.99331	2.681	205.002	13.88
<b>Core 2</b>	0.98886	2.680	204.977	13.88
<b>Core 3</b>	0.98501	2.683	205.487	13.88
<b>Core 4</b>	0.98910	2.681	205.460	13.88
<b>Core 5</b>	0.97445	2.676	205.359	13.88
<b>Core 6</b>	0.98893	2.682	205.472	13.88

After the first refuel, the cores lasted between 300-400 days, as opposed to the fresh core which lasted between 500-600 days. It therefore makes sense that the 13.88 GWd/MTU of

burnup achieved in the second burn cycle was less than that achieved in the first burn cycle. The difference was roughly 7 GWd/MTU. Once again the average Q-value was about 205 MeV and the number of neutrons released per fission was roughly 2.68 in each case.

Next, the used fuel composition after the cycle was examined. The composition of some of the key actinides present can be seen in the following table.

Table 3.9. Normalized Weight % of Key Actinides Found in Fuel After Burn Cycle 2

	<b>Core 1</b>	<b>Core 2</b>	<b>Core 3</b>	<b>Core 4</b>	<b>Core 5</b>	<b>Core 6</b>
<b>Np-237</b>	0.0556	0.0548	0.0525	0.0549	0.0529	0.0531
<b>Pu-238</b>	0.0186	0.0178	0.0169	0.0182	0.0171	0.0177
<b>Pu-239</b>	0.8342	0.8349	0.8389	0.8278	0.8284	0.8304
<b>Am-241</b>	0.0026	0.0028	0.0025	0.0027	0.0027	0.0025
<b>Am-243</b>	0.0084	0.0085	0.0083	0.0079	0.0067	0.0086
<b>Cm-242</b>	0.0009	0.0009	0.0007	0.0099	0.0078	0.0080
<b>Other</b>	0.0797	0.0803	0.0802	0.0797	0.0844	0.0796

After Cycle 2, isotopes of Americium and Curium began to become significant, while  $^{239}\text{Pu}$  remained the most abundant transuranic isotope. The transuranic content for the second refuel cycle was again made into a stacked bar graph to compare the impact of each isotope. This can be seen in the following figure.

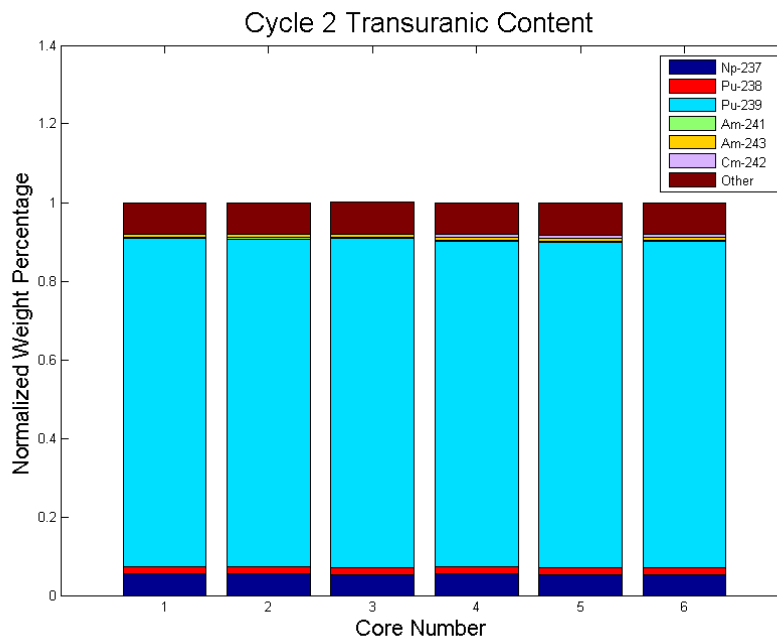


Figure 3.24. Normalized Weight Percentages of Transuranics Present in Fuel After Cycle 2

The next calculations performed were the two-dimensional core neutron flux profiles. These can be seen in the following figures.

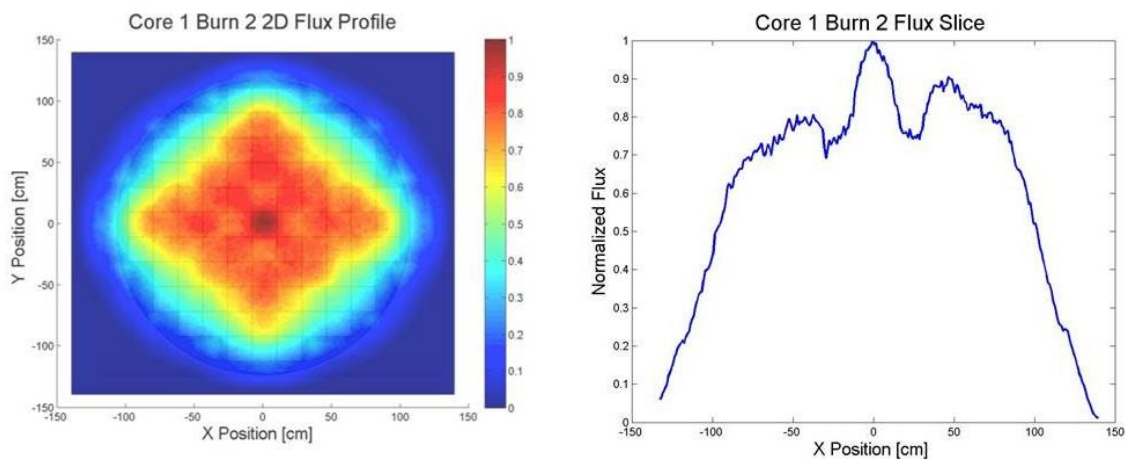


Figure 3.25. Burn Cycle 2 Core 1 Normalized Radial Flux Profile and Flux Slice

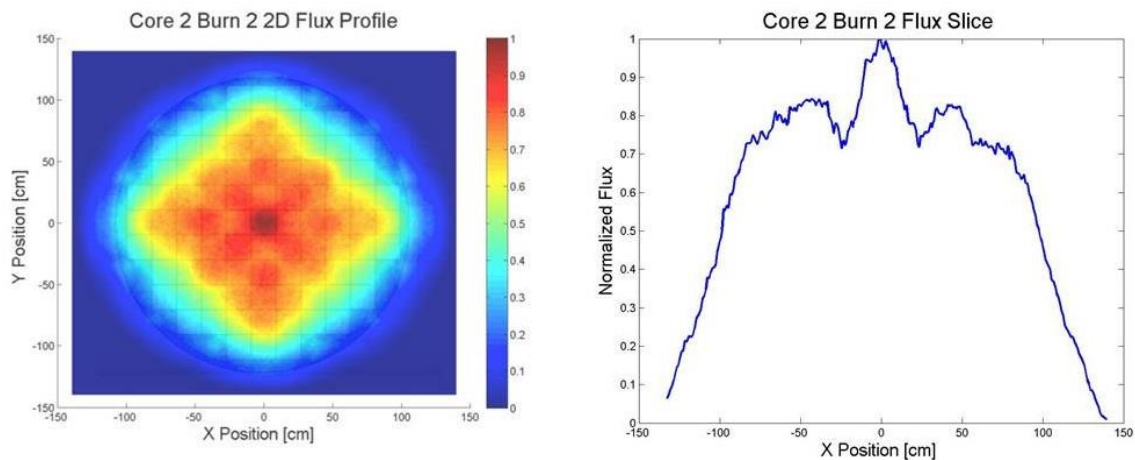


Figure 3.26. Burn Cycle 2 Core 2 Normalized Radial Flux Profile and Flux Slice

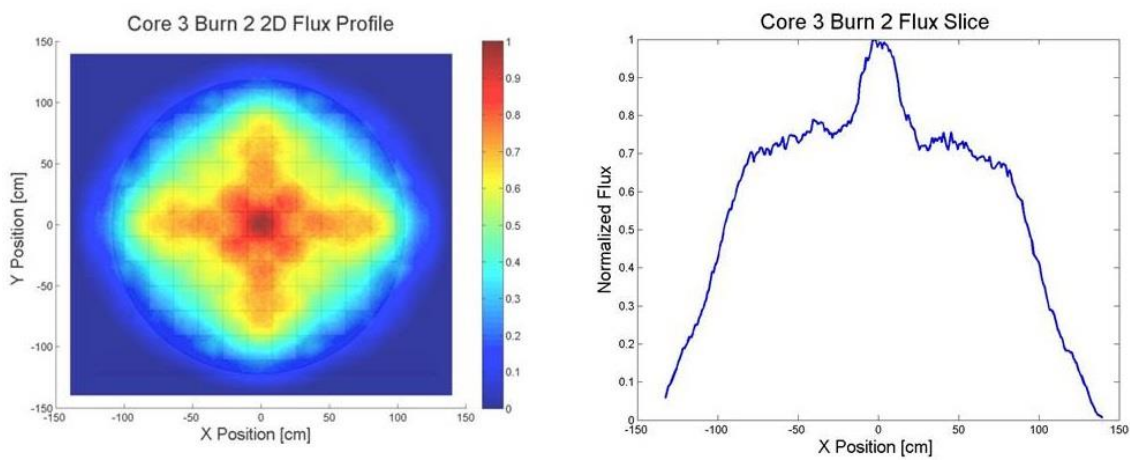


Figure 3.27. Burn Cycle 2 Core 3 Normalized Radial Flux Profile and Flux Slice

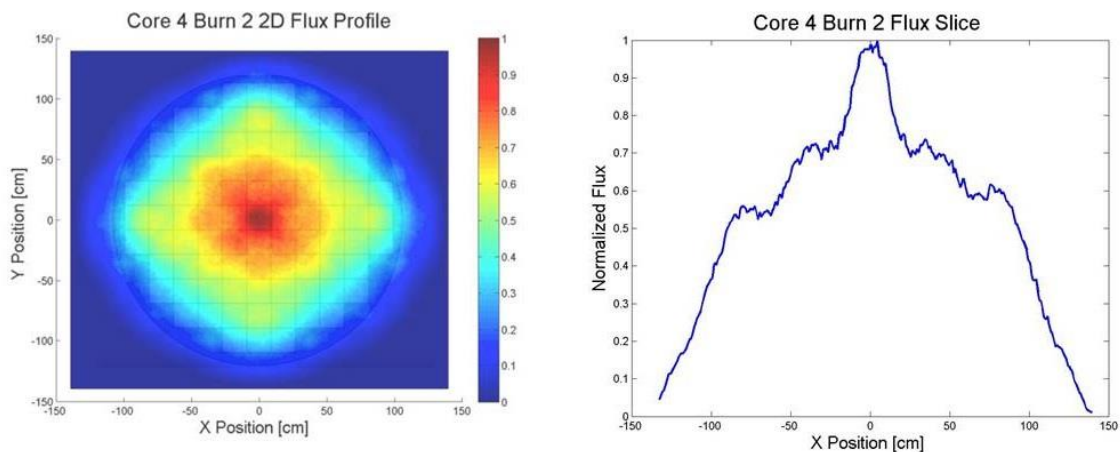


Figure 3.28. Burn Cycle 2 Core 4 Normalized Radial Flux Profile and Flux Slice

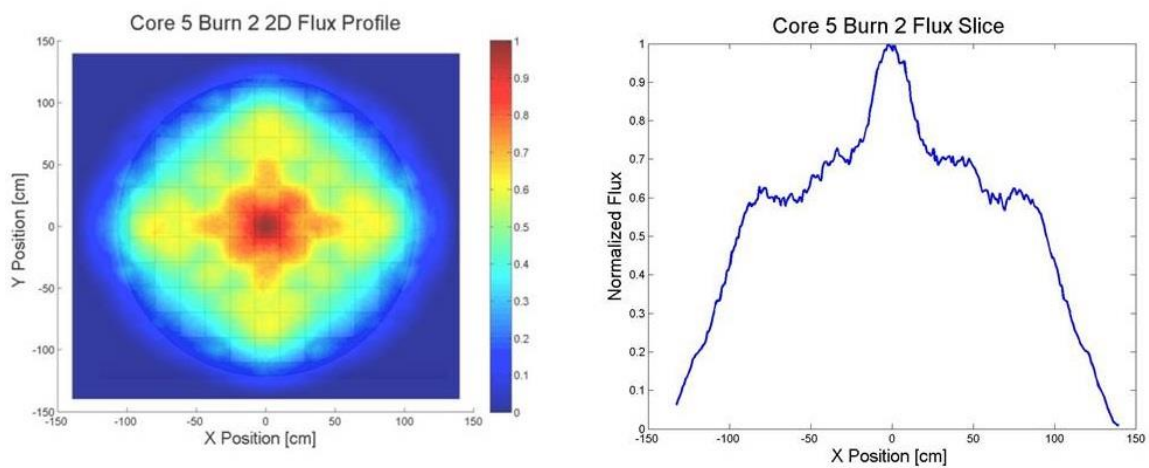


Figure 3.29. Burn Cycle 2 Core 5 Normalized Radial Flux Profile and Flux Slice

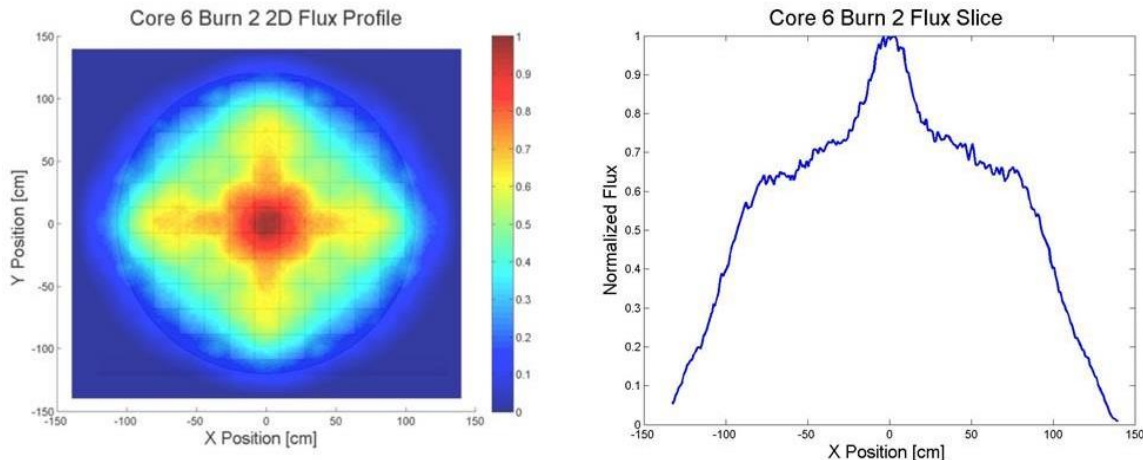


Figure 3.30. Burn Cycle 2 Core 6 Normalized Radial Flux Profile and Flux Slice

One pattern that began to emerge was that while Cores 1-4 had a relatively spread out flux density, Cores 5 and 6 appeared to have a higher flux density near the center of the core. This was something to keep in mind when deciding which of these cores shows the best overall performance, since a flat flux profile is desirable. The maximum to average ratios were calculated for this cycle as well, and these results can be found in the following table.

Table 3.10. Burn Cycle 2 Peak to Average Flux Ratios

	<b>Maximum to Average Ratio</b>
<b>Core 1</b>	2.3713
<b>Core 2</b>	2.4768
<b>Core 3</b>	2.6909
<b>Core 4</b>	2.8959
<b>Core 5</b>	2.8231
<b>Core 6</b>	2.8864



400 days after the first refuel, the maximum to average flux ratios have fallen compared to where they were after 600 days and at the beginning of the cycle. All six cores show a value under 3. It is the goal to lower the peak to average ratio, so a decrease in this value was a positive outcome.

**3.2.3. Burn Cycle 3.** For a third and final time, a burn cycle was carried out in MCNP. 36 assemblies were replaced in each core in accordance with Fig. 2.16. The neutronics data from this run can be seen in the following table.

Table 3.11. Burn Cycle 3 Numerical Results (400 days)

	$k_{\text{eff}}$	$v_{\text{avg}}$	$Q_{\text{avg}}$ (MeV)	Burnup (GWd/MTU)
<b>Core 1</b>	0.99543	2.682	205.443	13.88
<b>Core 2</b>	0.98764	2.680	205.406	13.88
<b>Core 3</b>	0.97713	2.691	205.609	13.88
<b>Core 4</b>	0.99056	2.681	205.422	13.88
<b>Core 5</b>	0.95575	2.673	205.599	13.88
<b>Core 6</b>	0.98428	2.689	205.573	13.88

As was the case in the second burn cycle, all six cores became subcritical before the 400 day time break. Overall the  $k_{\text{eff}}$  values were slightly lower on average at the end of this cycle than at the end of the previous cycle, which makes sense because there was less fresh fuel and therefore more depleted fuel present at the beginning of the third cycle than at the beginning of the second cycle. The same level of burnup was achieved in this cycle, 13.88 GWd/MTU.

After the burn cycle was complete, the composition of the fuel 400 days after the beginning of the cycle was analyzed. The normalized weight fractions of some key actinides in the fuel can be seen in the following table.

Table 3.12. Normalized Weight % of Key Actinides Found in Fuel After Burn Cycle 3

	<b>Core 1</b>	<b>Core 2</b>	<b>Core 3</b>	<b>Core 4</b>	<b>Core 5</b>	<b>Core 6</b>
<b>Np-237</b>	0.0542	0.0537	0.0546	0.0538	0.511	0.0544
<b>Pu-238</b>	0.0186	0.0182	0.0197	0.0184	0.0168	0.0197
<b>Pu-239</b>	0.8291	0.8308	0.8291	0.8314	0.8224	0.8275
<b>Am-241</b>	0.0024	0.0025	0.0026	0.0024	0.0022	0.0025
<b>Am-243</b>	0.0141	0.0138	0.0144	0.0140	0.0118	0.0146
<b>Cm-242</b>	0.0010	0.0010	0.0011	0.0010	0.0010	0.0011
<b>Other</b>	0.0806	0.0799	0.0786	0.0789	0.0948	0.0802

Once again Americium and Curium were present in the used fuel. The  $^{238}\text{Pu}$  content has risen by roughly 1% since Cycle 1. These transuranic compositions were once again plotted and can be seen in the figure below.

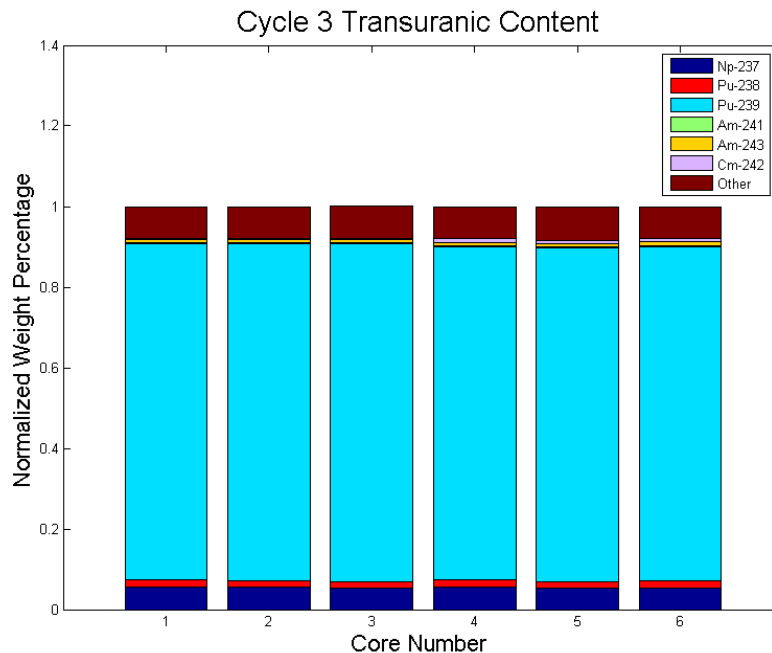


Figure 3.31. Normalized Weight Percentages of Transuranics Present in Fuel After Cycle 3

Next, the two-dimensional radial flux profiles were found using an FMESH4 tally for the fourth and final time. The resulting flux maps can be seen in the figures below.

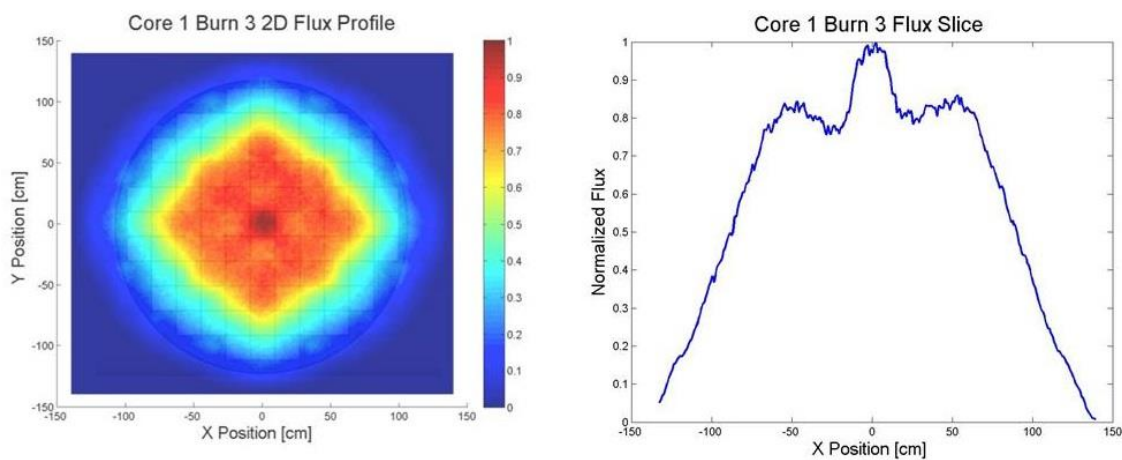


Figure 3.32. Burn Cycle 3 Core 1 Normalized Radial Flux Profile and Flux Slice

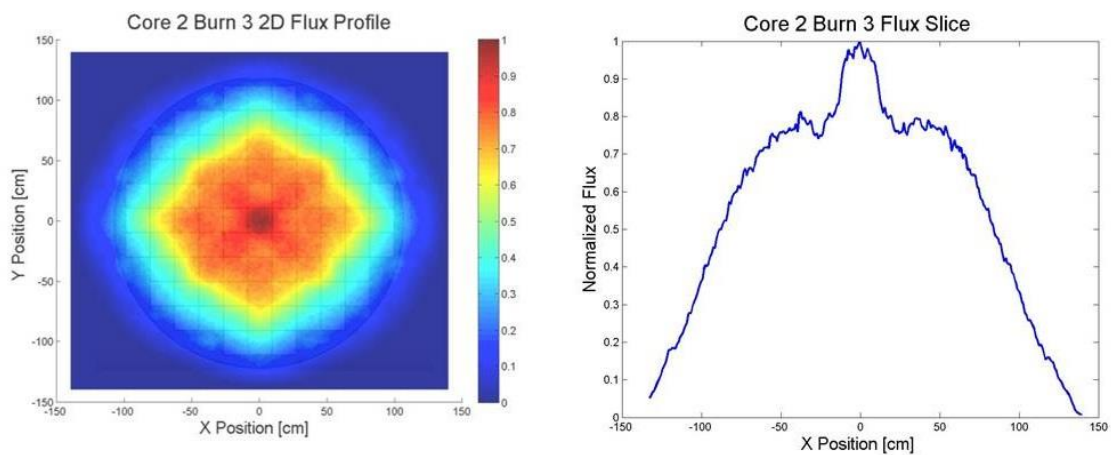


Figure 3.33. Burn Cycle 3 Core 2 Normalized Radial Flux Profile and Flux Slice

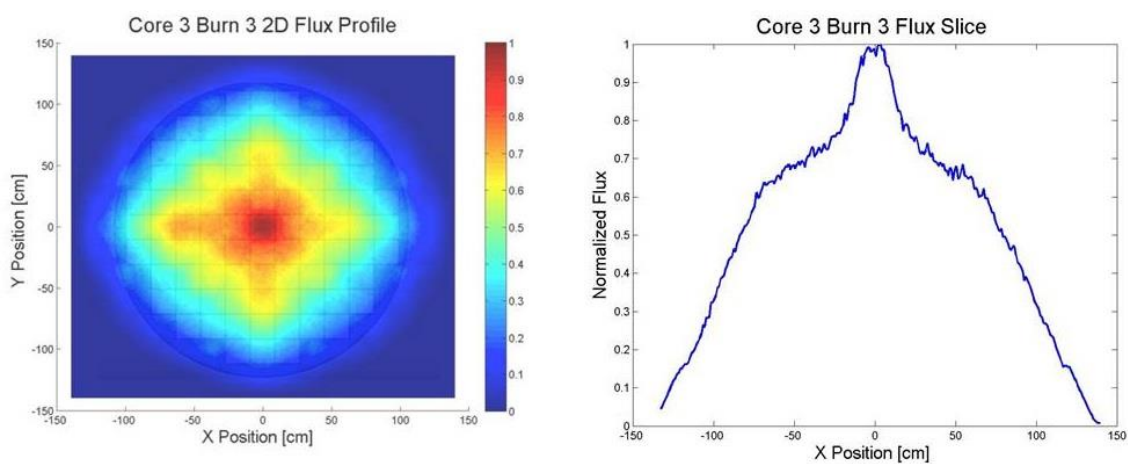


Figure 3.34. Burn Cycle 3 Core 3 Normalized Radial Flux Profile and Flux Slice

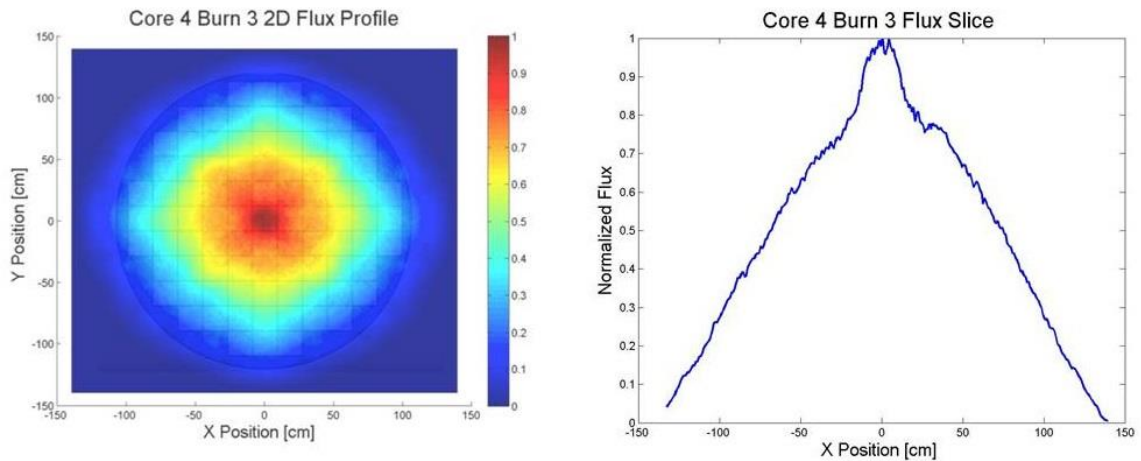


Figure 3.35. Burn Cycle 3 Core 4 Normalized Radial Flux Profile and Flux Slice

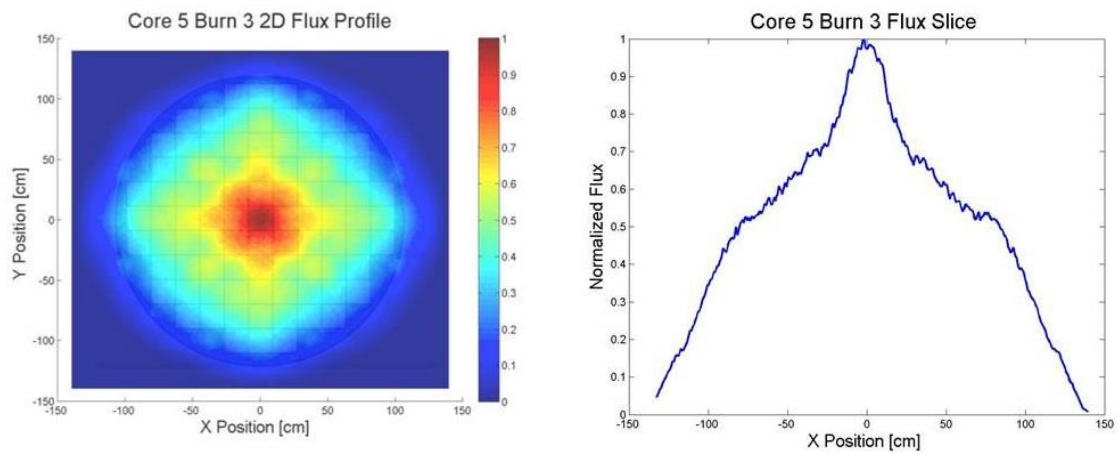


Figure 3.36. Burn Cycle 3 Core 5 Normalized Radial Flux Profile and Flux Slice

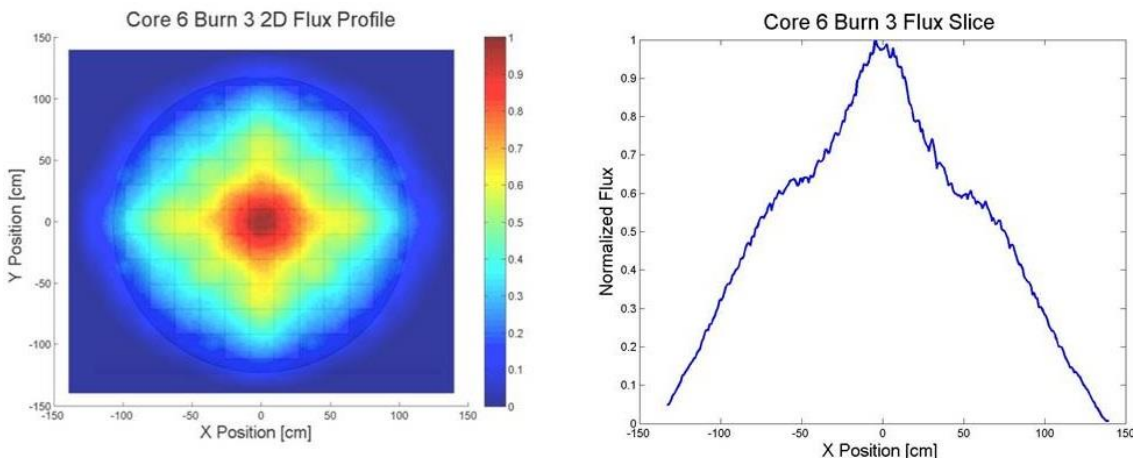


Figure 3.37. Burn Cycle 3 Core 6 Normalized Radial Flux Profile and Flux Slice

The pattern in the flux maps observed after the second cycle continued to be visible here at the end of the third cycle. Both Core 5 and Core 6 have a higher power density towards the middle of the core and a rather abrupt drop off. In these two cores, at distances of 50 cm from the center, the flux values that have dropped to merely 55% or less, whereas the rest of the cores have all inner assemblies at about 65% of the maximum or higher at that range. The maximum to average flux ratios were calculated and can be found in the following table.

Table 3.13. Burn Cycle 3 Peak to Average Flux Ratios

	<b>Maximum to Average Ratio</b>
<b>Core 1</b>	2.6286
<b>Core 2</b>	2.7414
<b>Core 3</b>	3.0853
<b>Core 4</b>	3.2331
<b>Core 5</b>	3.1273
<b>Core 6</b>	3.3040

Not only did Cores 5 and 6 have the least spread-out flux density, but they also had the third highest and highest peak to average flux ratios respectively. Overall the average peak to average ratio for the third cycle was higher than the second cycle and a bit lower than the first burn cycle.

#### 4. CONCLUSIONS

Six variations for the Westinghouse SMR core have been proposed in this research. Based on the simulations and subsequent calculations performed, it can be concluded that all six core configurations are at least viable in that they produce results within the realm of expectation for a PWR-type reactor core such as the AP1000. However some of these cores show better or worse performance than others. The clear outlier among the group is Core 5, whose high number of IFBA rods decreases the initial excess reactivity significantly compared to the other cores. For this reason, the fuel was depleted and the reactor became subcritical faster, and a higher concentration of borated water was required to reduce the reactor state to  $k_{\text{eff}}=1$ . Furthermore, the flux profiles of both Core 5 and Core 6 were shown to be less than ideal, with most of the flux density found closer to the center as opposed to a more spread out flux density that would be more desirable. This was particularly noticeable when examining the results from the burn cycles. Cores 5 and 6 had the lowest delayed neutron fraction at a value between 0.0068 and 0.0069. With the AP1000 design goal of 0.0075 in mind, Core 4 came the closest to this with a delayed neutron fraction of 0.00726. Core 6 also had a total reactivity coefficient roughly 1 pcm/K smaller in magnitude than the rest of the cores. In terms of production of troublesome actinides, none of the cores had a clear advantage or disadvantage. The levels of  $^{238}\text{Pu}$ , a key contributor to decay heat, were fairly even after each burn cycle for all six cores. One issue that persisted throughout the burn cycles was that the reactors all became subcritical earlier than the 18-months design goal. A likely explanation for this is that as a simplification for this project, during the refueling process each assembly was directly replaced in its spot in the core with no shuffling pattern. In reality, an assembly shuffling



pattern would be developed in order to optimize and lengthen the lifetime of the fuel. It is therefore suggested that Cores 1-4 be investigated for further study and optimization, while several instances of poorer performance relative to the other cores indicate that Cores 5 and 6 should not be considered as part of the design for the Westinghouse SMR core.

APPENDIX A.

BEGINNING OF LIFE NEUTRONICS DATA

Table A1. Criticality and Delayed Neutron Fraction Calculations

	$k_{\text{eff}}$	$\sigma_k$	$\beta_{\text{eff}}$	$\sigma_\beta$
<b>Core 1</b>	1.18257	0.00015	0.006943	$1.25 \times 10^{-6}$
<b>Core 2</b>	1.16806	0.00014	0.007037	$1.20 \times 10^{-6}$
<b>Core 3</b>	1.17902	0.00014	0.007092	$1.19 \times 10^{-6}$
<b>Core 4</b>	1.17229	0.00014	0.007260	$1.23 \times 10^{-6}$
<b>Core 5</b>	1.13702	0.00015	0.006860	$1.24 \times 10^{-6}$
<b>Core 6</b>	1.18451	0.00015	0.006855	$1.19 \times 10^{-6}$

Table A2. Excess Reactivity and Shutdown Margin Calculations

	$P_{\text{ex}}$	$\sigma_p$	<b>SDM</b>	$\sigma_{\text{SDM}}$
<b>Core 1</b>	0.15438	0.00003	0.03156	0.00003
<b>Core 2</b>	0.14388	0.00002	0.04576	0.00004
<b>Core 3</b>	0.15184	0.00003	0.03633	0.00003
<b>Core 4</b>	0.14697	0.00002	0.04083	0.00004
<b>Core 5</b>	0.12050	0.00002	0.07302	0.00007
<b>Core 5</b>	0.15577	0.00003	0.03146	0.00003

APPENDIX B.

SAMPLE MCNP INPUT FILE

## Kirby Compton SMR Test Core 1

```

c -----
c Universe Codes
c Various Rods
c 2.61 fuel rods: 11,51,52,53,54,55
c 3.78 fuel rods: 12,70,75
c 4.95 fuel rods: 14,56,57,58,90,81,82
c 3.78 IFBA rods: 13,71,76
c 4.95 IFBA rods: 15,59,60,61,83,84,85
c instrumentation tube: 17
c pyrex rod: 18,72,77,86,87,88
c black control rod: 19
c guide tube with pyrex: 16,73,78,91,92,93
c guide tube with control rod: 90
c Rod Assemblies
c 2.61 0I 0P: 20,62,63,64,65,66
c 3.78 88I 24P: 21
c 3.78 44I 24P: 22,74,79
c 3.78 28I 24P: 23
c 4.95 72I 24P: 24
c 4.95 88I 12P: 25,40,42,44
c 4.95 88I 9P: 26,46,48,50
c 4.95 112I 0P: 27,67,68,69
c 4.95 28I 0P:28
c Core configuration: 29
c -----
c 2.61 fuel rods 1
1      12 -10.4 -1 -2 u=11 imp:n=1 vol=128.6055156
2      2 -1e-4 (1:2) -3 u=11 imp:n=1
3      3 -6.5 3 -4 u=11 imp:n=1
4      4 -.67 4 u=11 imp:n=1
c -----
c 2.61 fuel rods 2
1001  22 -10.4 -1 -2 u=51 imp:n=1 vol=128.6055156
1002  2 -1e-4 (1:2) -3 u=51 imp:n=1
1003  3 -6.5 3 -4 u=51 imp:n=1
1004  4 -.67 4 u=51 imp:n=1
c -----
c 2.61 fuel rods 3
2001  32 -10.4 -1 -2 u=52 imp:n=1 vol=128.6055156
2002  2 -1e-4 (1:2) -3 u=52 imp:n=1
2003  3 -6.5 3 -4 u=52 imp:n=1
2004  4 -.67 4 u=52 imp:n=1
c -----
c 2.61 fuel rods 4
3001  42 -10.4 -1 -2 u=53 imp:n=1 vol=128.6055156
3002  2 -1e-4 (1:2) -3 u=53 imp:n=1

```

```

3003  3 -6.5 3 -4 u=53 imp:n=1
3004  4 -.67 4 u=53 imp:n=1
c -----
c 2.61 fuel rods 5
4001  52 -10.4 -1 -2 u=54 imp:n=1 vol=128.6055156
4002  2 -1e-4 (1:2) -3 u=54 imp:n=1
4003  3 -6.5 3 -4 u=54 imp:n=1
4004  4 -.67 4 u=54 imp:n=1
c -----
c 2.61 fuel rods 6
5001  62 -10.4 -1 -2 u=55 imp:n=1 vol=128.6055156
5002  2 -1e-4 (1:2) -3 u=55 imp:n=1
5003  3 -6.5 3 -4 u=55 imp:n=1
5004  4 -.67 4 u=55 imp:n=1
c -----
c 3.78 fuel rods 1
5      11 -10.4 -1 -2 u=12 imp:n=1 vol=128.6055156
6      2 -1e-4 (1:2) -3 u=12 imp:n=1
7      3 -6.5 3 -4 u=12 imp:n=1
8      4 -.67 4 u=12 imp:n=1
c -----
c 3.78 fuel rods 2
1005  21 -10.4 -1 -2 u=70 imp:n=1 vol=128.6055156
1006  2 -1e-4 (1:2) -3 u=70 imp:n=1
1007  3 -6.5 3 -4 u=70 imp:n=1
1008  4 -.67 4 u=70 imp:n=1
c -----
c 3.78 fuel rods 3
2005  41 -10.4 -1 -2 u=75 imp:n=1 vol=128.6055156
2006  2 -1e-4 (1:2) -3 u=75 imp:n=1
2007  3 -6.5 3 -4 u=75 imp:n=1
2008  4 -.67 4 u=75 imp:n=1
c -----
c 4.95 fuel rods 1
9      10 -10.4 -1 -2 u=14 imp:n=1 vol=128.6055156
10     2 -1e-4 (1:2) -3 u=14 imp:n=1
11     3 -6.5 3 -4 u=14 imp:n=1
12     4 -.67 4 u=14 imp:n=1
c -----
c 4.95 fuel rods 2
1009  20 -10.4 -1 -2 u=56 imp:n=1 vol=128.6055156
1010  2 -1e-4 (1:2) -3 u=56 imp:n=1
1011  3 -6.5 3 -4 u=56 imp:n=1
1012  4 -.67 4 u=56 imp:n=1
c -----
c 4.95 fuel rods 3
2009  30 -10.4 -1 -2 u=57 imp:n=1 vol=128.6055156

```

```

2010  2 -1e-4 (1:2) -3 u=57 imp:n=1
2011  3 -6.5 3 -4 u=57 imp:n=1
2012  4 -.67 4 u=57 imp:n=1
c -----
c 4.95 fuel rods 4
3009  40 -10.4 -1 -2 u=58 imp:n=1 vol=128.6055156
3010  2 -1e-4 (1:2) -3 u=58 imp:n=1
3011  3 -6.5 3 -4 u=58 imp:n=1
3012  4 -.67 4 u=58 imp:n=1
c -----
c 4.95 fuel rods 5
4009  90 -10.4 -1 -2 u=80 imp:n=1 vol=128.6055156
4010  2 -1e-4 (1:2) -3 u=80 imp:n=1
4011  3 -6.5 3 -4 u=80 imp:n=1
4012  4 -.67 4 u=80 imp:n=1
c -----
c 4.95 fuel rods 6
5009  100 -10.4 -1 -2 u=81 imp:n=1 vol=128.6055156
5010  2 -1e-4 (1:2) -3 u=81 imp:n=1
5011  3 -6.5 3 -4 u=81 imp:n=1
5012  4 -.67 4 u=81 imp:n=1
c -----
c 4.95 fuel rods 7
6009  110 -10.4 -1 -2 u=82 imp:n=1 vol=128.6055156
6010  2 -1e-4 (1:2) -3 u=82 imp:n=1
6011  3 -6.5 3 -4 u=82 imp:n=1
6012  4 -.67 4 u=82 imp:n=1
c -----
c 3.78 IFBA fuel rods 1
13   61 -10.4 -1 -2 u=13 imp:n=1 vol=128.6055156
14   7 -6.08 1 -2 -5 u=13 imp:n=1 vol=1.612592598
15   2 -1e-4 (2:5) -3 u=13 imp:n=1
16   3 -6.5 3 -4 u=13 imp:n=1
17   4 -.67 4 u=13 imp:n=1
c -----
c 3.78 IFBA fuel rods 2
1013  31 -10.4 -1 -2 u=71 imp:n=1 vol=128.6055156
1014  57 -6.08 1 -2 -5 u=71 imp:n=1 vol=1.612592598
1015  2 -1e-4 (2:5) -3 u=71 imp:n=1
1016  3 -6.5 3 -4 u=71 imp:n=1
1017  4 -.67 4 u=71 imp:n=1
c -----
c 3.78 IFBA fuel rods 3
2013  51 -10.4 -1 -2 u=76 imp:n=1 vol=128.6055156
2014  67 -6.08 1 -2 -5 u=76 imp:n=1 vol=1.612592598
2015  2 -1e-4 (2:5) -3 u=76 imp:n=1
2016  3 -6.5 3 -4 u=76 imp:n=1

```

```

2017 4 -.67 4 u=76 imp:n=1
c -----
c 4.95 IFBA fuel rods 1
18 50 -10.4 -1 -2 u=15 imp:n=1 vol=128.6055156
19 17 -6.08 1 -2 -5 u=15 imp:n=1 vol=1.612592598
20 2 -1e-4 (2:5) -3 u=15 imp:n=1
21 3 -6.5 3 -4 u=15 imp:n=1
22 4 -.67 4 u=15 imp:n=1
c -----
c 4.95 IFBA fuel rods 2
1018 60 -10.4 -1 -2 u=59 imp:n=1 vol=128.6055156
1019 27 -6.08 1 -2 -5 u=59 imp:n=1 vol=1.612592598
1020 2 -1e-4 (2:5) -3 u=59 imp:n=1
1021 3 -6.5 3 -4 u=59 imp:n=1
1022 4 -.67 4 u=59 imp:n=1
c -----
c 4.95 IFBA fuel rods 3
2018 70 -10.4 -1 -2 u=60 imp:n=1 vol=128.6055156
2019 37 -6.08 1 -2 -5 u=60 imp:n=1 vol=1.612592598
2020 2 -1e-4 (2:5) -3 u=60 imp:n=1
2021 3 -6.5 3 -4 u=60 imp:n=1
2022 4 -.67 4 u=60 imp:n=1
c -----
c 4.95 IFBA fuel rods 4
3018 80 -10.4 -1 -2 u=61 imp:n=1 vol=128.6055156
3019 47 -6.08 1 -2 -5 u=61 imp:n=1 vol=1.612592598
3020 2 -1e-4 (2:5) -3 u=61 imp:n=1
3021 3 -6.5 3 -4 u=61 imp:n=1
3022 4 -.67 4 u=61 imp:n=1
c -----
c 4.95 IFBA fuel rods 5
4018 120 -10.4 -1 -2 u=83 imp:n=1 vol=128.6055156
4019 77 -6.08 1 -2 -5 u=83 imp:n=1 vol=1.612592598
4020 2 -1e-4 (2:5) -3 u=83 imp:n=1
4021 3 -6.5 3 -4 u=83 imp:n=1
4022 4 -.67 4 u=83 imp:n=1
c -----
c 4.95 IFBA fuel rods 6
5018 130 -10.4 -1 -2 u=84 imp:n=1 vol=128.6055156
5019 87 -6.08 1 -2 -5 u=84 imp:n=1 vol=1.612592598
5020 2 -1e-4 (2:5) -3 u=84 imp:n=1
5021 3 -6.5 3 -4 u=84 imp:n=1
5022 4 -.67 4 u=84 imp:n=1
c -----
c 4.95 IFBA fuel rods 7
6018 140 -10.4 -1 -2 u=85 imp:n=1 vol=128.6055156
6019 97 -6.08 1 -2 -5 u=85 imp:n=1 vol=1.612592598

```



```

6020 2 -1e-4 (2:5) -3 u=85 imp:n=1
6021 3 -6.5 3 -4 u=85 imp:n=1
6022 4 -.67 4 u=85 imp:n=1
c -----
c Instrumentation Tube
23 4 -.67 -6 u=17 imp:n=1
24 5 -8 6 -7 u=17 imp:n=1
25 4 -.67 7 u=17 imp:n=1
c -----
c Pyrex Rods 1
26 2 -1e-4 (-8:2) -12 u=18 imp:n=1
27 5 -8 8 -9 -2 u=18 imp:n=1
28 2 -1e-4 9 -10 -2 u=18 imp:n=1
29 6 -2.23 10 -11 -2 u=18 imp:n=1 vol=95.24213138
30 2 -1e-4 11 -12 -2 u=18 imp:n=1
31 5 -8 12 -13 u=18 imp:n=1
32 4 -.67 13 u=18 imp:n=1
c -----
c Pyrex Rods 2
1026 2 -1e-4 (-8:2) -12 u=72 imp:n=1
1027 5 -8 8 -9 -2 u=72 imp:n=1
1028 2 -1e-4 9 -10 -2 u=72 imp:n=1
1029 16 -2.23 10 -11 -2 u=72 imp:n=1 vol=95.24213138
1030 2 -1e-4 11 -12 -2 u=72 imp:n=1
1031 5 -8 12 -13 u=72 imp:n=1
1032 4 -.67 13 u=72 imp:n=1
c -----
c Pyrex Rods 3
2026 2 -1e-4 (-8:2) -12 u=77 imp:n=1
2027 5 -8 8 -9 -2 u=77 imp:n=1
2028 2 -1e-4 9 -10 -2 u=77 imp:n=1
2029 26 -2.23 10 -11 -2 u=77 imp:n=1 vol=95.24213138
2030 2 -1e-4 11 -12 -2 u=77 imp:n=1
2031 5 -8 12 -13 u=77 imp:n=1
2032 4 -.67 13 u=77 imp:n=1
c -----
c Pyrex Rods 4
3026 2 -1e-4 (-8:2) -12 u=86 imp:n=1
3027 5 -8 8 -9 -2 u=86 imp:n=1
3028 2 -1e-4 9 -10 -2 u=86 imp:n=1
3029 36 -2.23 10 -11 -2 u=86 imp:n=1 vol=95.24213138
3030 2 -1e-4 11 -12 -2 u=86 imp:n=1
3031 5 -8 12 -13 u=86 imp:n=1
3032 4 -.67 13 u=86 imp:n=1
c -----
c Pyrex Rods 5
4026 2 -1e-4 (-8:2) -12 u=87 imp:n=1

```

```

4027 5 -8 8 -9 -2 u=87 imp:n=1
4028 2 -1e-4 9 -10 -2 u=87 imp:n=1
4029 46 -2.23 10 -11 -2 u=87 imp:n=1 vol=95.24213138
4030 2 -1e-4 11 -12 -2 u=87 imp:n=1
4031 5 -8 12 -13 u=87 imp:n=1
4032 4 -.67 13 u=87 imp:n=1
c -----
c Pyrex Rods 6
5026 2 -1e-4 (-8:2) -12 u=88 imp:n=1
5027 5 -8 8 -9 -2 u=88 imp:n=1
5028 2 -1e-4 9 -10 -2 u=88 imp:n=1
5029 56 -2.23 10 -11 -2 u=88 imp:n=1 vol=95.24213138
5030 2 -1e-4 11 -12 -2 u=88 imp:n=1
5031 5 -8 12 -13 u=88 imp:n=1
5032 4 -.67 13 u=88 imp:n=1
c -----
c Black Control Rods (Ag-In-Cd)
36 8 -9.32 -12 30 -2 u=19 imp:n=1
37 5 -8 12 -13 30 -2 u=19 imp:n=1
38 4 -.67 13 u=19 imp:n=1
39 4 -.67 -13 -30 u=19 imp:n=1
43 2 -1e-4 -13 2 u=19 imp:n=1
c -----
c Guide tube with Pyrex rods inserted 1
33 like 23 but fill=18 u=16 imp:n=1
34 like 24 but u=16 imp:n=1
35 like 25 but u=16 imp:n=1
c -----
c Guide tube with Pyrex rods inserted 2
1033 like 23 but fill=72 u=73 imp:n=1
1034 like 24 but u=73 imp:n=1
1035 like 25 but u=73 imp:n=1
c -----
c Guide tube with Pyrex rods inserted 3
2033 like 23 but fill=77 u=78 imp:n=1
2034 like 24 but u=78 imp:n=1
2035 like 25 but u=78 imp:n=1
c -----
c Guide tube with Pyrex rods inserted 4
3033 like 23 but fill=86 u=91 imp:n=1
3034 like 24 but u=91 imp:n=1
3035 like 25 but u=91 imp:n=1
c -----
c Guide tube with Pyrex rods inserted 5
4033 like 23 but fill=87 u=92 imp:n=1
4034 like 24 but u=92 imp:n=1
4035 like 25 but u=92 imp:n=1

```

```

c -----
c Guide tube with Pyrex rods inserted 6
5033 like 23 but fill=88 u=93 imp:n=1
5034 like 24 but u=93 imp:n=1
5035 like 25 but u=93 imp:n=1
c -----
c Guide tube with Black rods inserted
40 like 23 but fill=19 u=90 imp:n=1
41 like 24 but u=90 imp:n=1
42 like 25 but u=90 imp:n=1
c -----
c Assembly Constructions
c -----
c 2.61 no pyrex, no IFBA 1
100 4 -.67 -15 14 16 -17 u=20 imp:n=1 lat=1 fill=-8:8 -8:8
0:0
    11 11 11 11 11 11 11 11 11 11 11 11 11 11 11 11 11
    11 11 11 11 11 11 11 11 11 11 11 11 11 11 11 11 11
    11 11 11 11 11 90 11 11 90 11 11 90 11 11 11 11 11
    11 11 11 90 11 11 11 11 11 11 11 11 11 90 11 11 11
    11 11 11 11 11 11 11 11 11 11 11 11 11 11 11 11 11
    11 11 90 11 11 90 11 11 90 11 11 90 11 11 90 11 11
    11 11 11 11 11 11 11 11 11 11 11 11 11 11 11 11 11
    11 11 11 11 11 11 11 11 11 11 11 11 11 11 11 11 11
    11 11 90 11 11 90 11 11 90 11 11 90 11 11 90 11 11
    11 11 11 11 11 11 11 11 11 11 11 11 11 11 11 11 11
    11 11 11 90 11 11 11 11 11 11 11 11 11 11 90 11 11
    11 11 11 11 11 90 11 11 90 11 11 90 11 11 11 11 11
    11 11 11 11 11 11 11 11 11 11 11 11 11 11 11 11 11
    11 11 11 11 11 11 11 11 11 11 11 11 11 11 11 11 11
c -----
-
c 2.61 no pyrex, no IFBA 2
101 4 -.67 -15 14 16 -17 u=62 imp:n=1 lat=1 fill=-8:8 -8:8
0:0
    51 51 51 51 51 51 51 51 51 51 51 51 51 51 51 51 51
    51 51 51 51 51 51 51 51 51 51 51 51 51 51 51 51 51
    51 51 51 51 51 90 51 51 90 51 51 90 51 51 51 51 51
    51 51 51 90 51 51 51 51 51 51 51 51 51 90 51 51 51
    51 51 51 51 51 51 51 51 51 51 51 51 51 51 51 51 51
    51 51 90 51 51 90 51 51 90 51 51 90 51 51 90 51 51
    51 51 51 51 51 51 51 51 51 51 51 51 51 51 51 51 51
    51 51 51 51 51 51 51 51 51 51 51 51 51 51 51 51 51
    51 51 90 51 51 90 51 51 90 51 51 90 51 51 90 51 51

```

```

51 51 51 51 51 51 51 51 51 51 51 51 51 51 51 51
51 51 51 51 51 51 51 51 51 51 51 51 51 51 51 51
51 51 90 51 51 90 51 51 90 51 51 90 51 51 90 51 51
51 51 51 51 51 51 51 51 51 51 51 51 51 51 51 51
51 51 51 90 51 51 51 51 51 51 51 51 51 90 51 51 51
51 51 51 51 51 90 51 51 90 51 51 90 51 51 51 51 51
51 51 51 51 51 51 51 51 51 51 51 51 51 51 51 51
51 51 51 51 51 51 51 51 51 51 51 51 51 51 51 51

```

c -----

-

c 2.61 no pyrex, no IFBA 3

102 4 -.67 -15 14 16 -17 u=63 imp:n=1 lat=1 fill=-8:8 -8:8  
0:0

```

52 52 52 52 52 52 52 52 52 52 52 52 52 52 52 52
52 52 52 52 52 52 52 52 52 52 52 52 52 52 52 52
52 52 52 52 52 90 52 52 90 52 52 90 52 52 52 52 52
52 52 52 90 52 52 52 52 52 52 52 52 52 90 52 52 52
52 52 52 52 52 52 52 52 52 52 52 52 52 52 52 52
52 52 90 52 52 90 52 52 90 52 52 90 52 52 90 52 52
52 52 52 52 52 52 52 52 52 52 52 52 52 52 52 52
52 52 52 52 52 52 52 52 52 52 52 52 52 52 52 52
52 52 90 52 52 90 52 52 90 52 52 90 52 52 90 52 52
52 52 52 52 52 52 52 52 52 52 52 52 52 52 52 52
52 52 52 90 52 52 52 52 52 52 52 52 52 90 52 52 52
52 52 52 52 52 90 52 52 90 52 52 90 52 52 52 52 52
52 52 52 52 52 52 52 52 52 52 52 52 52 52 52 52
52 52 52 52 52 52 52 52 52 52 52 52 52 52 52 52

```

c -----

-

c 2.61 no pyrex, no IFBA 4

103 4 -.67 -15 14 16 -17 u=64 imp:n=1 lat=1 fill=-8:8 -8:8  
0:0

```

53 53 53 53 53 53 53 53 53 53 53 53 53 53 53 53
53 53 53 53 53 53 53 53 53 53 53 53 53 53 53 53
53 53 53 53 53 90 53 53 90 53 53 90 53 53 53 53 53
53 53 53 90 53 53 53 53 53 53 53 53 53 90 53 53 53
53 53 53 53 53 53 53 53 53 53 53 53 53 53 53 53
53 53 90 53 53 90 53 53 90 53 53 90 53 53 90 53 53
53 53 53 53 53 53 53 53 53 53 53 53 53 53 53 53
53 53 53 53 53 53 53 53 53 53 53 53 53 53 53 53
53 53 90 53 53 90 53 53 90 53 53 90 53 53 90 53 53
53 53 53 53 53 53 53 53 53 53 53 53 53 53 53 53
53 53 53 53 53 53 53 53 53 53 53 53 53 53 53 53
53 53 90 53 53 90 53 53 90 53 53 90 53 53 90 53 53

```

```

53 53 53 53 53 53 53 53 53 53 53 53 53 53 53 53
53 53 53 90 53 53 53 53 53 53 53 53 90 53 53 53
53 53 53 53 53 90 53 53 90 53 53 90 53 53 53 53
53 53 53 53 53 53 53 53 53 53 53 53 53 53 53 53
53 53 53 53 53 53 53 53 53 53 53 53 53 53 53 53

```

c -----

-

c 2.61 no pyrex, no IFBA 5

104 4 -.67 -15 14 16 -17 u=65 imp:n=1 lat=1 fill=-8:8 -8:8  
0:0

```

54 54 54 54 54 54 54 54 54 54 54 54 54 54 54 54
54 54 54 54 54 54 54 54 54 54 54 54 54 54 54 54
54 54 54 54 54 90 54 54 90 54 54 90 54 54 54 54
54 54 54 90 54 54 54 54 54 54 54 54 54 90 54 54
54 54 54 54 54 54 54 54 54 54 54 54 54 54 54 54
54 54 90 54 54 90 54 54 90 54 54 90 54 54 90 54
54 54 54 54 54 54 54 54 54 54 54 54 54 54 54 54
54 54 54 54 54 54 54 54 54 54 54 54 54 54 54 54
54 54 90 54 54 90 54 54 90 54 54 90 54 54 90 54
54 54 54 54 54 54 54 54 54 54 54 54 54 54 54 54
54 54 54 90 54 54 54 54 54 54 54 54 54 90 54 54
54 54 54 54 54 90 54 54 90 54 54 90 54 54 54 54
54 54 54 54 54 54 54 54 54 54 54 54 54 54 54 54
54 54 54 54 54 54 54 54 54 54 54 54 54 54 54 54

```

c -----

-

c 2.61 no pyrex, no IFBA 6

105 4 -.67 -15 14 16 -17 u=66 imp:n=1 lat=1 fill=-8:8 -8:8  
0:0

```

55 55 55 55 55 55 55 55 55 55 55 55 55 55 55 55
55 55 55 55 55 55 55 55 55 55 55 55 55 55 55 55
55 55 55 55 55 90 55 55 90 55 55 90 55 55 55 55
55 55 55 90 55 55 55 55 55 55 55 55 55 90 55 55
55 55 55 55 55 55 55 55 55 55 55 55 55 55 55 55
55 55 90 55 55 90 55 55 90 55 55 90 55 55 90 55
55 55 55 55 55 55 55 55 55 55 55 55 55 55 55 55
55 55 55 55 55 55 55 55 55 55 55 55 55 55 55 55
55 55 90 55 55 90 55 55 90 55 55 90 55 55 90 55
55 55 55 55 55 55 55 55 55 55 55 55 55 55 55 55
55 55 55 90 55 55 55 55 55 55 55 55 55 90 55 55
55 55 55 55 55 90 55 55 90 55 55 90 55 55 55 55

```

```

55 55 55 55 55 55 55 55 55 55 55 55 55 55 55 55
55 55 55 55 55 55 55 55 55 55 55 55 55 55 55
c 3.78 88 IFBA, 24 pyrex
110 4 -.67 -15 14 16 -17 u=21 imp:n=1 lat=1 fill=-8:8 -8:8
0:0
76 76 75 75 75 75 75 75 75 75 75 75 75 75 76 76
76 75 75 75 75 76 75 75 76 75 75 76 75 75 75 76
75 75 76 75 76 78 75 76 78 76 75 78 76 75 76 75 75
75 75 75 78 76 76 75 75 75 75 75 76 76 78 75 75 75
75 75 76 76 75 76 75 75 76 75 75 76 75 76 76 75 75
75 76 78 76 76 78 75 76 78 76 75 78 76 76 78 76 75
75 75 75 75 75 75 76 75 75 75 76 75 75 75 75 75 75
75 75 76 75 75 76 75 75 76 75 75 76 75 75 76 75 75
75 76 78 75 76 78 75 76 17 76 75 78 76 75 78 76 75
75 75 76 75 75 76 75 75 76 75 75 76 75 75 76 75 75
75 75 75 75 75 75 76 75 75 75 76 75 75 75 75 75 75
75 76 78 76 76 78 75 76 78 76 75 78 76 76 78 76 75
75 75 76 76 75 76 75 75 76 75 75 76 75 76 76 75 75
75 75 75 78 76 76 75 75 75 75 75 76 76 78 75 75 75
75 75 76 75 76 78 75 76 78 76 75 78 76 75 76 75 75
76 75 75 75 75 76 75 75 76 75 75 76 75 75 75 75 76
76 76 75 75 75 75 75 75 75 75 75 75 75 75 76 76
c 3.78 44 IFBA, 24 pyrex
120 4 -.67 -15 14 16 -17 u=22 imp:n=1 lat=1 fill=-8:8 -8:8
0:0
13 13 12 12 12 12 12 12 12 12 12 12 12 12 13 13
13 12 12 12 12 13 12 12 12 12 12 13 12 12 12 13
12 12 12 12 12 16 12 12 16 12 12 16 12 12 12 12
12 12 12 16 13 12 12 12 13 12 12 12 13 16 12 12 12
12 12 12 13 12 12 12 12 12 12 12 12 12 13 12 12 12
12 13 16 12 12 16 13 12 16 12 13 16 12 12 16 13 12
12 12 12 12 12 13 12 12 13 12 12 13 12 12 12 12 12
12 12 12 12 12 12 12 12 12 12 12 12 12 12 12 12 12
12 12 16 13 12 16 13 12 17 12 13 16 12 13 16 12 12
12 12 12 12 12 12 12 12 12 12 12 12 12 12 12 12 12
12 12 12 12 12 13 12 12 13 12 12 13 12 12 12 12 12
12 13 16 12 12 16 13 12 16 12 13 16 12 12 16 13 12
12 12 12 13 12 12 12 12 12 12 12 12 12 13 12 12 12
12 12 12 16 13 12 12 12 13 12 12 12 13 16 12 12 12
12 12 12 12 12 16 12 12 16 12 12 16 12 12 12 12 12
13 12 12 12 12 13 12 12 12 12 12 13 12 12 12 12 13
13 13 12 12 12 12 12 12 12 12 12 12 12 12 13 13
c 3.78 28 IFBA, 24 pyrex 1
130 4 -.67 -15 14 16 -17 u=23 imp:n=1 lat=1 fill=-8:8 -8:8
0:0
13 13 12 12 12 12 12 12 12 12 12 12 12 12 13 13
13 12 12 12 12 12 12 12 12 12 12 12 12 12 12 13

```

```

12 12 12 12 12 16 13 12 16 12 13 16 12 12 12 12 12
12 12 12 16 12 12 12 12 12 12 12 12 16 12 12 12
12 12 12 12 13 12 12 12 12 12 12 13 12 12 12 12
12 12 16 12 12 16 12 12 16 12 12 16 12 12 16 12 12
12 12 13 12 12 12 12 12 12 12 12 12 12 13 12 12
12 12 12 12 12 12 12 13 12 13 12 12 12 12 12 12
12 12 16 12 12 16 12 12 17 12 12 16 12 12 16 12 12
12 12 12 12 12 12 12 13 12 13 12 12 12 12 12 12
12 12 13 12 12 12 12 12 12 12 12 12 12 13 12 12
12 12 16 12 12 16 12 12 16 12 12 16 12 12 16 12 12
12 12 12 12 13 12 12 12 12 12 12 13 12 12 12 12
12 12 12 16 12 12 12 12 12 12 12 12 16 12 12 12
12 12 12 12 12 16 13 12 16 12 13 16 12 12 12 12
13 12 12 12 12 12 12 12 12 12 12 12 12 12 12 13
13 13 12 12 12 12 12 12 12 12 12 12 12 12 13 13

```

c 3.78 28 IFBA, 24 pyrex 2

131 4 -.67 -15 14 16 -17 u=74 imp:n=1 lat=1 fill=-8:8 -8:8  
0:0

```

71 71 70 70 70 70 70 70 70 70 70 70 70 70 71 71
71 70 70 70 70 70 70 70 70 70 70 70 70 70 70 71
70 70 70 70 70 73 71 70 73 70 71 73 70 70 70 70
70 70 70 73 70 70 70 70 70 70 70 70 73 70 70 70
70 70 70 70 71 70 70 70 70 70 70 70 71 70 70 70
70 70 73 70 70 73 70 70 73 70 70 73 70 70 73 70
70 70 71 70 70 70 70 70 70 70 70 70 70 71 70 70
70 70 70 70 70 70 70 71 70 71 70 70 70 70 70 70
70 70 73 70 70 73 70 70 73 70 70 73 70 70 73 70
70 70 70 70 71 70 70 70 70 70 70 71 70 70 70 70
70 70 70 73 70 70 70 70 70 70 70 70 73 70 70 70
70 70 70 70 70 73 71 70 73 70 71 73 70 70 70 70
71 70 70 70 70 70 70 70 70 70 70 70 70 70 70 71
71 71 70 70 70 70 70 70 70 70 70 70 70 70 71 71

```

c 4.95 72 IFBA, 24 pyrex

140 4 -.67 -15 14 16 -17 u=24 imp:n=1 lat=1 fill=-8:8 -8:8  
0:0

```

83 83 80 80 80 80 80 80 80 80 80 80 80 80 83 83
83 80 80 80 80 83 80 80 83 80 80 83 80 80 80 83
80 80 80 80 83 91 80 83 91 83 80 91 83 80 80 80
80 80 83 83 80 83 80 80 83 80 80 83 80 83 83 80
80 83 91 80 83 91 80 83 91 83 80 91 83 80 91 83
80 80 80 80 80 80 80 80 80 80 80 80 80 80 80 80
80 80 83 80 80 83 80 80 83 80 80 83 80 80 83 80
80 83 91 80 83 91 80 83 17 83 80 91 83 80 91 83

```

```

80 80 83 80 80 83 80 80 83 80 80 83 80 80 83 80 80
80 80 80 80 80 80 80 80 80 80 80 80 80 80 80 80
80 83 91 80 83 91 80 83 91 83 80 91 83 80 91 83 80
80 80 83 83 80 83 80 80 83 80 80 83 80 83 83 80 80
80 80 80 91 83 80 80 80 80 80 80 80 83 91 80 80 80
80 80 80 80 83 91 80 83 91 83 80 91 83 80 80 80 80
83 80 80 80 80 83 80 80 83 80 80 83 80 80 80 80 83
83 83 80 80 80 80 80 80 80 80 80 80 80 80 80 83 83

```

c 4.95 88 IFBA, 12 pyrex South

```

150 4 -.67 -15 14 16 -17 u=25 imp:n=1 lat=1 fill=-8:8 -8:8
0:0

```

```

84 84 81 81 81 81 81 81 81 81 81 81 81 81 81 84 84
84 81 81 81 81 84 81 81 84 81 81 84 81 81 81 81 84
81 81 84 81 84 17 81 84 17 84 81 17 84 81 84 81 81
81 81 81 17 84 84 81 81 81 81 81 84 84 17 81 81 81
81 81 84 84 81 84 81 81 84 81 81 84 81 84 84 81 81
81 84 17 84 84 17 81 84 17 84 81 17 84 84 17 84 81
81 81 81 81 81 81 84 81 81 81 84 81 81 81 81 81 81
81 81 84 81 81 84 81 81 84 81 81 84 81 81 84 81 81
81 84 92 81 84 92 81 84 17 84 81 92 84 81 92 84 81
81 81 84 81 81 84 81 81 84 81 81 84 81 81 84 81 81
81 81 81 81 81 81 84 81 81 81 84 81 81 81 81 81 81
81 84 92 84 84 17 81 84 92 84 81 17 84 84 92 84 81
81 81 84 84 81 84 81 81 84 81 81 84 81 84 84 81 81
81 81 81 92 84 84 81 81 81 81 81 84 84 92 81 81 81
81 81 84 81 84 92 81 84 92 84 81 92 84 81 84 81 81
84 81 81 81 81 84 81 81 84 81 81 84 81 81 81 81 84
84 84 81 81 81 81 81 81 81 81 81 81 81 81 81 84 84

```

c 4.95 88 IFBA, 12 pyrex East

```

250 4 -.67 -15 14 16 -17 u=40 imp:n=1 lat=1 fill=-8:8 -8:8
0:0

```

```

84 84 81 81 81 81 81 81 81 81 81 81 81 81 81 84 84
84 81 81 81 81 84 81 81 84 81 81 84 81 81 81 81 84
81 81 84 81 84 17 81 84 92 84 81 92 84 81 84 81 81
81 81 81 17 84 84 81 81 81 81 81 84 84 92 81 81 81
81 81 84 84 81 84 81 81 84 81 81 84 81 84 84 81 81
81 84 17 84 84 17 81 84 92 84 81 17 84 84 92 84 81
81 81 81 81 81 81 84 81 81 81 84 81 81 81 81 81 81
81 81 84 81 81 84 81 81 84 81 81 84 81 81 84 81 81
81 84 17 81 84 17 81 84 17 84 81 92 84 81 92 84 81
81 81 84 81 81 84 81 81 84 81 81 84 81 81 84 81 81
81 81 81 81 81 81 84 81 81 81 84 81 81 81 81 81 81
81 84 17 84 84 17 81 84 92 84 81 17 84 84 92 84 81
81 81 84 84 81 84 81 81 84 81 81 84 81 84 84 81 81
81 81 81 17 84 84 81 81 81 81 81 84 84 92 81 81 81
81 81 84 81 84 17 81 84 92 84 81 92 84 81 84 81 81
84 81 81 81 81 84 81 81 84 81 81 84 81 81 81 81 84

```



84 84 81 81 81 81 81 81 81 81 81 81 81 81 81 84 84  
 c 4.95 88 IFBA, 12 pyrex North  
 350 4 -.67 -15 14 16 -17 u=42 imp:n=1 lat=1 fill=-8:8 -8:8  
 0:0

84 84 81 81 81 81 81 81 81 81 81 81 81 81 81 84 84  
 84 81 81 81 81 84 81 81 84 81 81 84 81 81 81 81 84  
 81 81 84 81 84 92 81 84 92 84 81 92 84 81 84 81 81  
 81 81 81 92 84 84 81 81 81 81 81 84 84 92 81 81 81  
 81 81 84 84 81 84 81 81 84 81 81 84 81 84 84 81 81  
 81 84 92 84 84 17 81 84 92 84 81 17 84 84 92 84 81  
 81 81 81 81 81 81 84 81 81 81 84 81 81 81 81 81  
 81 81 84 81 81 84 81 81 84 81 81 84 81 81 84 81 81  
 81 84 92 81 84 92 81 84 17 84 81 92 84 81 92 84 81  
 81 81 84 81 81 84 81 81 84 81 81 84 81 81 84 81 81  
 81 81 81 81 81 81 84 81 81 81 84 81 81 81 81 81  
 81 84 17 84 84 17 81 84 17 84 81 17 84 84 17 84 81  
 81 81 84 84 81 84 81 81 84 81 81 84 81 84 84 81 81  
 81 81 81 17 84 84 81 81 81 81 81 84 84 17 81 81 81  
 81 81 84 81 84 17 81 84 17 84 81 17 84 81 84 81 81  
 84 81 81 81 81 84 81 81 84 81 81 84 81 81 81 81 84  
 84 84 81 81 81 81 81 81 81 81 81 81 81 81 81 84 84

c 4.95 88 IFBA, 12 pyrex West  
 450 4 -.67 -15 14 16 -17 u=44 imp:n=1 lat=1 fill=-8:8 -8:8  
 0:0

84 84 81 81 81 81 81 81 81 81 81 81 81 81 81 84 84  
 84 81 81 81 81 84 81 81 84 81 81 84 81 81 81 81 84  
 81 81 84 81 84 92 81 84 92 84 81 17 84 81 84 81 81  
 81 81 81 92 84 84 81 81 81 81 81 84 84 17 81 81 81  
 81 81 84 84 81 84 81 81 84 81 81 84 81 84 84 81 81  
 81 84 92 84 84 17 81 84 92 84 81 17 84 84 17 84 81  
 81 81 81 81 81 81 84 81 81 81 84 81 81 81 81 81  
 81 81 84 81 81 84 81 81 84 81 81 84 81 81 84 81 81  
 81 84 92 81 84 92 81 84 17 84 81 17 84 81 17 84 81  
 81 81 84 81 81 84 81 81 84 81 81 84 81 81 84 81 81  
 81 81 81 81 81 81 84 81 81 81 84 81 81 81 81 81  
 81 84 92 84 84 17 81 84 92 84 81 17 84 84 17 84 81  
 81 81 84 84 81 84 81 81 84 81 81 84 81 84 84 81 81  
 81 81 81 92 84 84 81 81 81 81 81 84 84 17 81 81 81  
 81 81 84 81 84 92 81 84 92 84 81 17 84 81 84 81 81  
 84 81 81 81 81 84 81 81 84 81 81 84 81 81 81 81 84  
 84 84 81 81 81 81 81 81 81 81 81 81 81 81 81 84 84

c 4.95 88 IFBA, 9 pyrex SE  
 160 4 -.67 -15 14 16 -17 u=26 imp:n=1 lat=1 fill=-8:8 -8:8  
 0:0

85 85 82 82 82 82 82 82 82 82 82 82 82 82 85 85  
 85 82 82 82 82 85 82 82 85 82 82 85 82 82 82 82 85  
 82 82 85 82 85 17 82 85 17 85 82 17 85 82 85 82 82

```

82 82 82 17 85 85 82 82 82 82 82 85 85 17 82 82 82
82 82 85 85 82 85 82 82 85 82 82 85 82 85 85 82 82
82 85 17 85 85 17 82 85 17 85 82 17 85 85 93 85 82
82 82 82 82 82 82 85 82 82 82 85 82 82 82 82 82 82
82 82 85 82 82 85 82 82 85 82 82 85 82 82 85 82 82
82 85 17 82 85 17 82 85 17 85 82 93 85 82 93 85 82
82 82 85 82 82 85 82 82 85 82 82 85 82 82 85 82 82
82 82 82 82 82 82 85 82 82 82 85 82 82 82 82 82 82
82 85 17 85 85 17 82 85 93 85 82 17 85 85 93 85 82
82 82 85 85 82 85 82 82 85 82 82 85 82 85 85 82 82
82 82 82 17 85 85 82 82 82 82 82 85 85 93 82 82 82
82 82 85 82 85 93 82 85 93 85 82 93 85 82 85 82 82
85 82 82 82 82 85 82 82 85 82 82 85 82 82 82 82 85
85 85 82 82 82 82 82 82 82 82 82 82 82 82 82 85 85

```

c 4.95 88 IFBA, 9 pyrex NE

260 4 -.67 -15 14 16 -17 u=46 imp:n=1 lat=1 fill=-8:8 -8:8  
0:0

```

15 85 82 82 82 82 82 82 82 82 82 82 82 82 85 85
85 82 82 82 82 85 82 82 85 82 82 85 82 82 82 85
82 82 85 82 85 93 82 85 93 85 82 93 85 82 85 82 82
82 82 82 17 85 85 82 82 82 82 82 85 85 93 82 82 82
82 82 85 85 82 85 82 82 85 82 82 85 82 85 85 82 82
82 85 17 85 85 17 82 85 93 85 82 17 85 85 93 85 82
82 82 82 82 82 82 85 82 82 82 85 82 82 82 82 82 82
82 82 85 82 82 85 82 82 85 82 82 85 82 82 85 82 82
82 85 17 82 85 17 82 85 17 85 82 93 85 82 93 85 82
82 82 85 82 82 85 82 82 85 82 82 85 82 82 85 82 82
82 82 82 17 85 85 82 82 82 82 82 85 85 17 82 82 82
82 82 85 82 85 17 82 85 17 85 82 17 85 82 85 82 82
85 82 82 82 82 85 82 82 85 82 82 85 82 82 82 82 85
85 85 82 82 82 82 82 82 82 82 82 82 82 82 82 85 85

```

c 4.95 88 IFBA, 9 pyrex NW

360 4 -.67 -15 14 16 -17 u=48 imp:n=1 lat=1 fill=-8:8 -8:8  
0:0

```

85 85 82 82 82 82 82 82 82 82 82 82 82 82 85 85
85 82 82 82 82 85 82 82 85 82 82 85 82 82 82 82 85
82 82 85 82 85 93 82 85 93 85 82 93 85 82 85 82 82
82 82 82 93 85 85 82 82 82 82 82 85 85 17 82 82 82
82 82 85 85 82 85 82 82 85 82 82 85 82 85 85 82 82
82 85 93 85 85 17 82 85 93 85 82 17 85 85 17 85 82
82 82 82 82 82 82 85 82 82 82 85 82 82 82 82 82 82
82 82 85 82 82 85 82 82 85 82 82 85 82 82 85 82 82
82 85 93 82 85 93 82 85 17 85 82 17 85 82 17 85 82
82 82 85 82 82 85 82 82 85 82 82 85 82 82 85 82 82

```

```

82 82 82 82 82 82 85 82 82 82 85 82 82 82 82 82
82 85 93 85 85 17 82 85 17 85 82 17 85 85 17 85 82
82 82 85 85 82 85 82 82 85 82 82 85 82 85 85 82 82
82 82 82 17 85 85 82 82 82 82 82 85 85 17 82 82 82
82 82 85 82 85 17 82 85 17 85 82 17 85 82 85 82 82
85 82 82 82 82 85 82 82 85 82 82 85 82 82 82 82 85
85 85 82 82 82 82 82 82 82 82 82 82 82 82 85 85

```

c 4.95 88 IFBA, 9 pyrex SW

460 4 -.67 -15 14 16 -17 u=50 imp:n=1 lat=1 fill=-8:8 -8:8  
0:0

```

85 85 82 82 82 82 82 82 82 82 82 82 82 82 85 85
85 82 82 82 82 85 82 82 85 82 82 85 82 82 82 85
82 82 85 82 85 17 82 85 17 85 82 17 85 82 85 82 82
82 82 82 17 85 85 82 82 82 82 82 85 85 17 82 82 82
82 82 85 85 82 85 82 82 85 82 82 85 82 85 85 82 82
82 85 93 85 85 17 82 85 17 85 82 17 85 85 17 85 82
82 82 82 82 82 82 85 82 82 82 85 82 82 82 82 82
82 82 85 82 82 85 82 82 85 82 82 85 82 82 85 82 82
82 85 93 82 85 93 82 85 17 85 82 17 85 82 17 85 82
82 82 85 82 82 85 82 82 85 82 82 85 82 82 85 82 82
82 82 82 82 82 82 85 82 82 82 85 82 82 82 82 82
82 85 93 85 85 17 82 85 93 85 82 17 85 85 17 85 82
82 82 85 85 82 85 82 82 85 82 82 85 82 85 85 82 82
82 82 82 93 85 85 82 82 82 82 82 85 85 17 82 82 82
82 82 85 82 85 93 82 85 93 85 82 93 85 82 85 82 82
85 82 82 82 82 85 82 82 85 82 82 85 82 82 82 82 85
85 85 82 82 82 82 82 82 82 82 82 82 82 82 85 85

```

c 4.95 112 IFBA, 0 pyrex 1

170 4 -.67 -15 14 16 -17 u=27 imp:n=1 lat=1 fill=-8:8 -8:8  
0:0

```

15 15 14 14 14 14 14 14 14 14 14 14 14 14 15 15
15 14 14 14 14 15 14 14 15 14 14 15 14 14 14 15
14 14 14 15 15 90 15 15 90 15 15 90 15 15 14 14 14
14 14 15 90 15 15 14 14 15 14 14 15 15 90 15 14 14
14 14 15 15 14 15 14 14 15 14 14 15 14 15 15 14 14
14 15 90 15 15 90 15 15 90 15 15 90 15 15 90 15 14
14 14 15 14 14 15 14 14 15 14 14 15 14 14 15 14 14
14 14 15 14 14 15 14 14 15 14 14 15 14 14 15 14 14
14 15 90 15 15 90 15 15 90 15 15 90 15 15 90 15 14
14 14 15 15 14 15 14 14 15 14 14 15 14 15 15 14 14
14 14 15 90 15 15 14 14 15 14 14 15 15 90 15 14 14
14 14 14 15 15 90 15 15 90 15 15 90 15 15 14 14 14
15 14 14 14 14 15 14 14 15 14 14 15 14 14 14 14 15
15 15 14 14 14 14 14 14 14 14 14 14 14 14 14 15 15

```

c 4.95 112 IFBA, 0 pyrex 2  
 171 4 -.67 -15 14 16 -17 u=67 imp:n=1 lat=1 fill=-8:8 -8:8  
 0:0

```

59 59 56 56 56 56 56 56 56 56 56 56 56 56 56 59 59
59 56 56 56 56 59 56 56 59 56 56 59 56 56 56 56 59
56 56 56 59 59 90 59 59 90 59 59 90 59 59 56 56 56
56 56 59 90 59 59 56 56 59 56 56 59 59 90 59 56 56
56 56 59 59 56 59 56 56 59 56 56 59 56 59 59 56 56
56 59 90 59 59 90 59 59 90 59 59 90 59 59 90 59 56
56 56 59 56 56 59 56 56 59 56 56 59 56 56 59 56 56
56 56 59 56 56 59 56 56 59 56 56 59 56 56 59 56 56
56 59 90 59 59 90 59 59 90 59 59 90 59 59 90 59 56
56 56 59 59 56 59 56 56 59 56 56 59 56 59 59 56 56
56 56 59 90 59 59 56 56 59 56 56 59 59 90 59 56 56
56 56 56 59 59 90 59 59 90 59 59 90 59 59 56 56 56
59 56 56 56 56 59 56 56 59 56 56 59 56 56 56 56 59
59 59 56 56 56 56 56 56 56 56 56 56 56 56 59 59

```

c 4.95 112 IFBA, 0 pyrex 3  
 172 4 -.67 -15 14 16 -17 u=68 imp:n=1 lat=1 fill=-8:8 -8:8  
 0:0

```

60 60 57 57 57 57 57 57 57 57 57 57 57 57 60 60
60 57 57 57 57 60 57 57 60 57 57 60 57 57 57 60
57 57 57 60 60 90 60 60 90 60 60 90 60 60 57 57 57
57 57 60 90 60 60 57 57 60 57 57 60 57 60 60 57 57
57 60 90 60 60 90 60 60 90 60 60 90 60 60 90 60 57
57 57 60 57 57 60 57 57 60 57 57 60 57 57 60 57 57
57 57 60 57 57 60 57 57 60 57 57 60 57 57 60 57 57
57 60 90 60 60 90 60 60 90 60 60 90 60 60 90 60 57
57 57 60 57 57 60 57 57 60 57 57 60 57 57 60 57 57
57 57 60 57 57 60 57 57 60 57 57 60 57 57 60 57 57
57 60 90 60 60 90 60 60 90 60 60 90 60 60 90 60 57
57 57 57 60 60 90 60 60 90 60 60 90 60 60 57 57 57
60 57 57 57 57 60 57 57 60 57 57 60 57 57 57 57 60
60 60 57 57 57 57 57 57 57 57 57 57 57 57 60 60

```

c 4.95 112 IFBA, 0 pyrex 4  
 173 4 -.67 -15 14 16 -17 u=69 imp:n=1 lat=1 fill=-8:8 -8:8  
 0:0

```

61 61 58 58 58 58 58 58 58 58 58 58 58 58 61 61
61 58 58 58 58 61 58 58 61 58 58 61 58 58 58 61
58 58 58 61 61 90 61 61 90 61 61 90 61 61 58 58 58
58 58 61 90 61 61 58 58 61 58 58 61 61 90 61 58 58

```

```

58 58 61 61 58 61 58 58 61 58 58 61 58 61 61 58 58
58 61 90 61 61 90 61 61 90 61 61 90 61 61 90 61 58
58 58 61 58 58 61 58 58 61 58 58 61 58 58 61 58 58
58 58 61 58 58 61 58 58 61 58 58 61 58 58 61 58 58
58 61 90 61 61 90 61 61 90 61 61 90 61 61 90 61 58
58 58 61 58 58 61 58 58 61 58 58 61 58 58 61 58 58
58 58 61 58 58 61 58 58 61 58 58 61 58 58 61 58 58
58 61 90 61 61 90 61 61 90 61 61 90 61 61 90 61 58
58 58 61 61 58 61 58 58 61 58 58 61 58 61 61 58 58
58 58 61 90 61 61 58 58 61 58 58 61 61 90 61 58 58
58 58 58 61 61 90 61 61 90 61 61 90 61 61 58 58 58
61 58 58 58 58 61 58 58 61 58 58 61 58 58 58 58 61
61 61 58 58 58 58 58 58 58 58 58 58 58 58 58 61 61

```

c 4.95 28 IFBA, 0 pyrex

180 4 -.67 -15 14 16 -17 u=28 imp:n=1 lat=1 fill=-8:8 -8:8  
0:0

```

15 15 14 14 14 14 14 14 14 14 14 14 14 14 14 15 15
15 14 14 14 14 14 14 14 14 14 14 14 14 14 14 14 15
14 14 14 14 14 90 15 14 90 14 15 90 14 14 14 14 14
14 14 14 90 14 14 14 14 14 14 14 14 14 90 14 14 14
14 14 14 14 15 14 14 14 14 14 14 14 14 15 14 14 14
14 14 90 14 14 90 14 14 90 14 14 90 14 14 90 14 14
14 14 15 14 14 14 14 14 14 14 14 14 14 14 15 14 14
14 14 14 14 14 14 14 15 14 15 14 14 14 14 14 14 14
14 14 90 14 14 90 14 14 90 14 14 90 14 14 90 14 14
14 14 14 14 15 14 14 14 14 14 14 14 15 14 14 14 14
14 14 14 90 14 14 14 14 14 14 14 14 14 90 14 14 14
14 14 14 14 14 90 15 14 90 14 15 90 14 14 14 14 14
15 14 14 14 14 14 14 14 14 14 14 14 14 14 14 14 15
15 15 14 14 14 14 14 14 14 14 14 14 14 14 14 15 15

```

c

c Core Configuration

c

200 4 -.67 -19 18 20 -21 u=29 imp:n=1 lat=1 fill=-6:6 -6:6  
0:0

```

29 29 29 29 29 29 29 29 29 29 29 29 29
29 29 29 29 29 26 25 50 29 29 29 29 29
29 29 29 69 67 24 63 24 67 69 29 29 29
29 29 69 68 27 65 23 65 27 68 69 29 29
29 29 67 27 66 74 62 74 66 27 67 29 29
29 26 24 65 74 64 21 64 74 65 24 50 29
29 40 63 23 62 21 20 21 62 23 63 44 29
29 46 24 65 74 64 21 64 74 65 24 48 29
29 29 67 27 66 74 62 74 66 27 67 29 29

```

```

29 29 69 68 27 65 23 65 27 68 69 29 29
29 29 29 69 67 24 63 24 67 69 29 29 29
29 29 29 29 29 46 42 48 29 29 29 29 29
29 29 29 29 29 29 29 29 29 29 29 29 29
201 0 -24 22 -23 fill=29 imp:n=1
202 5 -8 -25 24 22 -23 imp:n=1
203 4 -.67 (25:-22:23) -26 28 -29 imp:n=1
204 5 -8 26 -27 28 -29 imp:n=1
205 0 27:-28:29 imp:n=0

```

c Surface Cards

c

c -----rod structures-----

c

```

1   Cz .4096                               $ fuel radius
2   Pz 244                                 $ top of fuel pins
3   Cz .4179                               $ Helium gap
4   Cz .475                                $ cladding diameter
5   Cz .41216                              $ IFBA thickness
6   Cz .56                                 $ guide tube inner radius
7   Cz .60                                 $ guide tube outer radius
8   Cz .214                                $ Pyrex rod structure
9   Cz .231                                $ Pyrex rod structure
10  Cz .241                                $ Pyrex rod structure
11  Cz .427                                $ Pyrex rod structure
12  Cz .437                                $ Pyrex rod structure
13  Cz .484                                $ Pyrex rod structure

```

c

c -----assembly structures-----

```

14  Px -.63                                $ rod lattice pitch
15  Px .63                                 $ rod lattice pitch
16  Py -.63                                $ rod lattice pitch
17  Py .63                                 $ rod lattice pitch
18  Px -10.71                              $ fuel assembly dimension
19  Px 10.71                               $ fuel assembly dimension
20  Py -10.71                              $ fuel assembly dimension
21  Py 10.71                               $ fuel assembly dimension

```

c

c -----core level structures-----

```

22  Pz 0                                   $ bottom of fuel
23  Pz 260
24  Cz 135                                $ core barrel inner radius
25  Cz 140                                $ core barrel outer radius
26  Cz 200
27  Cz 275
28  Pz -10
29  Pz 270

```

30 Pz 270

\$ control rod level

c Data Cards

mode n

c TOTNU NO

kcode 100000 1.0 60 400

ksrc 1.26 1.26 130

burn TIME=100 5R

POWER=800

MAT=10 20 30 40 50 60 70 80 90 100 110 120 130 140 11  
21 31 41 51 61

12 22 32 42 52 62 6 16 26 36 46 56 7 17 27 37 47  
57 67 77 87 97

MATVOL=156384.307 156384.307 78192.153 156384.307  
115230.542 115230.542

57615.271 115230.542 197538.072 90538.283  
181076.566 74076.777

45269.141 90538.283 121403.607 242807.214  
28807.635

90538.283 45269.141 14403.818 33951.856  
135807.425 135807.425

135807.425 271614.849 135807.425 9143.245  
18286.489

9143.245 18286.489 4571.622 6857.433 180.610  
1444.883

1444.883 722.441 1444.883 361.221 567.633  
928.853 567.633 1135.265

OMIT=10,4,06014,07016,08018 09018  
20,4,06014,07016,08018 09018  
30,4,06014,07016,08018 09018  
40,4,06014,07016,08018 09018  
50,4,06014,07016,08018 09018  
60,4,06014,07016,08018 09018  
70,4,06014,07016,08018 09018  
80,4,06014,07016,08018 09018  
90,4,06014,07016,08018 09018  
100,4,06014,07016,08018 09018  
110,4,06014,07016,08018 09018  
120,4,06014,07016,08018 09018  
130,4,06014,07016,08018 09018  
140,4,06014,07016,08018 09018  
11,4,06014,07016,08018 09018  
21,4,06014,07016,08018 09018  
31,4,06014,07016,08018 09018  
41,4,06014,07016,08018 09018  
51,4,06014,07016,08018 09018  
61,4,06014,07016,08018 09018

12,4,06014,07016,08018 09018  
22,4,06014,07016,08018 09018  
32,4,06014,07016,08018 09018  
42,4,06014,07016,08018 09018  
52,4,06014,07016,08018 09018  
62,4,06014,07016,08018 09018  
6, 26, 06014,07016,08018 09018, 10021, 10022  
12023, 12027, 13026, 13028, 14027, 14031  
16031, 39087, 39092, 39093, 40089, 40097  
41091, 41092, 41096, 41097, 41098, 41099  
42091, 42093  
16, 26, 06014,07016,08018 09018, 10021, 10022  
12023, 12027, 13026, 13028, 14027, 14031  
16031, 39087, 39092, 39093, 40089, 40097  
41091, 41092, 41096, 41097, 41098, 41099  
42091, 42093  
26, 26, 06014,07016,08018 09018, 10021, 10022  
12023, 12027, 13026, 13028, 14027, 14031  
16031, 39087, 39092, 39093, 40089, 40097  
41091, 41092, 41096, 41097, 41098, 41099  
42091, 42093  
36, 26, 06014,07016,08018 09018, 10021, 10022  
12023, 12027, 13026, 13028, 14027, 14031  
16031, 39087, 39092, 39093, 40089, 40097  
41091, 41092, 41096, 41097, 41098, 41099  
42091, 42093  
46, 26, 06014,07016,08018 09018, 10021, 10022  
12023, 12027, 13026, 13028, 14027, 14031  
16031, 39087, 39092, 39093, 40089, 40097  
41091, 41092, 41096, 41097, 41098, 41099  
42091, 42093  
56, 26, 06014,07016,08018 09018, 10021, 10022  
12023, 12027, 13026, 13028, 14027, 14031  
16031, 39087, 39092, 39093, 40089, 40097  
41091, 41092, 41096, 41097, 41098, 41099  
42091, 42093  
7, 26, 06014,07016,08018 09018, 10021, 10022  
12023, 12027, 13026, 13028, 14027, 14031  
16031, 39087, 39092, 39093, 40089, 40097  
41091, 41092, 41096, 41097, 41098, 41099  
42091, 42093  
17, 26, 06014,07016,08018 09018, 10021, 10022  
12023, 12027, 13026, 13028, 14027, 14031  
16031, 39087, 39092, 39093, 40089, 40097  
41091, 41092, 41096, 41097, 41098, 41099  
42091, 42093  
27, 26, 06014,07016,08018 09018, 10021, 10022



```

12023, 12027, 13026, 13028, 14027, 14031
16031, 39087, 39092, 39093, 40089, 40097
41091, 41092, 41096, 41097, 41098, 41099
42091, 42093
37, 26, 06014,07016,08018 09018, 10021, 10022
12023, 12027, 13026, 13028, 14027, 14031
16031, 39087, 39092, 39093, 40089, 40097
41091, 41092, 41096, 41097, 41098, 41099
42091, 42093
47, 26, 06014,07016,08018 09018, 10021, 10022
12023, 12027, 13026, 13028, 14027, 14031
16031, 39087, 39092, 39093, 40089, 40097
41091, 41092, 41096, 41097, 41098, 41099
42091, 42093
57, 26, 06014,07016,08018 09018, 10021, 10022
12023, 12027, 13026, 13028, 14027, 14031
16031, 39087, 39092, 39093, 40089, 40097
41091, 41092, 41096, 41097, 41098, 41099
42091, 42093
67, 26, 06014,07016,08018 09018, 10021, 10022
12023, 12027, 13026, 13028, 14027, 14031
16031, 39087, 39092, 39093, 40089, 40097
41091, 41092, 41096, 41097, 41098, 41099
42091, 42093
77, 26, 06014,07016,08018 09018, 10021, 10022
12023, 12027, 13026, 13028, 14027, 14031
16031, 39087, 39092, 39093, 40089, 40097
41091, 41092, 41096, 41097, 41098, 41099
42091, 42093
87, 26, 06014,07016,08018 09018, 10021, 10022
12023, 12027, 13026, 13028, 14027, 14031
16031, 39087, 39092, 39093, 40089, 40097
41091, 41092, 41096, 41097, 41098, 41099
42091, 42093
97, 26, 06014,07016,08018 09018, 10021, 10022
12023, 12027, 13026, 13028, 14027, 14031
16031, 39087, 39092, 39093, 40089, 40097
41091, 41092, 41096, 41097, 41098, 41099
42091, 42093

```

c

c -----Flux Tally-----

```

FMESH4:n ORIGIN=-140 -140 0 IMESH=140 IINTS=280 JMESH=140
JINTS=280 KMESH=260

```

c

c -----

c -----Material Specificaitons-----

c -----

```

c
c-----4.95% enriched UO2-----
m10 8016.71c -.11853 92235.71c -.043634 92238.71c -.83786
m20 8016.71c -.11853 92235.71c -.043634 92238.71c -.83786
m30 8016.71c -.11853 92235.71c -.043634 92238.71c -.83786
m40 8016.71c -.11853 92235.71c -.043634 92238.71c -.83786
m50 8016.71c -.11853 92235.71c -.043634 92238.71c -.83786
m60 8016.71c -.11853 92235.71c -.043634 92238.71c -.83786
m70 8016.71c -.11853 92235.71c -.043634 92238.71c -.83786
m80 8016.71c -.11853 92235.71c -.043634 92238.71c -.83786
m90 8016.71c -.11853 92235.71c -.043634 92238.71c -.83786
m100 8016.71c -.11853 92235.71c -.043634 92238.71c -.83786
m110 8016.71c -.11853 92235.71c -.043634 92238.71c -.83786
m120 8016.71c -.11853 92235.71c -.043634 92238.71c -.83786
m130 8016.71c -.11853 92235.71c -.043634 92238.71c -.83786
m140 8016.71c -.11853 92235.71c -.043634 92238.71c -.83786
c-----3.78% enriched UO2-----
m11 8016.71c -.11853 92235.71c -.033320 92238.71c -.84817
m21 8016.71c -.11853 92235.71c -.033320 92238.71c -.84817
m31 8016.71c -.11853 92235.71c -.033320 92238.71c -.84817
m41 8016.71c -.11853 92235.71c -.033320 92238.71c -.84817
m51 8016.71c -.11853 92235.71c -.033320 92238.71c -.84817
m61 8016.71c -.11853 92235.71c -.033320 92238.71c -.84817
c-----2.61% enriched UO2-----
m12 8016.71c -.11853 92235.71c -.023043 92238.71c -.85849
m22 8016.71c -.11853 92235.71c -.023043 92238.71c -.85849
m32 8016.71c -.11853 92235.71c -.023043 92238.71c -.85849
m42 8016.71c -.11853 92235.71c -.023043 92238.71c -.85849
m52 8016.71c -.11853 92235.71c -.023043 92238.71c -.85849
m62 8016.71c -.11853 92235.71c -.023043 92238.71c -.85849
c-----
m2 2004.71c 1 $ Helium in the fuel rod gap
c-----
$ Helium in the fuel rod gap
m3 40000.66c -.9823 50000.42c -.0145 26000.42c -.0021
      24000.42c -.001 72000.60c -.001
$ Zirlo cladding
c-----
m4 8016.71c 1 1001.71c 2
$ Water
c m4 8016.71c 1e6 1001.71c 2e6
c      8016.71c 12000 1001.71c 12000 5010.71c 800
5011.71c 3200 $ Borated Water
c-----
m5 24052.71c -.16 28058.71c -.1 25055.71c -.02 14028.71c -
.0075

```

7014.71c -.001 6000.71c -.0008 15031.71c -.00045  
 16032.71c -.0003  
 42098.71c -.02 26056.71c -.68995  
 \$ SS 316  
 c -----Pyrex Material-----  
 m6 5010.71c -.00744139 5011.71c -.03293305 14028.71c -  
 .34355993  
 14029.71c -.01801744 14030.71c -.01237181 11023.71c  
 -.02967434  
 13027.71c -.01587757 8016.71c -.54012447  
 m16 5010.71c -.00744139 5011.71c -.03293305 14028.71c -  
 .34355993  
 14029.71c -.01801744 14030.71c -.01237181 11023.71c  
 -.02967434  
 13027.71c -.01587757 8016.71c -.54012447  
 m26 5010.71c -.00744139 5011.71c -.03293305 14028.71c -  
 .34355993  
 14029.71c -.01801744 14030.71c -.01237181 11023.71c  
 -.02967434  
 13027.71c -.01587757 8016.71c -.54012447  
 m36 5010.71c -.00744139 5011.71c -.03293305 14028.71c -  
 .34355993  
 14029.71c -.01801744 14030.71c -.01237181 11023.71c  
 -.02967434  
 13027.71c -.01587757 8016.71c -.54012447  
 m46 5010.71c -.00744139 5011.71c -.03293305 14028.71c -  
 .34355993  
 14029.71c -.01801744 14030.71c -.01237181 11023.71c  
 -.02967434  
 13027.71c -.01587757 8016.71c -.54012447  
 m56 5010.71c -.00744139 5011.71c -.03293305 14028.71c -  
 .34355993  
 14029.71c -.01801744 14030.71c -.01237181 11023.71c  
 -.02967434  
 13027.71c -.01587757 8016.71c -.54012447  
 c -----IFBA (ZrB2) Material-----  
 -  
 m7 5010.71c -.03531503 5011.71c -.03293305 40090.71c -  
 .40990457  
 40091.71c -.09038548 40092.71c -.13967492 40094.71c  
 -.14463039  
 40096.71c -.0237937  
 m17 5010.71c -.03531503 5011.71c -.03293305 40090.71c -  
 .40990457  
 40091.71c -.09038548 40092.71c -.13967492 40094.71c  
 -.14463039  
 40096.71c -.0237937

m27 5010.71c -.03531503 5011.71c -.03293305 40090.71c -  
 .40990457  
     40091.71c -.09038548 40092.71c -.13967492 40094.71c  
 -.14463039  
     40096.71c -.0237937  
 m37 5010.71c -.03531503 5011.71c -.03293305 40090.71c -  
 .40990457  
     40091.71c -.09038548 40092.71c -.13967492 40094.71c  
 -.14463039  
     40096.71c -.0237937  
 m47 5010.71c -.03531503 5011.71c -.03293305 40090.71c -  
 .40990457  
     40091.71c -.09038548 40092.71c -.13967492 40094.71c  
 -.14463039  
     40096.71c -.0237937  
 m57 5010.71c -.03531503 5011.71c -.03293305 40090.71c -  
 .40990457  
     40091.71c -.09038548 40092.71c -.13967492 40094.71c  
 -.14463039  
     40096.71c -.0237937  
 m67 5010.71c -.03531503 5011.71c -.03293305 40090.71c -  
 .40990457  
     40091.71c -.09038548 40092.71c -.13967492 40094.71c  
 -.14463039  
     40096.71c -.0237937  
 m77 5010.71c -.03531503 5011.71c -.03293305 40090.71c -  
 .40990457  
     40091.71c -.09038548 40092.71c -.13967492 40094.71c  
 -.14463039  
     40096.71c -.0237937  
 m87 5010.71c -.03531503 5011.71c -.03293305 40090.71c -  
 .40990457  
     40091.71c -.09038548 40092.71c -.13967492 40094.71c  
 -.14463039  
     40096.71c -.0237937  
 m97 5010.71c -.03531503 5011.71c -.03293305 40090.71c -  
 .40990457  
     40091.71c -.09038548 40092.71c -.13967492 40094.71c  
 -.14463039  
     40096.71c -.0237937  
 c -----  
 m8 47000.55c -.805 48000.42c -.049 49000.42c -.146  
     \$ Ag-In-Cd for control rods

## BIBLIOGRAPHY

1. "Small Modular Nuclear Reactors." Energy.gov. Accessed March 2<sup>nd</sup>, 2015. <<http://www.energy.gov/ne/nuclear-reactor-technologies/small-modular-nuclear-reactors>>.
2. "Westinghouse Small Modular Reactor: Taking Proven Technology to the Next Level." Iaea.org. Accessed March 5<sup>th</sup>, 2015. <[https://www.iaea.org/INPRO/3rd\\_Dialogue\\_Forum/12.SMR-Westinghouse.pdf](https://www.iaea.org/INPRO/3rd_Dialogue_Forum/12.SMR-Westinghouse.pdf)>.
3. Smith, Matthew C., and Richard F. Wright. "Westinghouse Small Modular Reactor Passive Safety System Response to Postulated Events." *Proc. of ICAPP'12* (2012).
4. Ames, David Elroy. "High-Fidelity Nuclear Energy System Optimization Towards an Environmentally Benign, Sustainable, and Secure Energy Source." PhD diss., Texas A&M University, 2010.
5. Farkas, Gabriel, Svetozár Michálek, and Ján Haščík. "MCNP5 Delayed Neutron Fraction ( $\beta_{eff}$ ) Calculation In Training Reactor VR-1." *Journal of Electrical Engineering* 59, no. 4 (2008): 221-224.
6. Duderstadt, James J., and Louis J. Hamilton. *Nuclear Reactor Analysis*. New York: Wiley, 1976.
7. Lamarsh, John R. *Introduction to Nuclear Engineering*. 2nd ed. Reading, Mass.: Addison-Wesley, 1983.
8. United States Nuclear Regulatory Commission, "AP1000 Design Control Document".
9. United States Nuclear Regulatory Commission, "NUREG-0800, 15.4.6 Inadvertant Decrease in Boron in the Reactor Coolant System", (2007).
10. Housiadas, C., and M. Antonopoulos-Domis. "Estimation of the Moderator Temperature Coefficient of Reactivity Via Noise Analysis Using Closed-Loop Transfer Functions." *Annals of Nuclear Energy* 28, no. 10 (2001): 983-991.
11. Thilagam, L., C. Sunil Sunny, K. V. Subbaiah, K. Devan, Young-Seok Lee, and V. Jagannathan. "Doppler Coefficient Of Reactivity—Benchmark Calculations For Different Enrichments of UO<sub>2</sub>." *Joint International Topical Meeting on Mathematics & Computation and Supercomputing in Nuclear Applications (M&C+SNA 2007)*. Monterey, California. 2007.

12. Liang, C., and W. Ji. "A Neutronic Feasibility Study of the AP1000 Design Loaded With Fully Ceramic Micro-Encapsulated Fuel." American Nuclear Society, 555 North Kensington Avenue, La Grange Park, IL 60526 (United States), 2013.
13. Kindred, Thomas. "Westinghouse SMR Primary Systems." Uxc.com. 2012. Accessed March 9<sup>th</sup>, 2015.  
<<http://www.uxc.com/smr/Library%5CDesign%20Specific/Westinghouse%20SMR/Presentations/2012%20-%20W-SMR%20Primary%20Systems.pdf>>

## VITA

Kirby Compton was born in St. Louis, Missouri in 1990. He graduated from John Burroughs High School in St. Louis in 2009, and then began his studies at Connecticut College in New London, Connecticut. In May 2013 he was awarded a BA in Physics with a concentration in Astrophysics. He then started graduate school at Missouri University of Science and Technology in the department of Nuclear Engineering. As an NRC Fellowship recipient, Kirby began a research project that consisted of a reactor physics analysis of the variations in core configurations of the Westinghouse Small Modular Reactor using the transport code MCNP. He completed his Master's Degree in Nuclear Engineering in May 2015.